

## Precise Leveling survey around mount Io, Kirishima Volcano (2012 - 2016)

\*Takeshi Matsushima<sup>1</sup>, Kazunari Uchida<sup>1</sup>, Rintaro Miyamachi<sup>1</sup>, Shiori Fujita<sup>1</sup>, Manami Nakamoto<sup>1</sup>, Hitoshi Y. Mori<sup>2</sup>, Masayuki Murase<sup>3</sup>, Takahiro Ohkura<sup>4</sup>, Hiroyuki Inoue<sup>4</sup>

1.Institute of Seismology and Volcanology, Faculty of Science, Kyushu University, 2.Institute of Seismology and Volcanology, Faculty of Science, Hokkaido University, 3.Department of Geosystem Sciences, College of Humanities and Sciences, Nihon University, 4.Institute for Geothermal Sciences, Graduate School of Science, Kyoto University

### Introduction

Since the magma eruption of Kirishima Shinmoedake in southern Kyushu in 2011, volcanic activity of the Kirishima mountain range had been followed by a calm situation.

However, the number of volcanic earthquakes is increased around Ebino plateau (Mount Io) a distance of about 5km northwest from Shinmoedake since December 2013.

In August 2014 occurred volcanic tremor that epicenter near mount Io and, it was also observed tilt change at the same time. Furthermore, geothermal field appeared in the summit area of Mount Io in December 2015, then also it began ejection of volcanic gas.

Mount Io is the vents of dacitic lava flow of 16 and 17th centuries in the eastern part of Ebino plateau. Although in the summit area had also been mining of sulfur up to 1962, in recent years it had declined rapidly its volcanic activity.

In the Kirishima volcanic area, level route has been established in 1968 by the University of Tokyo Earthquake Research Institute, and the phenomenon of subsidence and contraction of Mount Io have been observed in several times (Koyama et al., 1991). Ozawa et al. (2003) reported the local subsidence of Mount Io by using the interference SAR. We thought that activation of volcanic activity in the vicinity of Ebino plateau from the end of 2013 is a new magmatic activity, in order to understand the crustal deformation associated with this magma intrusion in detail, was carried out the leveling of near Ebino plateau.

### Data and methods

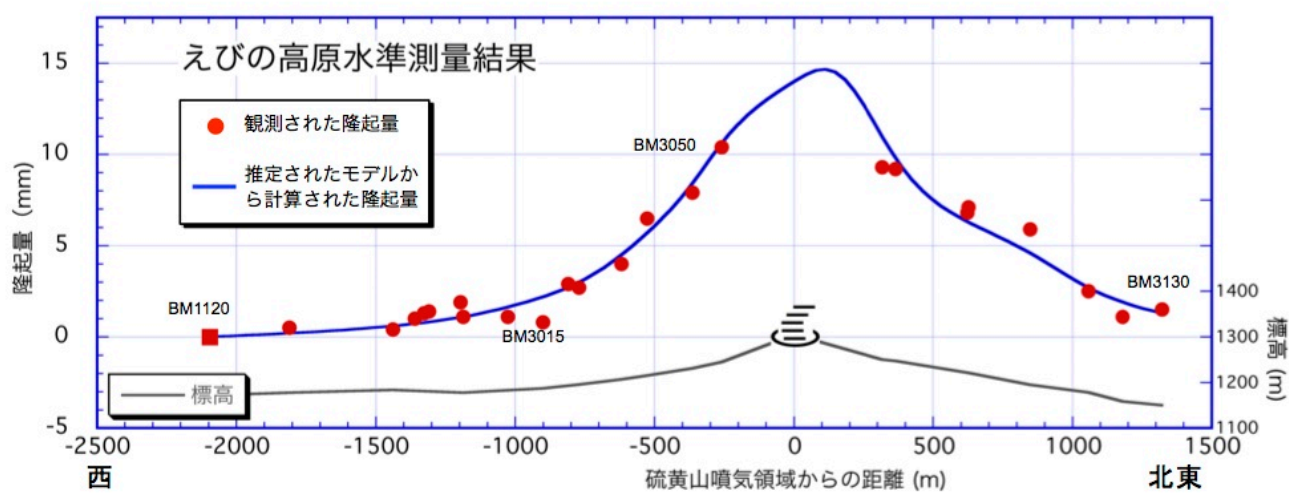
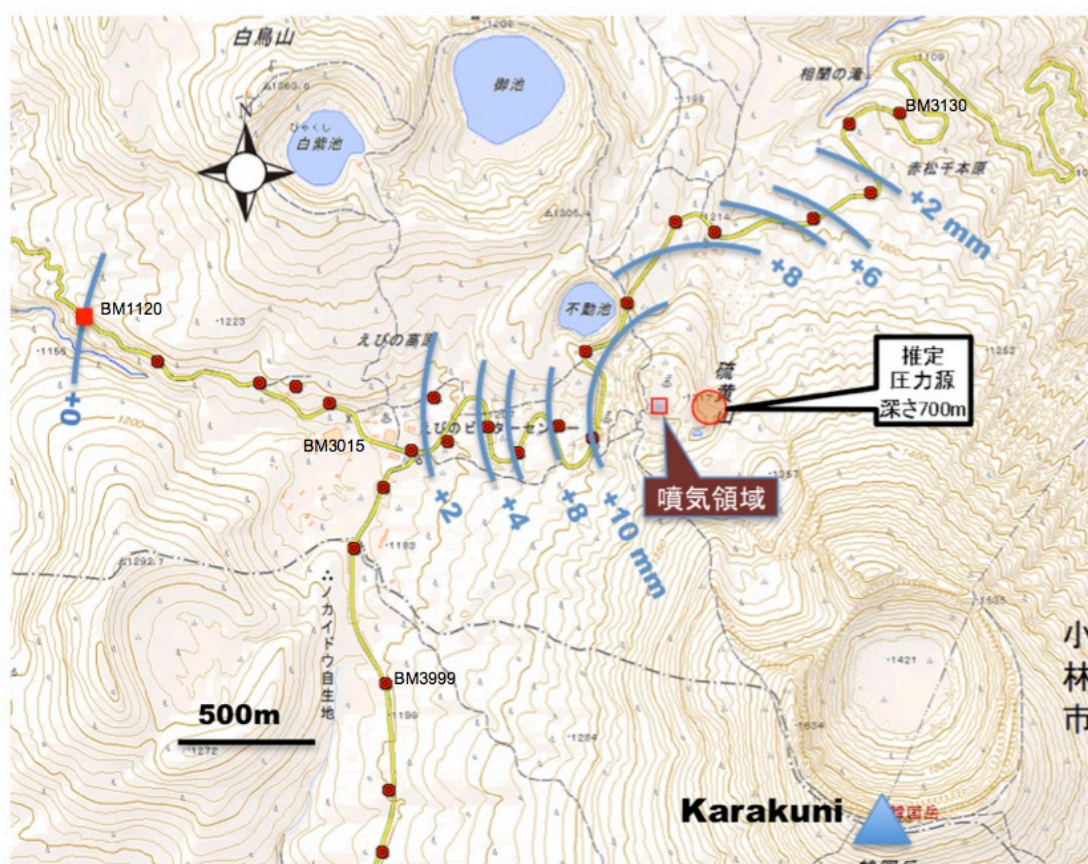
Immediately after the eruption of Shinmoedake in 2011, Hokkaido University made a leveling of three times with about 25km section of Ebino city- Ebino plateau - Kirishima Shin'yu hot spring (Mori et al., 2012) . We carried out a re-measurement of about 8km section between Ebino plateau - Kirishima Shin'yu in June, 2015, and we have established a new route of about 2.5km in Mount Io direction. Also in 2015 December 19 to 22 we carried out to re-survey in the vicinity of Ebino plateau.

### Result

With reference to the level point BM1120 level route western margin, the difference between the June measurement value and in December 2015 measured value at each level point are shown in the figure. Uplift amount is larger as it approaches the Mount Io from Ebino plateau (BM3015), uplift of up to 10.4 mm was recorded in west trailhead of Mount Io (BM3050). Uplift becomes gradually smaller when cross the mountain pass, and have returned to almost 0mm in BM3130 route northeast end.

Using the MaGCAP-V which the Meteorological Research Institute has developed, the elevation corrected Mogi model was determined by grid search. As a result, increasing pressure source of  $3.1 \times 10^4 \text{ m}^3$  East 150m of Mount Io fumarole area, was estimated at an altitude of 600m. The vertical variation, which is calculated from this model is consistent with the crustal deformation observed by Earth Science and Disaster Prevention Research Institute using interference SAR analysis. The depth of the pressure source, which corresponds to the lower surface of the low-resistivity layer (impermeable layer) that has been estimated by Aizawa et al. (2013).

Keywords: Kirishima Volcano, Mount Io, Ebino Plateau, Precise Leveling Survey, Volcanic Ground Deformation



## Probabilistic Prediction of Vulcanian Eruptions at the Showa Crater of Sakurajima Based on Ground Inflation

\*Masato Iguchi<sup>1</sup>

1.Sakurajima Volcano Research Center, Disaster Prevention Research Institute, Kyoto University

Ground inflation was detected prior to 4422 vulcanian eruptions at Sakurajima by strainmeters. Frequency distributions of duration, amount, mean rate of strain change and ratio of inflation to deflation strain changes associated with eruptions show lognormal distribution. By using the lognormal distribution of the frequency as probability function, it is possible to stochastically forecast occurrence time and scale of the vulcanian eruptions.

Keywords: vulcanian eruption, precursory inflation, Probabilistic forecasting

## Comparison between ground deformation events at Sakurajima from January to June 2015 and on August 15, 2015

\*Kohei Hotta<sup>1,2</sup>, Masato Iguchi<sup>2</sup>, Takahiro Ohkura<sup>1</sup>, Keigo Yamamoto<sup>2</sup>, Takeshi Tameguri<sup>2</sup>

1.Graduate School of Science, Kyoto University, 2.DPRI, Kyoto University

We applied some source models to the ground deformations in different stages of volcanic activity of Sakurajima to make clear style and process of magma intrusion.

One is slow ground inflation with highly eruptive activity at the Showa crater during the period from January to June 2015 (first-half 2015 event). This event is similar to that during the period from October 2011 to March 2012 (2011 event). A pressure source analysis based on Mogi model (Mogi, 1958, BERI) during the 2011 event revealed inflation sources to be located at a depth of 9.6 km below sea level beneath the Aira caldera and 3.3 km below sea level beneath Kita-dake, and a deflation source is located at a depth of 0.7 km below sea level beneath Minami-dake (Hotta et al., 2016, JVGR). The characteristics of ground deformation during the first-half 2015 event is similar to that of the 2011 event, and inflation sources beneath Aira caldera and Kita-dake and a deflation source beneath Minami-dake are considered.

The other is much rapider and larger ground deformation on August 15, 2015, when eruptive activity was decreasing from July 2015 (August 2015 event). The pattern of horizontal displacement during the period from August 14 to 16, 2015 shows a WNW-ESE extension, which suggests a tensile fault. A nearly vertical dike with a strike of NNE-SSW is obtained at a depth of 1.0 km below sea level beneath Minami-dake. The length and width are 2.3 km and 0.6 km, respectively. The opening 1.97 m yields its volume increase +2.7 million cubic meters (Hotta et al., under revision, EPS).

Associated with the August 2015 event, 887 volcano-tectonic (VT) earthquakes occurred beside the dike, differently from the first-half 2015 event while only 63 VT earthquakes occurred for the 6 months. Half of the total amount of deformation of the August 2015 event was concentrated from 10:27 to 11:54. It is estimated that the intrusion rate of magma was 1 million cubic meters per hour during the period. This rate is 200 times larger than that of magma intrusion rate beneath Minami-dake prior to the vulcanian eruption on July 24, 2012 (5 thousand cubic meters per hour; Iguchi, 2013, Study on volcanic eruption process by multi-parameter observation at Sakurajima). The quite rapid intrusion rate caused extremely high-rate accumulation of strain in surrounding rocks, and this forced significant increase in seismicity. The first-half 2015 event is considered to be a process of magma accumulation and migration among the pre-existing spherical reservoirs, similarly to the previous activities such as the 2011 event. Conversely, the August 2015 event is dike-creating event at a different place from the pre-existing reservoir beneath the Showa crater, and magma stopped at a shallow depth of 1.0 km. The direction of the opening of the dike coincides with the T-axes of the VT earthquakes at the SW flank and is influenced by tectonic stress around the Sakurajima volcano. The VT earthquakes at the SW flank during the periods of 1976-1978 and 2003-2004 are inferred to be the magma pass from southwestern part of Sakurajima (Kamo, 1989, Proceedings of Kagoshima International Conference on Volcanoes) and vertical tensile crack that across Sakurajima from NE to SW (Hidayati et al., 2007, BVJSJ), respectively. The first-half 2015 event was accompanied by the VT earthquakes at the SW flank during the period from March 31 to early April, 2015, similarly to 1976-1978 and 2003-2004. Magma might migrate beneath the dike intruded on the August 2015 event along the magma pass from southwestern part of Sakurajima or along vertical tensile crack that across Sakurajima from NE to SW accompany with the swarm of VT earthquakes at the southwestern part of Sakurajima in the first-half 2015 event.

Keywords: Sakurajima volcano, ground deformation, geodetic data, VT earthquake

## Continuous relative gravity observation at Sakurajima Volcano: Tilt and gravity changes during the dike intrusion event

\*Takahito Kazama<sup>1</sup>, Keigo Yamamoto<sup>2</sup>, Masato Iguchi<sup>2</sup>

1.Kyoto University, 2.DPRI, Kyoto University

At Sakurajima Volcano (Kagoshima Prefecture, Western Japan), rapid tilt changes due to the inflation of the mountain body were observed on 15 August 2015, along with the increase of volcanic earthquakes (Japan Meteorological Agency, 2015). Geodetic investigations also showed that the inflation was caused by the intrusion of a dike, whose strike direction was close to the north-south axis (Geospatial Information Authority of Japan, 2015). Ascending volcanic fluid may be related to the dike intrusion, but physical properties of the fluid such as density cannot be directly identified from the observations of earthquakes and crustal deformations because these observations only detect indirect deformations of the volcanic medium.

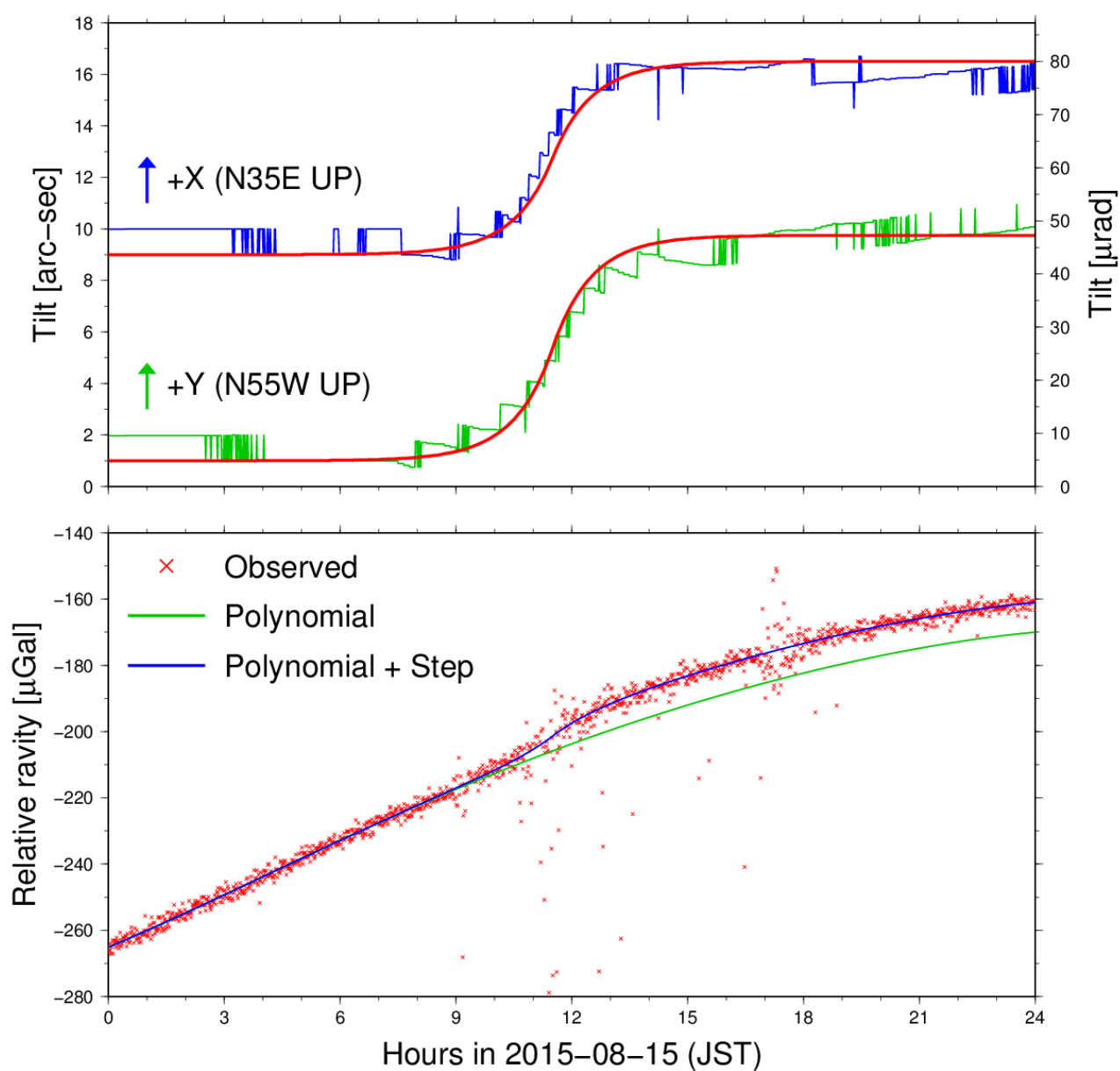
We thus utilize the minutely continuous data of relative gravity and tilts collected by a Scintrex CG-3M gravimeter at Arimura Observatory (2.1 km south-southeast of the Showa crater), in order to discuss the mass movement process during the dike intrusion event on 15 August 2015. Note that we already corrected several disturbances in the raw data of the gravity and tilts (such as the tidal effect and instrumental drift), which will be presented in the "Gravity and Geoid" session in detail.

Tilt change: The blue and green lines in the upper panel of the attached figure show the time variations in tilt for the N35E and N55W axes on 15 August 2015, respectively. Two tilt values increased rapidly around noon, suggesting that the ground uplifted at the north of Arimura Observatory (i.e., at the area of the volcanic craters). We estimated the time constant and amplitudes of the tilt variations by fitting the exponential functions of  $\exp(x)$  for  $x < 0$  and  $2 - \exp(-x)$  for  $x \geq 0$  through the trial-and-error approach. The peak-to-peak tilt amplitudes are +36 and +42 micro-rad for the N35E and N55W axes, respectively, so the absolute value of the tilt changes is calculated to be 56 micro-rad, which is about 65 % of that recorded in the Arimura tunnel (Japan Meteorological Agency, 2015). In addition, the time constant of the exponential functions is 1.0 hour, and the two tilt components varied most rapidly at 11:30 in JST.

Relative gravity change: The red lines in the lower panel of the attached figure show the relative gravity change in 15 August 2015, recorded by the CG-3M gravimeter. Although a part of the gravity data scatters due to the active seismicity, a gravity step can be identified in the instrumental drift with a period of a few days. By applying the regression of a fifth-order function and the above exponential function to the gravity time series, the peak-to-peak amplitude of the gravity step is calculated to be +9 micro-Gal. However, this gravity change is inconsistent with that observed by an absolute gravimeter at Arimura Observatory (-5 micro-Gal; Okubo et al., 2015) in terms of the sign and absolute amplitude. One of the possible reasons is that the relative gravity data was disturbed by apparent gravity changes due to the significant tilt changes. In our presentation, we will report the investigation results of the tilt-derived apparent gravity changes to discuss the mass movement process from the gravity signals associated with the dike intrusion.

Keywords: relative gravity, gravity change, tilt change, Sakurajima Volcano, dike, magma

## Scintrex CG-3M Gravimeter at Arimura



# Gravity vs Strain/Tilt Changes at Sakurajima Volcano from the Dyke Intrusion Event in August 2015 through Resumption of Frequent Explosions in February 2016

\*Shuhei Okubo<sup>1</sup>, Keigo Yamamoto<sup>2</sup>, Masato Iguchi<sup>2</sup>, Yoshiyuki Tanaka<sup>1</sup>, Yu Takagi<sup>1</sup>

1.Earthquake Research Institute, The University of Tokyo, 2.Disaster Prevention Research Institute, Kyoto University

In this paper, we deal with short-term gravity signals based on continuous absolute gravity measurements from July 2015 through February 2015. During this period, significant seismicity and crustal deformations were observed on Aug. 15, 2015, followed by unusual quiescence from late September 2015 through early February 2016.

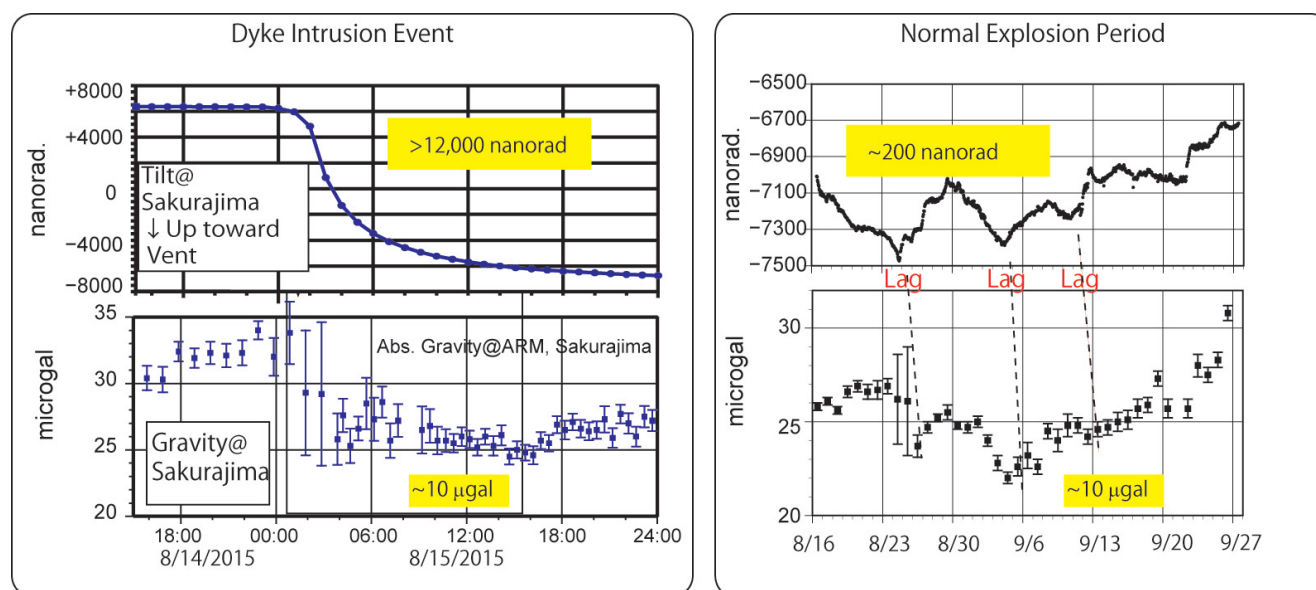
We compared gravity  $g(t)$  with strain or tilt record  $e(t)$  on Sakurajima volcano. Two aspects are noteworthy to point out. That is,

(1) The ratio  $|g(t) / e(t)|$  during the dyke intrusion (Aug. 15, 2015) is 100 times smaller than that during the other explosion period.

(2) Time lag between  $g(t)$  and  $e(t)$  is negligibly small during the dyke intrusion (Aug. 15, 2015) while  $g(t)$  during the other period shows significant time lag (~1 day) to  $e(t)$ .

These characteristics are well explained in terms of the conduit status (open/closed). When the conduit is closed as in the case of the dyke intrusion event, both strain/tilt and gravity are principally governed by instantaneous elastic deformation, which implies absence of time lag. On the other hand, when the conduit is open as in the explosion period other than the dyke intrusion event, inflation/deflation of magma chamber does not cause effective elastic deformation, which means larger  $|g(t) / e(t)|$  compared to the case of closed conduit and significant time lag of  $g(t)$  to  $e(t)$  because magma migration in a conduit requires certain amount of time.

Keywords: Gravity, Sakurajima, Magma Head, Crustal Deformation, Open Conduit, Vulcanian Eruption





## Vertical deformation associated with the 15 August 2015 dike intrusion at Sakurajima volcano measured by leveling survey

\*Keigo Yamamoto<sup>1</sup>, Shin Yoshikawa<sup>2</sup>, Takeshi Matsushima<sup>3</sup>, Takahiro Ohkura<sup>2</sup>, Akihiko Yokoo<sup>2</sup>, Hiroyuki Inoue<sup>2</sup>, Kazunari Uchida<sup>3</sup>, Tadaomi Sonoda<sup>1</sup>, Manami Nakamoto<sup>3</sup>, Yusuke Yamashita<sup>1</sup>, Daisuke Miki<sup>1</sup>, Satoshi Matsumoto<sup>3</sup>, Koki Aizawa<sup>3</sup>, Mie Ichihara<sup>4</sup>

1.Disaster Prevention Research Institute, Kyoto University, 2.Graduate School of Science, Kyoto University, 3.Faculty of Sciences, Kyushu University, 4.Earthquake Research Institute, University of Tokyo

We conducted the precise leveling survey in and around Sakurajima volcano, in order to detect the vertical ground deformation associated with the dike intrusion event occurred on August 15, 2015. The leveling routes measured in this survey are about 69 km long in total, including Sakurajima coast route, Sakurajima western flank route, Sakurajima northern flank route, Kurokami route in the eastern side of this volcano and Kagoshima Bay western coast route located outside Sakurajima. These leveling routes were measured during the periods from August 16 to September 24 and on December 18, 2015, immediately after the occurrence of the intrusion event. Mean square errors of the conducted survey were achieved with a good accuracy as the range from  $\pm 0.17$  to  $\pm 0.33$  mm/km. From the survey data measured in Sakurajima, we calculate the relative height of each bench mark referred to the reference bench mark BM.S.17 which is located at the western coast of Sakurajima. The calculated relative heights of the bench marks are then compared with those of the previous survey conducted in November 2014 (Yamamoto et al., 2015), resulting in the relative vertical displacements of the bench marks during the period from November 2014 to August-September 2015. As to the measured data of Kagoshima Bay western coast route, the reference bench mark is taken at BM.2469 located in Kagoshima city to the west of Sakurajima, and we calculate the relative vertical displacements of the bench marks during the period from November 2013 (when the previous survey was conducted in this route) to August 2015.

The resultant displacements indicate the remarkable ground uplifts around the northern part of Sakurajima, at Arimura (to the south of craters) and at Kurokami (to the east of craters). The amount of the maximum uplift is as much as about 16.8 mm referred to BM.S.17. The obtained uplifts at Arimura and Kurokami are consistent with the vertical ground deformation expected from the dike intrusion models inferred by other researches using InSAR, GNSS, tilt and strain data associated with the August 15 event (Geospatial Information Authority of Japan, 2015; Hotta et al., 2016). The uplifts around the northern part of Sakurajima suggest the inflation of the magma reservoir beneath the northern part of Sakurajima or beneath Aira caldera, which was not simultaneous with the August 15 event.

Keywords: Sakurajima volcano, dike intrusion, precise leveling survey, vertical ground deformation

## Earthquake Swarm Activity at Sakurajima Volcano on August 15, 2015

\*Takeshi Tameguri<sup>1</sup>, Kohei Hotta<sup>1</sup>, Masato Iguchi<sup>1</sup>

1.Sakurajima Volcano Research Center, Disaster Prevention Research Institute, Kyoto University

Explosive eruptions of vulcanian type have occurred at the summit crater Minamidake at Sakurajima volcano, Japan, since 1955. Principal eruptive activity shifted to the Showa crater at the eastern flank of the summit in 2006. The eruptions at the Showa crater were phreatic in 2006-2007 and vulcanian eruptions started from 2008. Minor vulcanian eruptions occurred about 500-1,000 times per year in 2010-2014. The eruptions occurred about 100 times every month until June in 2015. However, the eruptive activity gradually decreased from July. Active earthquake swarm and rapid ground deformation occurred on August 15, 2015 after decrease of the eruptive activity from July. In this study, we research temporary change of the earthquake activity, hypocenter distribution, source mechanism, and relationship the earthquake swarm between the rapid ground deformation.

The earthquake swarm are almost VT (Volcano-Tectonic) earthquake type, reached to 887 events on August 15. This swarm was obvious abnormal activity because the VT earthquakes occurred at most 40 events per month in Sakurajima. Location of hypocenters are calculated by using arrival times of P-wave first motion (more than 12 stations) and S-wave (more than 6 stations) assuming homogeneous half-space  $V_p=2.5\text{km/s}$  and  $V_p/V_s=1.73$ . Hypocenters are located beneath active craters Minamidake and Showa at depths 1.5 to 3.5 km. Source mechanisms determined using polarities of the first motions are normal fault (shallower than 2km) and strike slip types (deeper than 2km). The hypocenter location and source mechanism are similar pattern to general VT earthquake activities of the Sakurajima volcano (Hidayati et al., 2007, Bull. Volcanol. Soc. Japan).

Rapid and large ground deformation was also observed on August 15 accompanied with the earthquake swarm. Pattern of horizontal displacement showed extension to WNW-ESE, which suggested open of tensile crack by magma intrusion. A nearly vertical dike with strike of NNE-SSW was obtained at a depth of 1.0km beneath the Minamidake. Length and width of the dike were 2.3km and 0.6km, respectively. The dike opening was about 2m and its volume increased 2.7 million cubic meter (Hotta et al., submit to EPS).

The hypocenters of the VT earthquakes are close to opening of the dike estimated from ground deformation data. The earthquake swarm started at 07:05. Then, larger earthquake (M1.5 and M1.7) and the largest earthquake (M2.3) occurred at 09:03 and 10:47, respectively. The seismicity was increase during after the largest earthquake to before 12 a.m. The ground deformation was clear from 8 a.m. and inflation rate increased from 9 a.m. Half of the total amount of the inflation was going on 10:27 to 11:54 of the same time as the active seismicity. The inflation rate changed to decrease after 11:54. Two large low-frequency earthquakes (LF events) occurred at 11:32 and 11:43 before the change of inflation rate at 11:54. The decrease of the inflation rate may be related to the occurrence of the LF events. First motions of the LF events were compression (up and away from the summit crater in the vertical and radial components, respectively) at the all stations. We determined the source mechanism of the LF events by waveform inversion. The LF events were generated by isotropic expansion at the depth of 1.0km beneath the Minamidake crater. The hypocenter location and the first motions of the LF events were similar to those of explosion earthquakes accompanied with explosive eruptions from the Showa and Minamidake craters. However, the LF events are not accompanied with eruptions from the active craters. It is thought that the LF events were probably generated in closing magma system.

Keywords: Sakurajima Volcano, Earthquake Swarm

Failed eruption observed by seismic arrays during the Sakujirama volcano activity on Aug. 15, 2015.

\*Eisuke Fujita<sup>1</sup>, Hideki Ueda<sup>1</sup>, Taku Ozawa<sup>1</sup>, Yosuke Miyagi<sup>1</sup>, Takahiro Miwa<sup>1</sup>, Ryohei Kawaguchi<sup>1</sup>

1.National research Institute for Earth science and Disaster prevention, Volcanic research department

NIED conducts seismic array observation at two sites (north of Kitadake and Kurokami) in Sakurajima volcano from March 2015. Each array consists of nine 1Hz seismometers and 1 infrasonic sensor with 200Hz data loggers. We analyzed seismic data observed during the failed eruption on Aug. 15, 2015. The observed waveforms have significant characteristics as below: 1) P-arrival times at Kitadake-array leads 0.2s to those at Kurokami-array around 7:00. At 6:00 seismic signal is clear at Kitadake-array but not at Kurokami-array. 2) Rough estimates of epicenters are around east of Minamidake-Nakadake. 3) Waveforms at all stations of Kitadake-array are coherent, but at Kurokami-array, seismic stations at east of Nabeyama and others show different features. 4) Waveforms in 12:00 have lower frequency components. 6) LP vents have precursory high frequency noises.

Temporal change of cross-correlation factors of these seismic waveforms indicate that there are three different periods, i.e., A: 6:00 - 10:30, B: 10:30 - 12:00, and C: 12:00 - 24:00. There are no family waves between these three periods. In A period, many family earthquakes were observed but not in B period. During C period, some pairs separated as long as hours have high cross-correlation factors. It is implicated that, in the A period, some similar fault slip occurred successively in the initial phase of dike intrusion, in the B period, VT events may suggest random fractures, and there occurred some similar slips all around the intruded dike in the C period.

Keywords: Sakurajima, magma intrusion, VT earthquakes

## Unknown later arrivals in cross-line shooting seismograms of the repeating seismic experiments in Sakurajima Volcano

\*Tomoki Tsutsui<sup>1</sup>, Takeshi Tameguri<sup>2</sup>, Masato Iguchi<sup>2</sup>, Haruhisa Nakamichi<sup>2</sup>, Hiromitsu Oshima<sup>3</sup>, Hiroshi Aoyama<sup>3</sup>, Sadato Ueki<sup>4</sup>, Mare Yamamoto<sup>4</sup>, Kenji Nogami<sup>5</sup>, Minoru Takeo<sup>6</sup>, Takao Ohminato<sup>6</sup>, Mie Ichihara<sup>6</sup>, Jun Oikawa<sup>6</sup>, Takao Koyama<sup>6</sup>, Yuta Maeda<sup>7</sup>, Takahiro Ohkura<sup>2</sup>, Hiroshi Shimizu<sup>8</sup>, Takeshi Matsushima<sup>8</sup>, Hiroki Miyamachi<sup>9</sup>, Reiji Kobayashi<sup>9</sup>, Hiroshi Yakiwara<sup>9</sup>

1.Akita University, 2.Kyoto University, 3.Hokkaido University, 4.Tohoku University, 5.Tokyo Institute of Technology, 6.University of Tokyo, 7.Nagoya University, 8.Kyushu University, 9.Kagoshima University

Clear unknown later arrivals will be presented, which are detected through reconsideration on cross-line shooting seismograms in Sakurajima Volcano. The later arrivals are interpreted as PP reflections or PS conversions beneath eastern flank of Kitadake.

The repeating seismic experiments in Sakurajima Volcano has been conducted on every December since 2009 through 2014 (Tsutsui et al. 2010; 2011; 2012; 2013; 2014). The experiment includes two seismic profiles in the northern and the eastern Sakurajima, and fourteen or fifteen chemical shots have been recorded at over 250 temporary stations on each experiment. The active reflector "Alpha" at 5.8km below sea level has been reported as a result of the experiments, which is located in the northeastern part of Sakurajima. However, only a portion of the active reflector has been presented in the paper under processing, which locates just beneath the seismic line.

On the other hand, the cross-line shooting seismograms have been waiting for analysis. We have obtained sets of the cross-line shooting seismograms due to continuous recording over the shootings. We detected and interpreted some clear later arrivals in the cross-line shooting seismograms as followings;

A clear later arrival appears on 2.9 through 3 seconds in the eastern stations for northern shots and also in their reversed configuration, in the source distance range of 4.0 to 4.8 km. The arrival only appears in the seismograms corresponding to path passing through 2 km ENE of Kitadake summit. The arrival is interpreted as PP reflections because they appear high apparent velocity and also been found in reversed geometry of the station and the shot. A PP reflector at 4.7 to 4.8km below sea level gives well explanation on the arrival time. It is of interest that the modeled reflector is located in the south of the reflector "Alpha", and is shallower than "Alpha".

Moreover, other clear later arrival appears in seismograms in northern Sakurajima for the eastern shot, which appears about 5.2 s in the range 4.5 through 5.5 km. The arrival has high apparent velocity, disappears in the seismograms at the reversed geometry, and shows larger amplitude than that expected in PP arrival time. The arrival is interpreted to be PS conversion because of those above feature in seismograms. Assuming  $V_p/V_s$  is 1.73, the conversion at 5.8 km below sea level in NE of Kitadake can explain its travel time. It is significant that the converting points locate just at the same depth of the active reflector "Alpha", and locate between previous reflector and the reflection "Alpha". Moreover, amplitude of the conversion has been changing through the seismic rounds.

Later arrivals have been detected in cross-line shooting seismograms on 2014 of which an association with the latest intrusion event on August 2015 is of interest.

Those seismic horizons beneath eastern to northeastern flank of Kitadake will be reported and their association with the intrusion event on August 2015 will be discussed.

Keywords: Volcanology, Sakurajima Volcano, Volcanic structure, Seismology

## Depth of pre-eruptive magma reservoir of Sakurajima Volcano estimated from melt inclusions

\*Naoki Araya<sup>1</sup>, Michihiko Nakamura<sup>1</sup>, Satoshi Okumura<sup>1</sup>, Atsushi Yasuda<sup>2</sup>, Daisuke Miki<sup>3</sup>, Masato Iguchi<sup>3</sup>

1.Department of Earth Science, Graduate School of Science, Tohoku University, 2.Earthquake Research Institute, University of Tokyo, 3.Sakurajima Volcano Research Center, Disaster Prevention Research Institute, Kyoto University

To interpret magmatic processes of the ongoing Vulcanian explosions and to forecast possible future activity in Sakurajima Volcano, determining pre-eruptive magmatic conditions of the historic eruptions, especially depths of the magma reservoirs, is crucial. We therefore analyzed volatile contents and major element compositions of melt inclusions (MIs) and their host phenocrysts in the three historic Plinian eruptions (1471 A.D., 1779 A.D., and 1914 A.D.) and recent Vulcanian eruptions (1955–present).

The water contents of 110 MIs were analyzed with a FT-IR micro-reflectance spectroscopy (Yasuda, 2014). Most of the pyroxene-hosted melt inclusions (MIs) were dacitic to rhyolitic ( $\text{SiO}_2 = 65\text{--}72$  wt.%) and gradually shifted to mafic compositions with time as observed for bulk rock compositions after the 1471 eruption (Uto et al., 2005; Nakagawa et al., 2011). The water contents of the MIs in the three historic Plinian eruptions have similar frequency distributions ranging from 1.2 to 3.5 wt.%. More than 95% of the data were within 1.2–2.9 wt.%. By contrast, those of melt inclusions in the recent Vulcanian ejecta were less than 2.3 wt.%. The lower maximum water content of the erupted materials of the Vulcanian explosions compared to those of the Plinian eruptions are interpreted as a result of degassing before quenching upon eruption. The MIs containing up to 40 ppm  $\text{CO}_2$  were rarely found (Sato et al., 2012, JpGU), but most of the MIs did not contain detectable  $\text{CO}_2$  content. The saturation pressure for the water content of 1.2–2.9 wt.% was calculated at 15–73 MPa, which corresponds to the depth of 0.6–3.1 km assuming that density of the upper crust is  $2400 \text{ kg/m}^3$ . The depth of the shallowest magma reservoir estimated from the geodetic observations on the present Vulcanian explosions are located at a depth of 4 km beneath the Minamidake summit (Iguchi et al., 2013), which is deeper than the depth ranges for most of the MIs (0.6–3.1 km) and in accordance with the maximum depth (4.1 km, corresponding to 3.5 wt%  $\text{H}_2\text{O}$ ). Considering the erupted volumes of these Plinian eruptions ( $0.3\text{--}0.8 \text{ km}^3$  for the Plinian eruptions and  $0.8\text{--}2.0 \text{ km}^3$  including lava flows in DRE, Kobayashi et al., 2013), the obtained depth range (2.5 km) may be largely explained by the difference in the position of the magma reservoir.

Keywords: Sakurajima Volcano, magma reservoir, melt inclusion, water content

## Volcanic gas composition of Sakurajima volcano, Japan

\*Hiroshi Shinohara<sup>1</sup>, Ryunosuke KAZAHAYA<sup>1</sup>, Urumu Tsunogai<sup>2</sup>, Takao Ohminato<sup>3</sup>, Takayuki Kaneko<sup>3</sup>

1.Geological Survey of Japan, AIST, 2.Graduate School of Environmental Studies, Nagoya University, 3.Earthquake Research Institute, University of Tokyo

We conducted volcanic gas composition measurements applying Multi-GAS and alkaline-filter techniques at Sakurajima volcano, which continues persistent degassing and frequent small-scale Vulcanian eruptions for several decades. The Multi-GAS and alkaline-filter needs to be conducted in a dense plume for precise measurement. However, we cannot access to the summit area of the volcano because of the frequent eruption and we applied various techniques to approach the volcanic plume at Sakurajima, including 1) air-borne measurement with a Cessna aircraft, 2) air-borne measurement with an unmanned helicopter and 3) automatic measurement at a flank of the volcano. Accuracy of the estimated gas composition depends on measured volcanic gas concentration which is quite variable depending on wind speed, direction, volcanic activity and distance from the summit crater.

We started the measurement in 2012. Until the early 2015, Sakurajima volcano continues the intensive persistent degassing with SO<sub>2</sub> flux larger than 1,000 t/d and with frequent explosions at Showa crater, but SO<sub>2</sub> flux decreased to around 100 t/d in the late 2015 with quite limited number of explosions. The volcanic gas compositions are fairly well estimated during the high flux period. The estimated average composition is; CO<sub>2</sub>/SO<sub>2</sub> = 0.5, H<sub>2</sub>O/SO<sub>2</sub>=110, SO<sub>2</sub>/H<sub>2</sub>S=8, H<sub>2</sub>/SO<sub>2</sub>=0.15 and SO<sub>2</sub>/Cl=10 (mol ratio). This composition is similar to composition of other high-temperature gases in Japan with an exception of larger H<sub>2</sub>O/SO<sub>2</sub> than others (i.e., about 40 at Asama, Miyake and Aso volcanoes). The CO<sub>2</sub>/SO<sub>2</sub> ratios vary between 0.5-1.5 but negatively correlate with the measured SO<sub>2</sub> concentration. The similar correlations observed at Asama volcano were interpreted as the results of mixing of low-temperature gases with low SO<sub>2</sub> and high CO<sub>2</sub> concentrations. At Sakurajima volcano, however, distribution of low-temperature fumaroles are limited and the cause of the correlation is not clear. The SO<sub>2</sub>/Cl ratios vary 5-20, which is consistent with the SO<sub>2</sub>/HCl ratios measured in 2009-2013 by FT-IR for the gas plume from the Showa crater (Mori et al., 2004).

During the low flux period in the late 2015 and the early 2016, the estimated ratios are different from those during the high flux periods; SO<sub>2</sub>/H<sub>2</sub>S=0.6-2.5 and CO<sub>2</sub>/SO<sub>2</sub> = 20-150. During the low flux period, the measured gas concentrations were quite low (with maximum SO<sub>2</sub> concentration of 0.1-0.5 ppm) and the estimated ratios are likely associated with quite large uncertainty, in particular for CO<sub>2</sub>/SO<sub>2</sub> ratios. We measured δ<sup>13</sup>C of CO<sub>2</sub> in the plume samples collected during the flight when CO<sub>2</sub>/SO<sub>2</sub> ratios were estimated as 150 and estimated the large CO<sub>2</sub>/SO<sub>2</sub> ratio was caused by CO<sub>2</sub> with low δ<sup>13</sup>C (about -25 per mil) which is quite different from a common volcanic gas CO<sub>2</sub> and the large ratio is unlikely represent that of the gases from the summit vent. The SO<sub>2</sub>/H<sub>2</sub>S ratios during the low flux period are lower than those during the high flux period. The low values can be caused by various reasons, however, most likely cause might be pressure difference of magma degassing. Since SO<sub>2</sub>/H<sub>2</sub>S ratio at constant oxygen fugacity and temperature inversely proportional to pressure, 10 times increase of the degassing pressure can cause the ten times decrease of the SO<sub>2</sub>/H<sub>2</sub>S ratios.

Keywords: Volcanic gas, volcanic plume, Sakurajima



## Detection of abrupt increase in CO<sub>2</sub> flux from a submarine volcano, Wakamiko, in the innermost part of Kagoshima Bay in July 2015

\*Toshiro Yamanaka<sup>1</sup>, Kazuna Kondo<sup>1</sup>, Mari Kobayashi<sup>1</sup>, Takuro Noguchi<sup>2</sup>, Kei Okamura<sup>3</sup>, Tomoko Yamamoto<sup>4</sup>, Urumu Tsunogai<sup>5</sup>, Jun-ichiro Ishibashi<sup>6</sup>

1. Graduate School of Natural Science and Technology, Okayama University, 2. Multidisciplinary Science Cluster, Research and Education Faculty, Kochi University, 3. Center for Advanced Marine Core Research, Kochi University, 4. Faculty of Fisheries, Kagoshima University, 5. Graduate School of Environmental Studies, Nagoya University, 6. Graduate School of Science, Kyushu University

CO<sub>2</sub> flux from a submarine volcano, Wakamiko, Southern Kyushu, Japan, has been measured since 2007. The CO<sub>2</sub> flux from the volcano were varied ranging from 160 to 360 ton/day from 2007 to 2014, but in 2015 the flux is significantly increased up to 500 ton/day calculated using the data obtained in July. In the next month, August 2015, significant volcanic tremors were started beneath Sakurajima Volcano, so large-scale eruption of the volcano had been expected. After that, volcanic tremors beneath Sakurajima Volcano declined within two weeks, and also CO<sub>2</sub> flux from Wakamiko Volcano observed in December was decreased to similar range before 2014. Magma chamber beneath Aira Caldera has been considered to provide magmatic volatile to Wakamiko Volcano and to be connected with another shallower magma chamber beneath Sakurajima Volcano. The volcanic tremors were considered to be associated with ascending of magma from the shallower magma chamber. Therefore, the detected abrupt increase of CO<sub>2</sub> flux from Wakamiko Volcano may reflect those magma activities.

Keywords: Wakamiko submarine volcano, CO<sub>2</sub> flux, Volcanic activity of Sakurajima Volcano

## Hydrophone observations of volcanic activity from the sea area surrounding the Nishinoshima volcano

\*Yozo Hamano<sup>1</sup>, Hiroko Sugioka<sup>2</sup>, Aki Ito<sup>1</sup>, Mie Ichihara<sup>3</sup>, Masanao Shinohara<sup>3</sup>, Kiwamu Nishida<sup>3</sup>, Minoru Takeo<sup>3</sup>

1.Department of Deep Earth Structure and Dynamics Research, JAMSTEC, 2.Department of Planetology, Kobe University, 3.Earthquake Research Institute, University of Tokyo

We develop a remote island volcano monitoring system using an autonomous sea-going platform (Sugioka et al. 2016). The system is planned to be capable of observing 1) volcanic eruptions with infrasound signals, 2) deep volcanic activity by seismic signals, 3) eruptive activity by photographs, and 4) ocean waves due to collapse of island slope. During the KR15-03 cruise of R/V KAIREI, we tested the performance of the sensors for these observations. And, five Ocean Bottom Seismometers (OBS) were deployed on the seafloor surrounding the Nishinoshima for more general purpose of monitoring the seismic activity around the volcano. Here, we report the results of the hydrophone observations, which is to be used for observing seismic activity of the volcano. Hydrophone observation was made at the site 7km east to the Nishinoshima with water depth of 1318 m. The hydrophone was lowered from the ship to the depth of 10m below sea level. During the hydrophone measurements from 2015/2/27 13:20 to 14:40 (JST), videos of the volcano were taken continuously, and both the infrasound recorders on top of the ship and the OBS at the site NI11 14km east to the Nishinoshima were also operating. These simultaneous observations provide a big progress of understanding the role of each observation, and constructing a monitoring system of island volcanoes.

During the observation period, the volcanic activity was very high and eruptions with durations of 20 to 30 seconds occur with the frequency of about 15 events in ten minutes. The sequence of eruptions correlates well with the OBS and infrasound records, suggesting the seismic and infrasound signals are closely related to the eruptive activity at the shallow part of the volcanic body (Ichihara et al., 2016).

On the other hand, the features of hydrophone records are completely different. The most prominent feature of the hydrophone record is the harmonic tremor lasting about 20 minutes, which seem to be generated by deeper activities of the volcano. Underwater sound velocity structure seems responsible for that the wave sources for the OBS and the hydrophone are different. As for the sound velocity structure around the Nishinoshima estimated by the CTD measurement, the sound speed of surface 200 m is almost constant with the speed of 1518m/s. Below this depth, the sound speed drastically decreases to 1480 m/s at 1000m depth, and then slowly increase to 1490 m/s at 2000m depth. This sound speed structure suggests shadow zone at the sea surface depending on the source depth of the sound wave. Assuming that the position of the hydrophone is within the shadow zone, wave source of the explosion earthquakes is estimated to be deeper than 200m, but not much deeper than this depth, whereas the source depth of the harmonic tremor observed by the hydrophone seems to be as deep as 1300m, which is the water depth of the observation site of the hydrophone. It is not clear why the harmonic tremor is not recorded in the OBS. Probably, the T-phase signals are too large due to the low attenuation of the sound wave propagating through the underwater channel. The observation results explained above is extremely important for establishing the observation plan of the remote island volcano monitoring system.

Keywords: Nishinoshima, Volcanic activity, Hydrophone observation



## Multi-parametric observation for assessing activity of Nishinoshima volcano

\*Mie Ichihara<sup>1</sup>, Masanao Shinohara<sup>1</sup>, Kiwamu Nishida<sup>1</sup>, Shin'ichi Sakai<sup>1</sup>, Tomoaki Yamada<sup>1</sup>, Minoru Takeo<sup>1</sup>, Hiroko Sugioka<sup>5</sup>, Yozo Hamano<sup>2</sup>, Yutaka Nagaoka<sup>3</sup>, Akimichi Takagi<sup>3</sup>, Taisei Morishita<sup>4</sup>, Azusa Nishizawa<sup>4</sup>

1.Earthquake Research Institute, University of Tokyo, 2.JAMSTEC, 3.JMA, Meteorological Research Institute, 4.Japan Coast Guard, 5.Kobe University

Nishinoshima started eruptive activity in November, 2013, and a new island is created. Few observation data are available to assess the eruptive activity at such a remote island. This study is intended to get more information of the volcanic activity at Nishinoshima and to develop methods for monitoring remote island volcanoes. We conducted continuous recordings of infrasound at the nearest accessible island and of seismic waves with OBSs around Nishinoshima. We also took movies and infrasonic data during the installation of the OBSs. Here we report the results.

**Observation:**

The continuous infrasonic observation is conducted at Chichijima island about 130 km east of Nishinoshima. An infrasonic array has been operated offline since April 26, 2014, and another online station was added on October 5, 2014. An automatic analysis is run once a day to detect infrasound from Nishinoshima using data from the online infrasonic station and a nearby seismic station operated by JMA. The offline array data is used for more detailed analyses. Ray-tracing for infrasound propagation from Nishinoshima to the stations is conducted using the atmospheric data measured at Chichijima observatory of JMA. The result is used to evaluate the atmospheric effect. Five OBSs were installed around Nishinoshima on February 27-28, 2015, during the KR15-03 cruise of R/V KAIREI (JAMSTEC), and retrieved on October 3-4 during the KS15-07 cruise of R/V KEIFU (JMA). The first OBS station (NI11) was installed about 13 km to the south-east of Nishinoshima. Then in the afternoon of February 27, the boat stayed to the east of Nishinoshima in the distance about 6 km, and the movies and infrasonic data were recorded. The other 4 OBS stations (NI21-NI51) were installed afterward around Nishinoshima in the distance about 7 km.

**Results:**

The movies are compared with the infrasonic data recorded on the boat and the seismic data recorded at NI11. The times of the infrasonic and seismic data are shifted forward considering the propagation time. The signals associated with eruptions are clear in the 1-7 Hz band of the infrasound and in the 4-8 Hz band in the seismic data. The movies show that ash emission occurs intermittently with a cluster of successive small explosions. The individual explosions generate impulsive infrasound and a spindle-shape seismic wave packet is observed associated with the ash emission.

The continuous data of the five OBSs from February 28 to October 3, is used to analyze the spindle-shape wave packets. The epicenters are estimated using the travel time differences for 15 events that occurred on February 28, and are determined around Nishinoshima. Such events are automatically detected by the STA/LTA method, and 363367 events are counted in the period. The occurrence changes in the mid July: the daily number starts decreasing and the duration of an event starts increasing. The maximum amplitude in an hour is small in March, grows from April to May, and then decreases. It seems growing again after the mid July.

The ray-tracing calculation shows that the atmospheric structure is good for the infrasound propagation only until the beginning of April, 2015. Few rays reach the station after June, and the change in mid July is not detectable, if any. In the latter half of May, there are some days when the atmospheric conditions allow the infrasound propagation to the station, but no signal is

detected. According to the OBS observation, Nishinoshima is seismically active in the period, as mentioned above.

The remote infrasonic observation can provide us with some information of the volcanic activity, but the atmospheric conditions do not always allow infrasound to reach the station from the volcano. Observation with OBSs installed close to the volcano is important. If we can at least obtain the results of such event analyses as presented above, the OBS observation would make a useful monitoring method.

Keywords: Volcano, Monitoring, Infrasound, OBS

## Volcanic activity of the Nishinoshima volcano detected by ocean bottom seismometers and remote sensing observations

\*Akimichi Takagi<sup>1</sup>, Yutaka Nagaoka<sup>1</sup>, Azusa Nishizawa<sup>2</sup>, Tomozo Ono<sup>2</sup>, Kenji Nakata<sup>3</sup>, Kazuhiro Kimura<sup>3</sup>, Keiichi Fukui<sup>1</sup>, Shinobu Ando<sup>3</sup>, Hiroaki Tsuchiyama<sup>4</sup>

1.Volcanology Research Department, Meteorological Research Institute, 2.Hydrographic and Oceanographic Department, Japan Coast Guard, 3.Seismology and Tsunami Research Department, Meteorological Research Institute, 4.Seismology and Volcanology Department, Japan Meteorological Agency

In order to detect seismic activity of the Nishinoshima Island volcano which continues to eruptions actively, the network of self-popup-type ocean-bottom seismometers (OBS) was deployed around the island by the Meteorological Research Institute. We report the brief summary of the seismic activity of Nishinoshima with reference to other remote sensing observations.

Five observation devices which have one three-component seismometer and one hydrophone were installed 4 - 5 km far from the center of Nishinoshima Island, and recorded seismic activity from June 12 to October 2, 2015. This observation revealed that micro-earthquake activity around Nishinoshima volcano was so active. Many micro earthquakes were estimated to be  $M -1 - 0$ . Duration time of waveform is around 30 seconds, and envelope of waveform is spindle shape without clear P and S phases. Initial part of waveform has high-frequency component. In later part, the low-frequency component is dominant. Hourly number of recorded waveform was 50 - 100 during the period of OBS. The number of waveforms was around 100 in June, 2015. But seismicity began to weaken in August, and then the number reached to 40 per hour in October. Amplitude of waveform has reached a large size gradually.

The gradual decrease trend of seismicity was consistent with variance of brightness temperature monitored by JMA's geostationary meteorological satellite Himawari-8 (JMA, 2016). In addition, though  $SO_2$  flux in volcanic plume was measured to be 900 ton per day in May, 2015 by the Differential Optical Absorption Spectroscopy (DOAS), decreased to 400 ton per day in October, 2015. Moreover, heat flux of plume by optical sensor on the artificial satellite has decreased, and also incoherent area of the volcanic island by satellite SAR has decreased. So the gradual decrease trend of seismicity must have been synchronized to thermal and gas-emission activity in Nishinoshima volcano.

Another OBS network had been deployed around Nishinoshima from June 25 to July 5, 2015 by Japan Coast Guard (JCG). OBS station St5, located 8 km south far from Nishinoshima, detected active seismic swarms of monochromatic earthquakes. These waveforms have steep dominant frequency of 9 - 10Hz, and decays slowly. All of waveform oscillations have same direction, and b value, estimated from frequency distribution of seismic scale, was calculated to be 1.3. St5, recorded these waveforms, was located near submarine volcano Nishinoshima-Minami Knoll. Around this area, discolored seawater and/or thermal anomaly were observed until now. Therefore this monochromatic-earthquakes swarm may have been recorded as an original volcanic activity different from Nishinoshima volcano.

### Acknowledgment

Keifu Maru, the marine weather observation ship managed by Global Environment and Marine Department, JMA, was used for installation and pickup of OBS.

Keywords: Nishinoshima, ocean bottom seismometer, monochromatic earthquake, remote sensing

## Development of a monitoring system of remote island volcanoes using an autonomous vehicle of the Wave Glider

\*Hiroko Sugioka<sup>1</sup>, Yozo Hamano<sup>2</sup>, Mie Ichihara<sup>3</sup>, Kiwamu Nishida<sup>3</sup>, Minoru Takeo<sup>3</sup>

1.Kobe University, 2.JAMSTEC, 3.Earthquake Research Institute, University of Tokyo

Nishinoshima is a remote island volcano 1000 km south of Tokyo. On November 20, 2013, a brand new island was born nearby the older Nishinoshima. Over the past two years with continued volcanic activity, it has grown up to 12 times the size of the original island, which is offering us a rare opportunity to study how volcanic island forms and grows.

We develop a remote island volcanic activity monitoring system using an unmanned vehicle of the Wave Glider (WG), manufactured by Liquid Robotics Inc. of California, USA. The WG is designed to go forward using the wave and solar energy without any fuel and is equipped with a satellite communication modem to transmit data message to the land station in real-time. It has led the way to make ocean data collection and communications easier and safer, lower risk and cost, and real-time. In order to investigate the feasibility of the WG for station-keeping operation, we made a long-term deployment in the sea off Miyagi. Based on the detailed analyzing of 5 months navigation data from September to May in 2014, the potential utility of the WG as a sea surface gateway has been confirmed to identify the operating parameters.

In the remote island volcano monitoring system the WG plays roles not only in a satellite relay device but also in a multi-parametric observatory platform with microphones for detecting infrasound waves associated with volcanic eruptions, with hydrophones for detecting acoustic and seismic waves associated with deep volcanic activities, with wave gauges for detecting heave displacements associated with volcano collapse, and with video cameras. We investigated the performance of these sensors except for the wave gauge close to the Nishinoshima volcano during the KR15-03 cruise of R/V KAIREI in February 2015 (Hamano et al., 2016; Ichihara et al. 2016) and obtained extremely important results to establish the remote island volcano monitoring system.

Keywords: island volcanic activity, Nishinoshima, remote monitoring



## Relative hypocenter determination of eruption earthquakes at Stromboli volcano based on a temporal observation in June 2015

\*Shunsuke Sugimura<sup>1</sup>, Takeshi Nishimura<sup>1</sup>, Hiroshi Aoyama<sup>2</sup>, Taishi Yamada<sup>2</sup>, Ryohei Kawaguchi<sup>3</sup>, Takahiro Miwa<sup>3</sup>, Eisuke Fujita<sup>3</sup>, Maurizio Ripepe<sup>4</sup>, Riccardo Genco<sup>4</sup>

1.Graduate School of Science, Tohoku University, 2.Graduate School of Science, Hokkaido University, 3.NIED, 4.University of Florence

Earthquakes associated with eruptions of magma or gases are repeatedly observed with intervals of several or tens of minutes or hours on Strombolian explosions. The source of these earthquakes is likely the source of magma explosions associated with the rapid change of pressure in a conduit. Hypocenter determination of these eruption earthquakes enables us to understand the shape or location of the conduit. However, they generally have obscure onsets of P or S phases, which disable us to use general hypocenter determination methods using arrival times of these phases. In our previous study, we developed a new relative hypocenter determination method using deconvolution and master event method (Sugimura et al., 2015, JpGU, VSJ). Deconvolution filter enables us to automatically obtain higher resolution of the arrival time difference between a master event and a slave event and to separate the arrivals of two or three explosion events occurring in a very short time. In June 2015, we developed a temporal seismic network at Stromboli volcano. In this study, we determine relative hypocenter locations of eruption earthquakes using our method and the temporal observation data.

In the observation, we deployed five short-period seismometers at 200 m-1 km from the crater at Stromboli volcano. To obtain higher accuracy of source locations, we deployed them at west of the crater or the lower altitude than the expected source. The signals were recorded with a sampling frequency of 250Hz (Kinkei System, EDR-X7000) or 200 Hz (Hakusan Kougyou, LS-8800). Observation period was about two days in the beginning of June 2015.

In addition to our data, we analyze the signals obtained by the two permanent broadband seismic stations of Department of Earth Sciences of the University of Florence. In our analysis, we use band pass filter for the signals at 0.2-0.4 Hz. We choose a master event and use deconvolution filter to obtain arrival time differences between the master event and the slave events. We further calculate time differences of the arrival time differences between two stations using cross correlation of the deconvoluted waveforms. This enables us to eliminate origin time differences and to express these time differences as linear functions of the relative source locations from the master event.

We assume ~200 m beneath SW crater for the master event and the wave velocity of 1000 m/s. The result shows that the relative source locations are distributed in the range of ~200m in depth and sub-vertically. In future, we will consider a more possible source location of a master event and compare the source of short-period signals to understand the mechanism of magma explosions in a conduit at Stromboli.

Keywords: hypocenter determination, eruption earthquake, deconvolution, Stromboli volcano

## Seismicity model of volcanic earthquakes for a quantitative assessment of volcanic activity

\*Yuichi Morita<sup>1</sup>

1. Earthquake Research Institute, University of Tokyo

The activity of volcanic earthquakes is one of the well-established indicators of volcanic activities and precursors to volcanic eruptions. An increasing seismicity is often followed by a volcanic eruption (e.g. Mt. Usu 2000, Mt. Ontake 2014 eruptions). The earthquakes are generated not only by the temporal change of stress field that is caused by magma intrusion and/or emplacement (e.g. Izu Oshima 1986, Miyake 2000 eruptions), but also by increasing pore pressure on pre-existing faults caused by upwelling volatiles emitted from magma (e.g. phreatic eruption at Hakone 2015). To utilize the seismicity for quantitative evaluations of volcanic activities, we need to discriminate the effect of pore pressure changes from stress changes. To realize a quantitative evaluation, we need a physical model of seismicity and apply it in real case, and assess the model by comparing the estimated and observed seismicity.

One of the models that can relate stress changes to seismicity is rate and state dependence friction (RSF) law proposed by Dieterich (1994). We have already presented that the seismicity at Izu-Oshima volcano well obey the RSF law under the temporally changing inflations and deflations of the volcanic edifice. To check its validity at other volcanoes, we analyze seismicity around the other volcanoes induced by the 2011 Tohoku great earthquake.

Just after the 2011 Tohoku great earthquake, induced seismicity were appeared around more than 20 volcanoes in Japan. The seismicity increased rapidly and then decreases gradually like the sequence of after-shocks that is well-known as Ohmori's law. We analyzed the seismicity around 3 volcanoes: Nikkoshirane, Hakone and Yake-dake, because many hypocenters were determined by JMA around these volcanoes. At the same time, we estimate stress field around them using GEONET daily position data provided by GIA, Japan. We calculate Coulomb stress from the data and applied it to the RSF law to get an expected seismicity. Then, we compare the expected seismicity to observed one. In this analysis, we suppose that the focal mechanisms of the earthquake swarms are coincide with the expecting ones inferred from the estimated stress field. The great earthquake made a large strain over Japan Islands, and the large after-slip is lasting still now. The earthquake swarm zones are affected by stress rate change as well as stress step generated by the great earthquake. The RSF law can realize the feature and the estimated seismicity well match with the observed one. From this analysis, we can conclude that the RSF law is acceptable model for volcanic earthquake. The parameters of RSF concerning the relation between the stress rate and seismicity are also estimated for each volcano from the decay time of seismicity.

In this presentation, we demonstrate that RSF law is applicable to the seismicity of volcanic earthquakes generated by temporal variations of stress field. The pore pressure change at hypocenter region results in the difference between observed seismicity and estimated one based on RSF law. Therefore, in the case that seismicity is much larger than the estimated one, the effect of the pore pressure is dominant. It represents that of rising volatile affects the fault surface and it is precursor to the eruption. Here, the results for three volcanoes are presented now and further study will be carried out at present.

Acknowledgements: We are grateful to JMA for providing earthquake catalogue, and also to GIA, Japan for providing GEONET data.

Keywords: volcanic earthquake, seismicity, stress response, rate and state dependence friction law

## Fluid properties estimated from frequencies of LP events using the analytical formula for crack resonance frequencies

\*Kimiko Taguchi<sup>1</sup>, Hiroyuki Kumagai<sup>1</sup>, Yuta Maeda<sup>1</sup>

1.Nagoya University Environmental Studies

The crack model has been considered as a model of the resonator at the source of long-period (LP) events, and fluid types and sizes of resonators are estimated by comparison between peak frequencies of the observed LP events and resonance frequencies of the crack model by numerical simulations. However, numerical simulations required an extensive computational time, which prevented the systematic comparison to identify the oscillation modes of observed peak frequencies. Therefore, it was difficult to constrain all parameters of the crack model. Recently, Maeda and Kumagai (GRL, 2013) proposed an analytical formula for the resonance frequencies of the crack model, and this formula enables the comparison in a simple and systematic way. In this study, we investigated the resonance modes of peak frequencies of the observed LP events based on the analytical formula to estimate the crack model parameters. We analyzed observed LP events with the method described below. (1) First, we take the ratio of the resonance frequencies calculated by the analytical formula. We vary the assumed mode in the denominator of the ratio from the lowest mode to higher mode. Then, this ratio is expressed by three parameters of the crack model,  $m$  (the oscillation mode in the numerator of the ratio),  $W/L$  (the ratio of crack width to length), and  $C$  (crack stiffness). Here,  $C$  is expressed as  $C = 3(a/\alpha)^2(\rho_f/\rho_s)(L/d)$ , where  $a$  is the sound speed of the fluid in the crack,  $\alpha$  is the  $P$  wave velocity of the solid,  $\rho_f$  and  $\rho_s$  are the densities of the fluid and solid, respectively, and  $d$  is the aperture of the crack. Next, we take the ratio of observed peak frequencies to the lowest one. By comparison of the frequency ratio between the analytical and observed ones varying the assumed mode in the denominator and  $W/L$  systematically, we estimate  $W/L$  and  $C$  that best explain the observed peak frequencies successively from the lowest one. (2) It is known that  $Q$  factor of the crack model strongly depends on  $\alpha/a$  (Kumagai and Chouet, JGR, 2000). So we estimate  $\alpha/a$  by comparison between synthetic and observed waveforms based on numerical simulations of the crack model. We analyzed two LP events based on the step (1) (2). These LP events were observed at Kusatsu-Shirane volcano on 11 August and 2 November 1992. Here we refer to the events on 11 August and 2 November as the events 1 and 2, respectively. We first analyzed the event 1, and four observed peak frequencies were explained. Then we found that the fluid in the crack was explained by a misty gas, and all parameters of the crack model were estimated. We analyzed the event 2 in the same way, and we found that the fluid in the crack was also a misty gas but the crack size was larger than that of the event 1. These results suggest that water vapor was supplied to the crack in an aquifer system by outgassing from magma, then water vapor was cooled to saturation temperature, so the crack was filled with a misty gas. The difference of the crack size between the event 1 and the event 2 suggests that the amount of water vapor supplied to the crack in the event 2 was larger than that in the event 1. In the previous study of Kumagai et al. (JGR, 2002), it was difficult to compare observed peak frequencies to resonance frequencies of the crack model, so crack parameters ( $W/L$ ,  $L/d$ ) and oscillation modes were assumed. But the method used in this study enables simple and systematic identification of the modes of observed peak frequencies, and all parameters of the crack model can be constrained.

## Acoustic VLP signals accompanying the continuous ash emission following Vulcanian eruptions

\*Taishi Yamada<sup>1</sup>, Hiroshi Aoyama<sup>1</sup>, Takeshi Nishimura<sup>2</sup>, Masato Iguchi<sup>3</sup>, Muhamad Hendrasto<sup>4</sup>

1.Graduate School of Science, Hokkaido University, 2.Graduate School of Science, Tohoku University, 3.DPRI, Kyoto University, 4.CVGHM

Acoustic observation of active volcanoes has been provided the considerable information to understand the source process of volcano explosions (e.g., Fee and Matoza, 2013). However, Very Long Period (VLP) signals of acoustic wave accompanying volcanic explosions are poorly understood. In 2012–2013, we have conducted broadband seismic and infrasound observations of Vulcanian eruptions at Lokon-Empung volcano in Indonesia. The temporal observation network consists of 4 broadband seismometers (Trillium 40, Nanometrics Inc., 0.025–50 Hz) and an infrasound microphone (SI 102, Haksan Co., 0.05–1500 Hz). About 80 % of observed vulcanian explosions are followed by the continuous ash emissions, which is recognized as the vibration in the seismic and infrasound waveforms. We find a VLP phase at the onset of the vibration in the band pass (0.03–0.1 Hz) vertical displacement waveforms and 0.1 Hz low pass pressure waveform. The apparent propagation velocity of the VLP phase at each station can be explained by the sound velocity near the ground from the vent. Hence, it is regarded that the VLP phase is induced by the acoustic wave accompanying the continuous ash emission. We analyze the broadband seismic data because the signals that have the period longer than 20 s (out of range of the flat pressure response of the microphone) dominate the band pass ground displacement waveforms. Similar VLP signals accompanying the continuous emission following the Vulcanian eruption can be seen in the broadband seismic records at Shinmoedake volcano in Japan in 2011. National research Institute for Earth science and Disaster prevention (NIED) has operated two broadband seismometers (Trillium 240, Nanometrics Inc., 0.004–200 Hz) and two barometers (AP270, Koshin Co.) near the active vent during the period of the activity of Shinmoedake in 2011. Seismic waveforms of Vulcanian eruptions on Jan. 27, 2011 show the explosive signals accompanying the explosion and subsequent tremor induced by the continuous ash emission. Two infrasound microphones operated by Japan Meteorological Association (JMA) also recorded the signals associated with continuous ash emission after the explosion. We see the VLP phase propagating from the vent with the sound velocity accompanying the ash emission in the band pass (0.01–0.05 Hz) vertical displacement waveforms. The pressure change similar to the VLP phase is seen from the filtered (0.01–0.05 Hz) pressure waveforms recorded by the barometers. The maximum amplitude of vertical velocity of the VLP phase at both Lokon-Empung and Shinmoedake is in order of  $10^{-7}$  m/s at 2–5000 m from the vent. The vertical velocity of the ground induced by the pressure change in the atmosphere is given by Ben-Menahem and Singh (1981). If we set the P-wave velocity and density of the ground as 2700 m/s and 2500 kg/m<sup>3</sup> as tentative values, we obtain the pressure change inducing the VLP phase at each station is in order of the  $10^1$  Pa. Since the signals having the wavelength about  $10^3$  m constitutes of the VLP phase, we can assume that the VLP phase can be excited by the point source at the vent and propagates as a linear sound wave. Based on this assumption, we can estimate the rate of mass outflow of the atmosphere (Lighthill, 2001) at the source. With the dry-air density in the atmosphere (1 kg/m<sup>3</sup>), we estimate the mass flow rate of atmosphere in order of the  $10^5$  m<sup>3</sup>/s. Although this estimation includes the effects of the amplification factor of the stations and wind noise, it is consistent to the mass flow rate of Vulcanian eruptions reported by the previous works (e.g., Koyaguchi, 2008). Therefore, the excitation of the VLP phase can be explained by the pressure change accompanying the formation of the ash column. Further investigation of the VLP phase can contribute to understand the dynamics of

the ash column and source process of Vulcanian eruptions.

Keywords: Ash column, Vulcanian eruptions, Infrasound

## Active source seismic experiment in Zao Volcano, Japan

\*Mare Yamamoto<sup>1</sup>, Satoshi Miura<sup>1</sup>, Masahiro Ichiki<sup>1</sup>, Hiroshi Aoyama<sup>2</sup>, Tomoki Tsutsui<sup>3</sup>, Kentaro Emoto<sup>1</sup>, Satoshi Hirahara<sup>1</sup>, Takashi NAKAYAMA<sup>1</sup>, Tatsuya Torimoto<sup>1</sup>, Takao Ohminato<sup>4</sup>, Atsushi Watanabe<sup>4</sup>, Miwako Ando<sup>4</sup>, Yuta Maeda<sup>5</sup>, Takeshi Matsushima<sup>6</sup>, Manami Nakamoto<sup>6</sup>, Rintaro Miyamachi<sup>6</sup>, Takahiro Ohkura<sup>7</sup>, Shin Yoshikawa<sup>7</sup>, Hiroki Miyamachi<sup>8</sup>, Hiroaki Yanagisawa<sup>9</sup>, Shinya Nagato<sup>9</sup>

1.Tohoku University, 2.Hokkaido University, 3.Akita University, 4.University of Tokyo, 5.Nagoya University, 6.Kyushu University, 7.Kyoto University, 8.Kagoshima University, 9.Japan Meteorological Agency

Zao volcano is a Quaternary stratovolcano located in the central part of the volcanic front of the northeastern Japan. The most recent activity of Zao volcano began at ca. 35 ka at the central part of the volcano, and many historic eruptive activities including occurrence of lahar from the crater lake named Okama have been documented. After the occurrence of the 2011 Tohoku Earthquake, the activities of both deep low-frequency earthquakes and shallow long-period events beneath Zao volcano become higher, and it is thus important to reveal the subsurface structure and fluid distribution to prepare against possible future eruptive activities. With this point of view, as a part of MEXT 'Earthquake and Volcano Hazards Observation and Research Program', we conducted an active source experiment in October, 2015.

In the experiment, 132 temporal seismic stations were deployed on and around the volcano by 21 researchers from 8 universities and JMA, and seismic waves excited by two underground dynamite shots whose charges were 200 kg and 300 kg were recorded at a sampling frequency of 500 Hz. The configuration of seismic network was designed for refraction and fan-shooting analyses. In addition to these underground shots, to enhance the resolution of shallowmost structure, we also utilized a dynamite shot at a nearby quarrying plant, which generate surface waves suitable for the surface wave dispersion analysis.

As the first step of our analysis, we manually pick the arrival time of first onset at each station, and estimate velocity and depth of the basement layer by analyzing the obtained travel-time curves. By applying the time-term method, the P wave velocity of the basement is estimated as 5.2-5.5 km/s. An interesting point of this analysis is that the depth of the basement is quite shallow and at a depth of around 0.5 km from the ground surface. Although the uncertainty of this depth is still remaining, the result of surface wave dispersion analysis also supports the existence of basement at a shallow depth. We then apply the fan-shooting analysis to elucidate the distribution and extent of shallow hydrothermal system. From this analysis, we reveal that an attenuative zone seems to exist beneath slightly northeast of Okama at a depth of around 1 km.

In the previous studies, the subsurface structure of Zao volcano has been discussed mainly based on the geological observations. The results of the active seismic experiment such as the existence of shallow basement are consistent with these previous studies, and provide more detailed images of the subsurface structure beneath the volcano. Further studies including the relocation of volcanic earthquakes and elucidation of hydrothermal system may contribute to a better understanding of volcanic activities at Zao volcano.

Keywords: Zao Volcano, Active seismic experiment, Volcanic structure

## Estimation of the low velocity region beneath Mt. Fuji revealed by inversion of receiver functions

\*Sawako Kinoshita<sup>1</sup>, Kiwamu Nishida<sup>1</sup>, Toshihiro Igarashi<sup>1</sup>, Yosuke Aoki<sup>1</sup>, Minoru Takeo<sup>1</sup>, Hideki Ueda<sup>2</sup>

1.Earthquake Research Institute, University of Tokyo, 2.National Research Institute for Earth Science and Disaster Prevention

Mt. Fuji, the largest stratovolcano in central Japan, has ejected a huge amount of basaltic products during the last 100,000 years. Although the reason for this high eruptive rate has not been well understood yet, a complicated tectonic setting is likely to be responsible for this uniqueness. Because the Izu-Bonin-Mariana arc (IBM) with a thickened crust is colliding and subducting below the Eurasian and Okhotsk plates around Mt. Fuji, a generic magma plumbing model for arc volcanoes is not readily applicable.

In this study, we conduct a receiver function (RF) analysis to investigate the seismic structure around Mt. Fuji including the distributions of the subducting IBM and the magma chamber below Mt. Fuji.

Cross sections of radial RF amplitudes reveal distinct positive velocity boundaries at depths of 40–60 km and 20–30 km around Mt. Fuji. We interpret the velocity boundary at 40–60 km depth as the lower boundary of the crust of IBM and that at 20–30 km depth as the lower boundary of the magma chamber of Mt. Fuji. Also, the velocity boundary representing the lower boundary of IBM crust does not continue just below Mt. Fuji at a depth of about 50 km, representing a locally weakened velocity contrast.

Next, we conducted an inversion analysis of receiver functions to investigate absolute S-wave velocities around Mt. Fuji, because the thick volcanic sediment layer and low velocity layers below Mt. Fuji change the amplitude of radial RFs. In RF inversions, there is a trade-off between the depth of the velocity boundary and the average velocity over the boundary, so we constrained results of the inversion by inverting receiver functions and dispersion curves of surface waves together. Our results are characterized by the following three features: 1) The north-south cross section of absolute velocities reveals that the width of IBM crust is developed down to a depth about 40 km. 2) Subducting oceanic crust, about 30–100 km to the southwest and 60–100 km to the northeast of Mt. Fuji, is represented by a low velocity body. 3) A distinct low velocity region exists below Mt. Fuji with a width of 40 km in horizontal direction and 20 km width in vertical direction, representing a crustal magma chamber of Mt. Fuji.

Our findings suggest that 1) Mt. Fuji has ejected mostly basaltic rocks because the crustal magma chamber is deep, and 2) an anomalously high eruption rate of Mt Fuji is because it hosts a large crustal magma chamber.

Keywords: Mt. Fuji, Receiver functions, Izu-Bonin-Mariana arc



## Characteristics of seismic velocity changes on volcanoes using noise correlation method: Analyses of JMA seismic data

\*Tomoya Takano<sup>1</sup>, Takeshi Nishimura<sup>1</sup>, Hisashi Nakahara<sup>1</sup>

1. Graduate School of Science, Tohoku University

Temporal changes of seismic velocity have been detected associated with the occurrence of large earthquakes and volcanic activities. The velocity changes are estimated to be about 0.1 ~ a few %. At active volcanoes, such seismic velocity changes are interpreted to be caused by the magma intrusion. To estimate seismic velocity changes preceding eruptions, it is important to examine the characteristic of seismic velocity changes during time periods having no volcanic activities. Therefore, we systematically investigate the characteristic of seismic velocity changes by applying seismic interferometry to ambient noise recorded at active volcanoes in Japan.

We estimate seismic velocity changes using continuous records of short period seismometers by Japan Meteorological Agency (JMA). We analyze 12 volcanoes which are observed by more than two seismometers and more than three GNSS stations: Hokkaido-Koma, Meakandake, Tokachidake, Tarumasan, Adatarayama, Nasudake, Kusatsu-Shirane, Izuoshima, Miyakejima, Unzendake, Bandaisan, and Sakurajima. We use data from 2012 to 2013. Distances between stations are within about 5 km, and the number of station pairs ranges from 1 to 45 at each volcano. The seismic data are first filtered at 0.5-1Hz, 1-2Hz, and 2-4Hz, and cross correlation functions (CCF) of ambient seismic noise are then calculated. Daily seismic velocity changes are estimated by comparing each 1-day stacked CCF with a whole period stacked CCF as a reference based on MWCS method (Poupinet et al., 1984).

We recognize annual or a few monthly seismic velocity changes with amplitudes of about 1 ~ 3 %. The seismic velocity change largely even when there is no volcanic activity or earthquake. Correlation coefficients of velocity changes between each station pair at Izuoshima and Miyakejima and Tarumasan are high in the 1-2 Hz, however coefficients of other volcanoes are less than 0.5. The result implies that there would be localized velocity changes within the limits of a few kilometers in many volcanoes. We also compare seismic velocity changes between the three frequency bands for the same station pair. At a few volcanoes, the amplitudes of seismic velocity change are different between frequency bands while time series of velocity changes are well correlated. At the other volcanoes, trends or phases of seismic velocity changes are different. These results suggest changes of seismic velocity with depth or complex wave properties of ambient noise.

We investigate the relationship between seismic velocity changes and strain changes at each volcano because some studies reported velocity changes associated with stress changes. We estimate areal strain changes using three GNSS stations operated by JMA. We analyze the data with areal strain amplitudes of more than  $2 \times 10^{-6}$  and those of less than  $-2 \times 10^{-6}$  considering measurement errors. We calculate the correlation coefficient between seismic velocity changes and areal strain changes using only time periods when the areal strain exceed the maximum shear strain. The high correlation coefficient between areal strain and seismic velocity changes are estimated at Izuoshima and Tarumasan. However, it doesn't appear that seismic velocity changes correlate with areal strain changes in Tokachidake where irregular patterns are recognized in seismic velocity changes at three frequency bands and at different station pairs.

Seismic velocity changes are estimated to be about 1 ~ 3 % at volcanoes during no eruptive periods. Some stations show the high correlation coefficient between areal strain and seismic velocity changes. We suggest that areal strain changes may affect seismic velocity changes.

Keywords: Seismic velocity changes, Seismic interferometry, Volcano deformation

## Shallow crustal velocity structures obtained from ambient noise study of dense broadband seismic array in the Tatun Volcano Group of Taiwan

\*Yu-Chih Huang<sup>1</sup>, Tsuneomi Kagiya<sup>1</sup>, Cheng-Horng Lin<sup>2,3</sup>

1.Aso Volcanological Laboratory, Institute of Geothermal Sciences, Graduate School of Science, Kyoto University, Kumamoto, Japan, 2.Institute of Earth Sciences, Academia Sinica, Taipei, Taiwan, 3.Taiwan Volcano Observatory at Tatun, Ministry of Science and Technology, Taipei, Taiwan

The Tatun Volcano Group (TVG) is located in the northern tip of Taiwan Island with a radius of 10 km. The TVG situates adjacent to the Taipei metropolis in the north and was predominantly active in the Quaternary period. Shanchiao Fault is an active normal fault transits the TVG in northeastern orientation. A sequence of normal faults and scarps inspected on the hanging wall of Shanchiao Fault and sub-parallel to its orientation in the extent of TVG. Since the major geothermal activities such as fumaroles, solfataras and hot springs also expose on the hanging wall of the Shanchiao Fault, it is thought to be the passage for volcanic-hydrothermal gas and fluid. Besides, Kanchiao Fault is a suspected active fault and known as the important geologic structures adjacent to the southeast of TVG.

The subjects about TVG is already extinct or still active are also under frequent discussion. Attribute to new technological advances and methodologies improvement, various types of observations and experiments were implemented to monitor the activities of TVG in recent years. Basing on the results of these recent researches, various evidence proved that TVG is not extinct, should be a potentially active volcano and cannot exclude the possibility of volcanic eruptions in the future. It is important to understand the magma chamber and detailed velocity structures below the TVG but are still not well resolved. The fundamental theory to obtain S-wave velocity structure from ambient seismic noise analysis has been already proofed and provided important constraints around the world in the past decade. We present the results of ambient seismic noise studies in the TVG with dense seismic monitoring network.

The seismic network in this research is composed with three sub-networks, totally there are 40 free-field seismic stations equipped with Güralp CMG-6TD broadband seismometers and GPS timing system. The interstation distances are between 0.6 km and 28 km, with an average of 8.5 km. The cross-correlation functions (CCFs) were calculated with the methodologies of one-bit cross-correlation and spectral whitening. We selected vertical component to obtain the CCFs in the period band 0.5-7 s for all station-pairs and derived with the selected daily recordings in 2014. The daily CCFs were stacked monthly and then the monthly CCFs were stacked again to further obtain TDEGFs and Rayleigh wave phase velocity dispersion curves. We stacked positive and negative lag times of TDEGF to enhance coherent signals and suppress the effect of uneven seismic noise sources distribution. The maximum period can be measured for each station-pair is related to the inter-station distance and phase velocity. For far-field approximation, the inter-station distance is required to be at least twice of propagating surface wave wavelengths in this study to assure surface wave can well develop between station-pair.

We focus on phase velocity maps in the period band 0.5-3 s in the TVG and the study region is parameterized by  $0.02^{\circ} \times 0.02^{\circ}$  grid points. Phase velocity maps show high velocities are dominate between Shanchiao Fault and Kanchiao Fault at study periods, which maybe relate to the solidified andesite lava. Especially in the south parts of Jinshan area, which locates the earliest stage of volcanic activities in the TVG. At periods longer than 2.5 s, high velocities separate into two major regions beneath the ChiShingShan and south parts of Jinshan area. At periods shorter than 1 s, there are some localized low velocity areas correlate well with the surface geothermal

activities. The regions north (footwall) of Shanchiao Fault show low velocities at the study periods maybe relate to the Tertiary strata already covered by andesite lava flows with dozens of meters thickness. The detailed S-wave velocity structures in the shallow crust will be investigated and searching for possible candidates of magma passages and hydrothermal reservoirs beneath TVG.

Keywords: ambient seismic noise tomography, Tatun Volcano Group, shallow crust

## Monitoring eruption activity using temporal stress changes at Mount Ontake volcano

\*Toshiko Terakawa<sup>1</sup>, Aitaro Kato<sup>1</sup>, Yuta Maeda<sup>1</sup>, Yoshiko Yamanaka<sup>1</sup>, Shinichiro Horikawa<sup>1</sup>, Kenjiro Matsuhira<sup>1</sup>, Takashi OKUDA<sup>1</sup>

1.Earthquake and Volcano Research Center, Graduate School of Environmental Studies, Nagoya University

On 27 September 2014, around 11:52 a.m. JST, Mt. Ontake volcano produced a hydrothermal eruption with a VEI value of 2. We examined temporal changes in the local stress field at Mt. Ontake over a period of 17 months (August 2014 to December 2015) with the 2014 eruption from focal mechanism solutions of 168 volcano-tectonic (VT) events (Terakawa et al., in press). In general, the local stress field around volcanoes represents the superposition of the regional stress field caused by plate motion and stress perturbation related to volcanic activity. The regional stress field does not change over periods of weeks to months, and so temporal stress changes over such time periods are attributed to volcanic activity.

We defined the angular difference between the observed slip vectors and theoretical slip vectors expected from the regional stress field as the misfit angle, based on the concept that seismic slip occurs in the direction of the resolved shear traction acting on a pre-existing fault. The misfit angles larger than the estimation errors of the regional stress field and focal mechanism solutions ( $>65^\circ$ ) mean that the local stress field was deviated from the regional stress field due to enhanced volcanic activity. The average misfit angles remarkably exceeded the threshold value ( $65^\circ$ ) two weeks before the eruption, but immediately after the eruption the values showed a marked decrease. The pre-eruption seismicity was dominated by normal faulting with ENE-WSW tension, indicating that the volcanic activity caused strong tension for the pre-eruption period. On the other hand, many reverse faulting with ESE-WNW compression for the post-eruption period corresponded to shrinkage of the volcanic edifice, controlled by the regional stress field.

The stress perturbation for the pre-eruption period suggests existence of dyke-type volcanic system beneath Mt. Ontake in which inflation is driven by magmatic/hydrothermal fluids propagating upwards in a vertical crack. This is consistent with the distribution of hypocenters of volcanic earthquakes relocated by a DD method (Kato et al., 2015), the alignment of craters from the 2014 eruption (GSI, 2014), and source mechanisms of VLP events prior to the 2007 and 2014 eruptions (Nakamichi et al., 2009, Maeda et al., 2015).

The time history of average misfit angles showed slight enhancements in November 2014, January-February 2015, June-July 2015, and October-December 2015. Especially, the final stage of the enhancement in June-July 2015 was synchronized with an unusual tiltmeter signal indicating summit upheaval. These observations suggest that some re-pressurization/de-pressurization processes repeated after the 2014 eruption. Temporal stress changes revealed in this study were well associated with physical processes at the active volcano. This indicates that the method has potential to contribute to eruption monitoring.

Keywords: Mount Ontake, stress fields, focal mechanism solutions

## Deflation source after the September 2014 eruption of Ontake Volcano, Japan detected by ALOS2/PALSAR2 InSAR

\*Shohei Narita<sup>1</sup>, Makoto MURAKAMI<sup>1</sup>

1. Institute of Seismology and Volcanology, Hokkaido Univ.

### 1. Introduction

On September 27<sup>th</sup>, a phreatic eruption occurred at Mt. Ontake, located on the border between Gifu and Nagano prefectures, central Japan. Preceding this event, the number of VT earthquakes gradually increased from early September, and their source was approaching ground surface during the final 10 minutes before the eruption. Simultaneously, the tilt meter located on the southeast flank recorded a rapid change suggesting inflation of the edifice. The eruption started on new eruptive fissures formed in Jigokudani, where there are many fumaroles and fissures formed in 1977. These activities then exponentially declined.

Multiple observations during the event suggest formation of co-eruptive crack just beneath Jigokudani area. Analysis of VLP event just before the eruption suggested that co-eruptive small crack opened at the depth of 300-1000m beneath the newly formed fissures, and its orientation was approximately east-west (Maeda et al., 2015). ALOS2-InSAR detected co-eruptive ground deformation, revealing that co-eruptive crack aligned along new fissures extends vertically downward from 100m to 1400m (GSI, 2015). On the other hand, deflation around Jigokudani area after the eruption is confirmed by ALOS2 InSAR. The goal of this study is to reveal the source causing the deflation and its relationship to pressure sources during pre and co-eruptive stages of 2014 eruption.

### 2. Data and Results

We processed 3 scenes of ALOS-2 data and computed 3 interferograms spanning 2014/10/03-2015/06/12 (8 month), 2014/10/03-2015/11/13 (13 month), 2015/06/12-2015/11/13 (5 month), respectively. All the interferograms were made from ascending and right looking observations having the same off-nadir angle (32.4°). Coherency of those interferograms is very good. We used RINC 0.36 version developed by Dr. Taku Ozawa at NIED.

In all the interferograms we detected LOS increase in the area of 2kmx1km around Jigokudani. The distance changes in LOS direction mean subsidence, and its maximum values are respectively 45cm in 13 month, 30cm in 8 month, and 12cm in 5 month. To estimate the source parameters causing the deformation, we carried out an inversion using Mogi model, which assumes point source buried in an elastic half-space. The depth of estimated sources is consistently about 400m beneath Jigokudani area. The volume changes are respectively  $3.7 \times 10^5 \text{ m}^3$  in 13 month,  $2.4 \times 10^5 \text{ m}^3$  in 8 month,  $1.1 \times 10^5 \text{ m}^3$  in 5 month.

### 3. Discussions and future challenges

The deflating source estimated in this study are consistently located about 400m below the surface. GNSS campaign observation from August 2005 to May 2007 detected local ground deformation near the summit of Ontake, and revealed that an inflating source was located about 1km under the area of new fissures. Although the depth of these sources location is not same, the horizontal location of the inflating source detected by GNSS is near the south edge of the deflating source in this study. Moreover, InSAR time-series analysis using ALOS-1 data from 2007 to 2010 revealed that there were displacements meaning inflation near the summit of Ontake and its speed was about 1cm/yr. To discuss the relation between these sources, it is necessary for us to track time-dependent ground deformation in detail and to relocate the source in this study with more precise method, i.e. finite element method, considering the topographic effect to the observed displacements.

Acknowledgements: The ALOS2 data were provided by JAXA. We used RINC software ver.0.36 developed by

Dr. Taku Ozawa at NIED. We also used 10m-DEM provided by the GSI.

Keywords: Ontake, phreatic eruption, volcano deformation

## Landform change detected from the airborne laser survey before and after the 2014 Eruption of Ontake Volcano, central Japan

\*Takehiko Suzuki<sup>1</sup>, Koshun Yamaoka<sup>2</sup>, Yoshimichi Senda<sup>3</sup>, Souta Unome<sup>3</sup>

1.Faculty of Urban Environmental Sciences, Tokyo Metropolitan University, 2.Earthquake and Volcano Research Center, Graduate School of Environmental Studies, Nagoya University, 3.Nakanihon Air Service

Reconstruction of landform change before and after the eruption is significant in evaluating influence around the volcano. However, it is commonly impossible to survey the landform change directly just after the beginning of the eruption by difficulties in access to the area close to the crater. So is the case of the 2014 Eruption of the Ontake Volcano, central Japan. This study aims to clarify the following landform changes by the airborne laser survey conducted in 2005, 2014 (after the eruption) and Sept. 5, 2015, such as fall-out of volcanic ashes, volcanic blocks, landform change around crater, and erosion/ deposition caused by volcanic mud flows.

Positive changes in altitude (Ridge of west Kenga-mine: +0.3–+0.6 m: Near the main craters: +10 m) are concordant of thickness of fall-out ashes shown by previous reports, indicating positive changes in altitude were caused by deposition of ashes. Deposition of ashes with a thickness of +8–+10 m along the valleys just in south slope of west Kenga-mine (Upper reach of Jigoku-dani) suggests passing the pyroclastic flow. This is first quantitative estimation of thickness in this area. This thick sediment filling the valley has disappeared by Sept. 2015, showing occurrence of erosion and transportation. Moreover, this erosion is not only removal of deposited ashes at the eruption but also deeper undercutting for former valley bed with a depth of –4––6 m, resulting a tendency of erosion in a long term.

On the west slope of Ichino-ike, an uplifted area with 190 m x 35 m stretching WNW-ESE existed just after the eruption. This was most likely formed associated with W1 Crater of the eruption, and is partly composed of mud flow deposit with a thickness of 2–1 m to the maximum. However, it was disappeared by Sept. 2015, probably by the formation of a gully with EW direction.

The most prominent landform change between 2014 and 2015 are erosion/ deposition along valleys (Upper reaches of Shaku-nanzo, Shira, Aka-Jigokudani, Minami-mata, and Yu Rivers) in a wide area. Depth of erosion are –1––6 m. Beside, positive changes in altitude less than 10 m were recognized in segments with 100 to 500 m long along the Shira and Yu Rivers, indicating depositions. These erosion and deposition are evident in comparison of airborne laser survey data collected in 2015 and 2005, resulting in over undercutting for former valley bed or depositional tendencies in a long term.

We attempted to clarify the distribution of volcanic blocks ejected at the 2014 eruption. However, it was difficult due to precision of data.

Keywords: Airborne laser survey, 2014 Eruption of Ontake Volcano, Landform change



## The September 14, 2015 phreatomagmatic eruption of Nakadake crater, Aso Volcano, Japan and its deposits

\*Yasuo Miyabuchi<sup>1</sup>, Chihoko Hara<sup>1</sup>, Yoshiyuki Iizuka<sup>2</sup>, Akihiko Yokoo<sup>3</sup>

1.Faculty of Education, Kumamoto University, 2.Institute of Earth Sciences, Academia Sinica,  
3.Graduate School of Science, Kyoto University

Following the November 2014-May 2015 magmatic activity including ash and strombolian eruptions, an explosive eruption occurred at Nakadake first crater, Aso Volcano in central Kyushu, southwestern Japan, on September 14, 2015. We performed fieldwork for observing and sampling of the related deposits in the proximal and distal areas immediately after the eruption. Based on these field observations, the eruption deposits were divided into ballistics, pyroclastic density current and ash-fall deposits.

A large number of ballistic clasts was scattered within about 500 m from the center of Nakadake first crater. Although the largest clast with a diameter of 1.6 m existed at the southwestern crater rim, most of ballistic clasts were less than 10 cm in diameter. We sampled all ballistic clasts from an area of 3.5 m<sup>2</sup> at the southwestern rim of Nakadake first crater. The total number of ballistic clasts deposited on the area was 158. Almost half of the ballistics appeared as fresh and unaltered basaltic andesite rocks interpreted to be derived from a fresh batch of magma, while the rest was weakly to highly altered clasts. An area of 2.3 km<sup>2</sup> was covered by a relatively thin ash interpreted to be derived from pyroclastic density currents (PDCs). The deposits were distributed with the SE-trending main axis and two minor axes of the NE and NW. The maximum thickness was less than 10 cm at the crater rim and the PDC deposits were wholly fine grained beds containing no block-sized clasts. Based on the isopach map, the mass of the PDC deposits was estimated at ca. 52,000 tons. The ash-fall deposit was finer grained and was clearly distributed about 8 km to the west of the source crater. The mass of the ash-fall deposit was calculated at about 27,000 tons. Adding the mass of the PDC deposits, the total eruptive mass of the September 14, 2015 event was 79,000 tons.

The polarizing microscope observations revealed that all samples of the September 14 deposits consisted of glass shards (20-30 %), crystal and lithic (40-50 %) grains. Most glass shards were unaltered poorly crystallized pale brown glasses which probably represented juvenile magma. Results of EPMA analysis indicate that chemical composition of glass shards included in the September 14 deposits were similar to those of glasses in the 1979, 1989-1990 and November 2014-May 2015 ash. These evidences including video footages suggest that the September 14, 2015 eruption of Nakadake first crater was phreatomagmatic origin. Similar phreatomagmatic eruptions occurred at Nakadake on September 6, 1979 and April 20, 1990 whose eruptive masses were one order larger than that of September 14, 2015 eruption. These eruptions impose a great hazard for areas within 1-2 km of the active Nakadake crater, yet efficiently impossible to predict due to the lack of any precursors.

Keywords: phreatomagmatic eruption, ballistic clasts, pyroclastic density current, Aso Volcano, Nakadake

## Fine sediment discharge after Sep. 14, 2015 Eruption in Aso volcano

\*Masayuki Sakagami<sup>1</sup>, Masaru Kunitomo<sup>1</sup>, Yamato Suzuki<sup>1</sup>

1.National Institute for Land and Infrastructure Management

Nakadake 1st Crater of Aso Volcano in southern Japan erupted on the 14<sup>th</sup> of September in 2015 where a phreatomagmatic eruptions was occurred and pyroclastic flow was observed, which distributed fine ash deposit around the crater. It is known that fine volcanic ash inducing the infiltration rate lowering, and causes disaster of lahar. Every volcanic eruption, however, may not result in lahar. Therefore, certain criteria is required to evaluate the possibility of a lahar. Survey of sediment deposition was performed three times after the eruption, and particle size was analyzed on the collected samples. In the watersheds around the Nakadake crater, gray mud deposit was detected coating the layer of black volcanic sand. These gray mud deposit consisted of fine particles was not observed at the previous three eruptions between 2014 and 2015. In this presentation, summaries of these observation results will be introduced.

Keywords: Aso-Nakadake Volcano, Lahar, Phreatomagmatic eruption, Pyroclastic flow

## Variation of fumarolic gas composition along the volcanic activity of Mt Hakone, Japan

\*Takeshi Ohba<sup>1</sup>, Muga Yaguchi<sup>1</sup>, Ken Ishida<sup>1</sup>, Soichiro Kumehara<sup>1</sup>, Masahiro Yamagishi<sup>1</sup>, Yasushi Daita<sup>2</sup>

1.Department of chemistry, School of Science, Tokai University, 2.Hot Spring Res. Inst. Kanagawa Pref.

The driving force of eruption is the degassing of magma or the explosion of hydrothermal reservoir. The volcanic gas contains the component originating in the degassing magma or the hydrothermal reservoir. Therefore, the volcanic gas is essentially important object for the understanding of eruption and the eruptive prediction.

At Mt Hakone, the swarm of volcanic earthquakes has been observed previously. For example, in 2001 the swarm of volcanic earthquakes was observed with the deformation of volcanic body suggesting a pressure source the depth of which was estimated to be 7km (Daita et al, 2009). In parallel to the swarm of earthquakes, the steam pressure in the borehole located in the geothermal area of Owakudani significantly increased. On 26th April 2015, a swarm of volcanic earthquake has started. On 30th June, a small steam eruption took place in the Owakudani geothermal area, which is the first historical eruption at Mt Hakone. The number of earthquake quickly decreased until September of 2015.

### Sampling and analysis of fumarolic gas

The Owakudani geothermal area is developed on Mt Kamiyama, one of the central cones of Hakone caldera. The fumarolic gases have been sampled and analyzed at two outlets in Owakudani geothermal area almost every month since May 2013 to Feb 2016. One fumarolic gas (T) is located near the parking of Owakudani geothermal area. Another fumarolic gas (S) is located on the north flank of Mt Kamiyama, 500m far from the fumarole T. The temperature of gas at the outlets was about 96°C, which is close to the boiling temperature of the altitude of the fumaroles. The fumarole T associates the discharge of hot spring water. The fumarolic gas was sampled in the evacuated glass bottle containing 20ml of 5M KOH solution. For the determination of SO<sub>2</sub>/H<sub>2</sub>S ratio, KI<sub>2</sub>-KI solution was reacted with fumarolic gas at the sampling site. For the sampling of condensed water of gas, a double glass tube was used for cooler. The solution in the evacuated glass bottle was analyzed along the method by Ozawa (1968) to determine the amount of H<sub>2</sub>O, CO<sub>2</sub>, total S (=H<sub>2</sub>S + SO<sub>2</sub>) and R-gas. The R-gas was analyzed by GC with Ar and He carrier gases to determine the relative concentration of He, H<sub>2</sub>, O<sub>2</sub>, N<sub>2</sub>, CH<sub>4</sub> and Ar. The isotopic ratio of condensed water was determined by use of an IR-laser cavity ring down analyzer (Picarro).

### Result and Discussion

Prior to the small steam eruption on 30th June 2015, definite changes were detected in the composition of fumarolic gas-T. The isotope ratio of H<sub>2</sub>O (δD) was -51 per mill in Jan 2015. It decreased to -67 per mill on 24th April which was 2 days before the start of earthquake swarm. After the start of earthquake swarm, it increased to -56 per mill on 8th May. Similar to the above change, He/N<sub>2</sub> ratio showed precursory change. The ratio was 3.3×10<sup>-4</sup> in Dec 2014, followed by the decrease down to 1.1×10<sup>-5</sup> on 24th April 2015. The ratio came back to 2.8×10<sup>-4</sup> on 8th May. The changes in δD and He/N<sub>2</sub> ratio suggest the suppressed supply of magmatic H<sub>2</sub>O into the shallow hydrothermal system. The suppression might be brought by the development of sealing zone surrounding the degassing magma. The sealing zone is a structure in crust where hydrothermal secondary minerals, such as silica, pyrite, alunite, anhydrite, deposit within the channel of fluid. The deposition of those minerals seals the channel by themselves. If the sealing is complete, the degassing fluid is stored within the sealing zone. The break of the sealing zone episodically injects the magmatic fluid to the shallow hydrothermal system. The increase of fluid

pressure after the injection induced the earthquake swarm stated on 26th April 2015.

#### Acknowledgments

This study was supported by the Ministry of Education, Culture, Sports, Science and Technology (MEXT) of Japan, under its Earthquake and Volcano Hazards Observation and Research Program.

Keywords: Volcanic gas, Mt Hakone, Magma

## Multi-GAS measurements at Mt.Tokachidake

\*Risa Okamoto<sup>1</sup>, Takeshi Hashimoto<sup>1</sup>

1.Institute of Seismology and Volcanology, Graduate School of Science, Hokkaido University

**Introduction:** The composition and flux of volcanic gases and those temporal changes are clues to understand degassing processes and their relevant structure below volcanoes.. The system so-called "Multi-GAS" device that consists of several gas sensors has been used to measure the chemical composition of volcanic gases on site (Shinohara, 2005). For the same purpose we started measuring volcanic gases at Mt. Tokachidake and Mt.Tarumae in 2014 using separate portable gas sensors of three kinds. We so far verified that even such a combination of off-the-shelf devices was able to provide reliable results, when applied to the plume with sufficient concentrations (Okamoto, 2015: JpGU).

At Mt.Tokachidake, localized ground inflation near 62-2 crater was detected since 2006 from GNSS by JMA and GSH. During May to August in 2015, further localized acceleration in ground deformation as well as the changes in thermal activity around the crater were found. For example, the fumarolic area called Furikozawa at the south of 62-2 crater extended eastward, whereas the bubbling in the hot ponds was seen at the bottom of 62-2 crater. We repeated our Multi-GAS measurements at Mt. Tokachidake in July and September in 2015 to monitor the temporal changes in gas chemistry associated with the recent volcanic activity.

**Field operation:** In this study, we used three separate gas sensors ( $\text{SO}_2$ ,  $\text{H}_2\text{S}$  and  $\text{CO}_2$ ). The detection range of each sensor was 0-100 ppm for  $\text{SO}_2$ , 0-100 ppm for  $\text{H}_2\text{S}$ , 0-9999 ppm for  $\text{CO}_2$ . The resolution was 1ppm for  $\text{SO}_2$ , 0.1ppm for  $\text{H}_2\text{S}$ , 1ppm for  $\text{CO}_2$ . The response time of the  $\text{CO}_2$  sensor was approximately one minute, which was considerably longer than the  $\text{H}_2\text{S}$ ,  $\text{SO}_2$  sensors. For this reason, we walked slowly in the plumes flowing on the crater rims, and took one-minute moving average on the time series of  $\text{H}_2\text{S}$  and  $\text{SO}_2$  in order to match them to the  $\text{CO}_2$  sensor with the longest time constant. Afterwards, cross-sensitivity between  $\text{H}_2\text{S}$  and  $\text{SO}_2$  sensors was calibrated and corrected. At Taisho-vent, due to the prevailing wind and topographic constraint, the plumes were flowing just on the rim. Therefore, we also profiled the gas concentrations to obtain the gas flux.

**Results:** We measured the plumes from Taisho-vent, 62-2 creator and Furikozawa fumarolic area in July and September in 2015. We obtained almost the same results between the two measurements. Molar ratios between compositions were estimated from the linear trends on the scatter plots as  $\text{SO}_2/\text{H}_2\text{S} \sim 6$ ,  $\text{CO}_2/\text{H}_2\text{S} \sim 5$  and  $\text{CO}_2/\text{SO}_2 \sim 1$  at Taisho-vent,  $\text{CO}_2/\text{SO}_2 \sim 0.5$  at 62-2 crater, and  $\text{CO}_2/\text{SO}_2 \sim 0.4$  at Furikozawa fumarolic area. Unlike the result from Taisho-vent,  $\text{H}_2\text{S}$  concentrations at 62-2 crater and Furikozawa fumarolic area were close to the detection limit. The  $\text{SO}_2$  emission rate was estimated as 6 to 7 t/d. These results were not significantly different from the measurement in 2014 and thus we considered that no essential change in degassing processes took place during this period. Meanwhile, total  $\text{SO}_2$  flux (based on the DOAS method) from the crater area in 2015 was reported as 100 to 200 t/d by JMA, which was almost double amount of the flux in 2014. Accordingly, it is likely that most of the  $\text{SO}_2$  flux in 2015 was the contribution from 62-2 crater and from the activation of Furikozawa fumaroles. Regarding the difference in gas component between Taisho-vent and others, we have not yet reached any consistent model that can explain all the results above, although we speculate some contribution of the shallow hydrothermal system beneath the crater area.

Keywords: Mt.Tokachidake, volcanic gas

## Improvement of the realtime volcano observation system based on the satellite infrared imagery and its application to the case of the 2015 Mt Raung eruption

\*Takayuki Kaneko<sup>1</sup>, ATSUSHI YASUDA<sup>1</sup>, Martin J. Wooster<sup>2</sup>, Fukashi Maeno<sup>1</sup>

1.Earthquake Research Institute, University of Tokyo, 2.King's College London

We are monitoring active volcanoes in east Asia using MODIS and MTSAT images. From 2015 through 2017, Japanese new optical satellites, Himawari-8/AHI and GCOM-C/SGLI start operation, which are next generation instruments of the ones we are currently using for monitoring. We plan to replace the MODIS-based realtime thermal monitoring system to a combination system consisting of Himawari-8/AHI and GCOM-C/SGLI. Further, for more precise non-realtime analysis, we also plan to use high-resolution images, in linkage with these two realtime datasets - combined analysis. The new type of Himawari, carrying the AHI sensor, can be used for thermal analysis, because of the improved resolution to be 2km. Also, its ultra-high frequency observation, every 10 minutes, will be particularly useful for thermal analysis of eruption sequences, which can change in a short period. We recently developed a prototype of realtime monitoring system based on Himawari-8/AHI. SGLI onboard GCOM-C is a moderate resolution sensor having resolution of 250m in the 1.6um and 11um channels. The satellite is being launched at the end of 2016 by JAXA. SGLI can be applied for more precise realtime monitoring than MODIS having resolution of 1 km, such as observing enlargement process of lava flows. Here, in non-realtime analysis, high-resolution images are used for specifying topographic change or type and distribution of erupted materials relating to the on-going eruptive process, which cannot be identified by the medium to coarse resolution images. In order to examine effectiveness of the combined analysis based on the three different datasets, we analyzed the 2015 eruption of Raung, as a test case.

Mt Raung, one of the most active volcanoes in Indonesia, is located in the easternmost of Java, Indonesia and has a large conical edifice with altitude of 3320 m. It has a summit caldera of 2km in diameter approximately 300 m in depth, of which topography is similar to the of Miyakejima formed in 2000. In June, 2015, the volcano erupted and lava continued to effuse in the summit caldera from the pyroclastic cone at the center of the floor. Analysis of high-resolution images (Landsat, SPOT, WV and GE) showed that the effused lava enlarged gradually and covered the entire areas of the caldera floor by the middle of July. At the same time, the accumulated lava bed increased in thickness. The total volume of effused lava and the average effusion rate were estimated to be  $5.3 \times 10^7 \text{ m}^3$  and  $1.1 \times 10^6 \text{ m}^3/\text{day}$ , respectively. We also analyzed Himawari-8/AHI images between 1st of June to 31st of August. The time series variations of thermal anomaly (1.6 um, 2.3 um, 3.9 um) showed that there were two pulses in the activity - Pulse I and II, which were divided by a low activity period at the end of July. Through examining the short term variations, we found that the eruption started at 4:30 on 20th of June (UTC) and ceased on 7th of August. Reactivation of the activity, i.e., start of Pulse II, occurred at 21:10 on 1st of August. The activity level was nearly constant through the majority of the period, which can be considered as a characteristic of the effusive eruption involving Strombolian lava fountaining. Several hours ahead of the onset of Pulse II, a small thermal pulse was observed. This can be a precursor to reactivation of the activity. In substitution for SGLI images, NPOSS/VIIRS images (resolution 380m) were analyzed to observe enlargement process of the lava bed on the caldera floor. We could recognize increase in the size of high-temperature areas at the summit on the 11 um images of VIIRS in the period from late June to early July. This is probably showing enlargement of the lava bed on the caldera floor. This result suggests that we can monitor detailed eruptive phenomena by using SGLI images in realtime. Also, the combined analysis proposed here is considered as a useful method for exploring

eruption sequence.

Keywords: satellite remote sensing, indrared imagery, Indonesia

## Estimating the total mass of tephra from radar echo-top height of eruption column

\*Keiichi Fukui<sup>1</sup>, Eiichi Sato<sup>1</sup>, Toshiki Shimbori<sup>1</sup>, Kensuke Ishii<sup>1</sup>

1.Meteorological Research Institute

We estimated the total mass of tephra from the time series of echo-top height of eruption cloud detected by the Japan Meteorological Agency radar network. We discussed the relation between the total mass of tephra evaluated by field survey and the total mass estimated from the radar data, and discussed the error in the total mass estimation.

Keywords: total mass of tephra, weather radar, radar echo-top height, eruption column height, estimation of eruptive mass, volcanic ash cloud



The morphology and effusion rate of deep submarine silicic lava flows and domes emplaced during the Havre 2012 eruption, Kermadec Arc, New Zealand

\*Fumihiko Ikegami<sup>1</sup>, Rebecca J Carey<sup>1</sup>, Jocelyn McPhie<sup>1</sup>, Adam Soule<sup>2</sup>, Kenichiro Tani<sup>3</sup>

1.University of Tasmania, 2.Woods Hole Oceanographic Institution, 3.National Museum of Nature and Science, Japan

## 1. Introduction

The eruption of Havre 2012 was the largest deep submarine silicic eruption in the modern history (Carey et al. 2014). The eruption was first detected by an airline passenger who saw extensive rafts of floating pumice on the ocean. The later investigation identified the onset of pumice dispersion on the 18th July 2012, which was accompanied by a subaerial plume and hotspot on the NASA MODIS satellite imagery. In addition, significant seismicity at the Havre caldera was measured during this time. Three months after the event, R/V Tangaroa of NIWA (National Institute of Water and Atmospheric Research, New Zealand) visited the Havre volcano and mapped the area using a EM120 multibeam system. This survey detected several new features along the caldera rim which did not exist in 2002. However, the resolution of the map did not permit the identification of the types of volcanic features present.

## 2. MESH Cruise

In 2014, the Mapping Exploration & Sampling at Havre (MESH) cruise was conducted to visit the seafloor and performed a geological field study of the 2012 eruption deposits. The R/V Roger Revelle (Scripps Institution for Oceanography, UCSD) and two unmanned vehicles, Sentry AUV (Autonomous Underwater Vehicle), and Jason ROV (Remotely Operated Vehicle) of WHOI (Woods Hole Oceanographic Institute) facilitated the voyage. The Sentry AUV mapped the full area of the 5-km wide Havre caldera with high-resolution bathymetry (1-m grid). The ROV Jason conducted traverses along the eruption products discovered by the Sentry high-resolution map, conducting sampling for the rocks and sediments at the seafloor.

## 3. Results and Discussions

The MESH cruise identified six lava flows (A~D,F,G), eight lava domes (H,I,K~P), two units of ash and lapilli deposits (AL,ABL), two debris avalanche deposit (MF1,2), and an extensively emplaced giant pumice deposit (GP) as the products of the 2012 eruption (Fig. 1). Most of the effusive products which this research focuses on have porphyritic textures with the phenocrysts of plagioclase, and pyroxene. Their whole rock composition ranges from 68~72% SiO<sub>2</sub> and inferred that the Havre 2012 magma was rhyodacitic.

The series of lava consists of both lava flows (length of 0.6~1.2 km) and lava domes (height of 70~250 m). Their vents were distributed along the fissures at the southern rim of the caldera which strongly infers structural control for magma ascent. The western part of the fissure is dominated by lava flows (A~G) which immediately descended the 30° slope of the caldera wall. They have clear levee structure with 70~150 m thickness, compression ridges for 10~30 m intervals, and talus with >20 degrees. The fissures from the middle to east formed small lava domes (H~P), although the easternmost one (O-P complex) is exceptionally large (1.1 x 0.8 km elliptical base with 250 m height). The total volume of these effusive products was 0.24 km<sup>3</sup>.

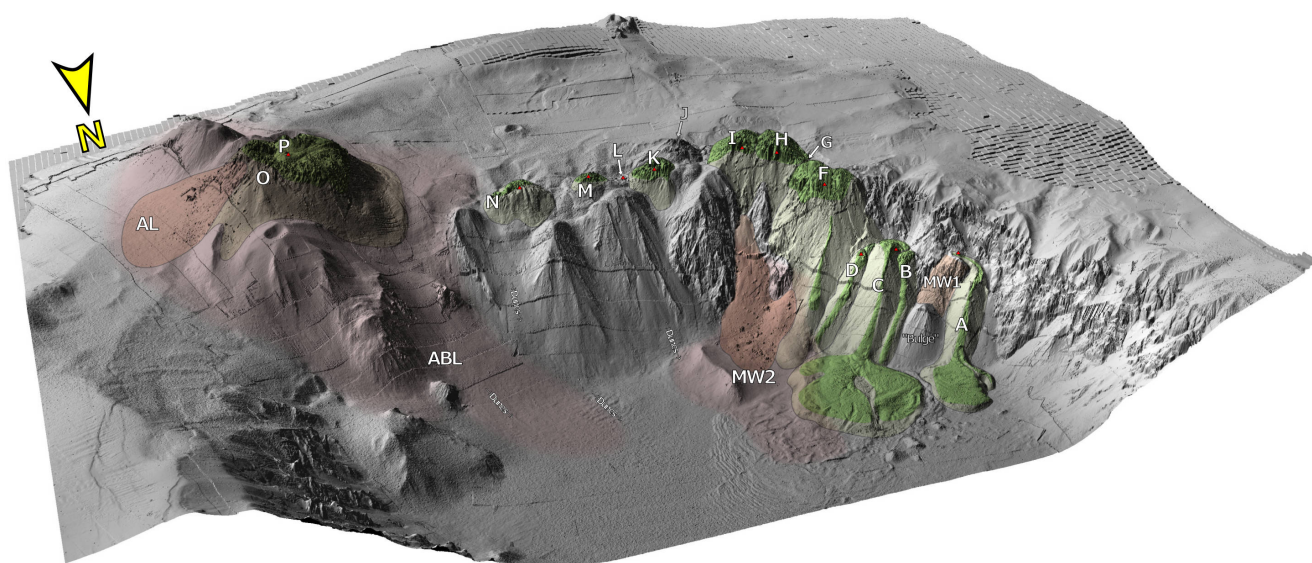
The chronology of the lava effusion has been investigated using the stratigraphical relationship to the GP unit, which was dispersed on 18th July. This enables constraints on the lava effusion rate between the 18th July to 19th August (NIWA voyage). The maximum volume of the lava post-dating GP (0.19 km<sup>3</sup> for A, F~P) draws the maximum effusion rate of 25 m<sup>3</sup>/s for 90-days average. This values comparable to other well-constrained subaerial silicic lavas, such as 50 m<sup>3</sup>/s for 20-days at

Cordon-Caulle 2011 eruption (Bertin et al. 2015), or  $66 \text{ m}^3/\text{s}$  for 14-days at Chaiten 2008 eruption (Pallister et al. 2013).

#### 4. Conclusion

The Havre 2012 eruption produced  $0.24 \text{ km}^3$  of rhyodacite lava flows and domes. The largest lava dome grew to the height of 250m and the longest lava flow advanced 1.2km from its vent despite the deep submarine environment. These investigations have calculated submarine silicic lava effusion rates ( $25 \text{ m}^3/\text{s}$ ) for the first time.

Keywords: Submarine volcano, Submarine caldera, Lava flow morphology, Effusion rate, Rhyolitic magma



## Evolution of magma ascent during the climactic phase of 2011 eruption of Shinmoe-dake, Japan, in view of groundmass microlite textures

\*Yuki Suzuki<sup>1</sup>, Mie Ichihara<sup>2</sup>, Fukashi Maeno<sup>2</sup>, Masashi NAGAI<sup>3</sup>, Hitomi Shibutani<sup>1</sup>, Syouhei Shimizu<sup>1</sup>, Setsuya Nakada<sup>2</sup>

1.Department of Earth Sciences, Faculty of Education and Integrated Arts of Sciences, Waseda University, 2.ERI, Univ. of Tokyo, 3.NIED

The climactic phase of the Shinmoe-dake 2011 eruption is characterized by three sub-Plinian events (Jan 26PM, 27AM, 27PM) and a lava accumulation stage in the crater (Jan 27-29), both of which were accompanied by vulcanian events. This study aimed at reconstructing magma ascent in conduit for this phase by using groundmass microlite textures. We then related the changes of magma ascent conditions with those of eruption intensity and style.

The analyzed samples include pumiceous clasts (gray and brown) and denser lava-like juvenile clasts from sub-Plinian (Layer 2-5, each with lower and upper subunits) and Jan 28 vulcanian deposits, and a lava block ejected from the crater on the Feb 1 vulcanian event. These are from magmas of the same chemical and storage conditions just prior to ascent from the reservoir. Representative samples for the textural analyses were selected based on bulk density that reflects syneruptive ascent rate and resultant degree of degassing. Subunits of Layer 2 to Layer 4 resemble one another in bulk density distribution ( $0.8\sim 1.7\text{ g/cm}^3$ ), except Layer3-up with extension to higher density ( $0.8\sim 2.1\text{ g/cm}^3$ ). Also, subunits of Layer 5 to Jan 28 resemble one another ( $0.8\sim 2.8\text{ g/cm}^3$ ) in having extension to much higher density than Layer3-up. The bulk density of Feb 1 lava ( $2.1\text{ g/cm}^3$ ) corresponds to high value observed in Layer 5 to Jan 28. The textural analyses were carried out for samples with maximum and minimum bulk densities in representative units (Layer2-up, 3-up, 4-up, 5-low, 5-up, Jan28, Feb 1 Lava).

The crystal size distributions (CSD) of plagioclase microlites are almost the same for all samples over the larger size (40-100 micrometer length in 3D). CSDs over smaller size change depending on the bulk density; dense samples from Layer 5-low, Layer 5-up, Jan 28 and Feb1 lava have steeper CSD than low density samples. These lines of evidence show magma ascent conditions at deeper part of conduit were constant throughout the climactic phase, but condition at shallow part was changing. The higher crystal numbers in dense samples can be explained by either a) higher ascent rate (when undercooling is relatively small, as a whole) or b) lower ascent rate (when undercooling is relatively large). Model b) is more likely in the present case, if decreasing trend of eruption intensity is considered. The bulk density distribution and correlation between bulk density and ascent rate show that the decrease of magma ascent rate at shallow part occurred gradually. The ascent rate variation widened in the third sub-Plinian event (Layer 5), by a little appearance of slowly ascended magmas. Only slowly ascended magmas came to occupy the conduit in the lava accumulation stage.

Suzuki *et al.* (2014 JPGU meeting) proposed that Layer3-up corresponds to the start of the second sub-Plinian event, based on that the bulk density distribution of Layer3-up has an extension to higher density, and degassed magma could have been formed in conduit during the resting phase (Jan 26, 19:00 –Jan 27, 2:00; between the first and second sub-Plinian events) due to decreased eruption rate. The textural study this time newly revealed CSD of plagioclase microlites of high density sample (ca.  $2.0\text{ g/cm}^3$ ) from Layer3-up resembles those of other pumiceous clasts from the first and second sub-Plinian events, implying conduit residence time of the degassed magma was not extremely long. This interpretation is consistent with the infrasound data indicating quasi-steady state magma flow for the resting phase.

Keywords: Shinmoe-dake, Bulk density, Groundmass microlite, Magma ascent, Degassing, Infrasonic

## Petrographic study of juvenile blocks of the 1783 A.D. (Agatsuma) pyroclastic flow in Asama Volcano

\*Sarina Sugaya<sup>1</sup>, Michihiko Nakamura<sup>1</sup>, Maya Yasui<sup>2</sup>

1.Department of Earth Sciences, Graduate School of Science, Tohoku University, 2.Department of Geosystem Sciences, College of Humanities and Sciences, Nihon University

The Agatsuma pyroclastic flow (APF) in the 1783 A.D. (Tenmei) eruption of the Asama volcano, central Japan, is characterized by occurrence of abundant rounded juvenile blocks with poorly vesiculated inner core and small proportion of fine ash matrix. The blocks have been referred to as cabbage for their shape and size. APF is a typical example of the "intermediate type" pyroclastic flow defined by Aramaki (1957), which have intermediate characters between the nuée ardente (dome-collapse type) and the pumice flows (column-collapse type) in terms of their volume, density of juvenile blocks and proportion of fine ash matrix. Because these characters may represent the magma outgassing and fragmentation processes, the intermediate type pyroclastic flow may be important to understand key processes that determine the bifurcation between explosive and effusive eruptions. Based on the observation that APF was composed of many (> 50) flow units, Takahashi and Yasui (2013) proposed that APF was generated through fountain collapses following Vulcanian explosions. They also suggested that lava lakes were formed by fall-backs of pyroclasts from the fountains during the Vulcanian activity on the basis of welding structures of the juvenile blocks. However, formation processes of these blocks are unclear. In this presentation, we propose that the cabbage-shaped juvenile blocks were formed repeatedly in the volcanic crater prior to each explosion.

On the surfaces of juvenile blocks ejected at the last stage of the 1783 A.D. eruption, we found the crusts impregnated with very fine (1–10  $\mu\text{m}$ ) ash particles and interstitial opal. The presence of opal shows that the juvenile blocks had been emplaced in a hydrothermal system after their rounded shape was formed. Since there is no geothermal area at the sampling location and its upper flank of the Maekake volcano, it is highly possible that silica precipitation from circulated geothermal water followed the formation of characteristic round shape of the juvenile blocks before generation of the APF. The weakly welded ash particles existed between the opal-bearing crust and the inner core; the welding process thus should have occurred before the crust formation. The surfaces of the juvenile blocks without opal-bearing crusts, which were collected from weakly-welded APF deposits, were covered instead with welded ash particles, which may have been formed at the higher temperature condition in the crater. These features indicate that the juvenile blocks were rounded probably via coagulation and welding and coated with volcanic ashes, and filled the crater before their eruption.

Keywords: Asama Volcano, Agatsuma pyroclastic flow, intermediate type pyroclastic flow, opal, welding

## Analysis of volcanic deformation at Tokachi-dake volcano by using 3-D boundary element method

\*Ryohei Kawaguchi<sup>1</sup>, Yosuke Miyagi<sup>1</sup>

### 1.NIED

Recent geodetic observations at active volcanoes succeeded in detecting small volcanic deformations associated with volcanic activities. These data can be used for quantitatively understanding the magma dynamics before eruptions. In this study, we calculated the volcanic deformation on the basis of 3-D boundary element method to explain the volcanic deformation data at Tokachi-dake volcano detected by SAR observation (Miyagi et al., 2016). Assuming an ellipsoidal shape pressure sources below the Maetokachi, deformation field at Tokachi-dake area, our forward modeling shows that ellipsoidal shape pressure source was locating at 300 m depth with about 3,000 m<sup>3</sup> volume increase could explain the deformation field observed at Tokachi-dake from SAR data. Using the temporal changes of ground deformation such as detected from GNSS data will enable us to constrain the pressure sources, which may give a new constraint on magma process prior to eruption.

Keywords: Tokachi, volcano deformation, BEM

## Finding the ruins from lahar deposit induced by the Heian eruption of Towada volcano, northeast Japan

\*Yusuke Minami<sup>1</sup>, Tsukasa Ohba<sup>2</sup>, Shintaro Hayashi<sup>3</sup>

1.Graduate School of Engineering and Resource Science, Akita University, 2.Faculty of International Resource Science, Akita University, 3.Faculty of Education and Human Studies, Akita University

At least 12 dwelling sites constructed during the Heian era was discovered at Katagai-Ienoshita ruins (Odate city, Akita prefecture) that is located 40 km far from the Towada volcano. These dwelling sites were buried by pyroclastic deposits, suggesting the occurrence of an ancient volcanic disaster. In this study, we describe and report these pyroclastic deposits. The pyroclastic deposits consist at least two layers: lower brownish orange volcanic ash and upper grayish lapilli tuff. The volcanic ash layer is four to seven cm thick and consisting of volcanic glass, pyroxene crystals, quartz crystals, and clasts of pumice, obsidian, and agate. Thickness of the volcanic ash is constant even on slopes such as the roof of the dwelling (up to 34°). The mantle bedding suggests that the layer is typical of ash fall deposits. The facies of the grayish lapilli tuff layer is massive and poorly sorted, consisting of clasts of pumice, mudstone, and alluvium conglomerate. The pumice clasts are 5 mm to 3 cm in diameter. Matrix of the lapilli tuff is composed of fine to medium sized clasts of volcanic glass, obsidian, agate, and quartz crystals. The grayish lapilli tuff is 100 to 150 cm thick. The lapilli tuff is thicker in depressions of the paleosurface, in other words, it ponded in the depressions. The lapilli tuff fills all the dwellings. Basal contact with the underlying volcanic ash layer is planar and shows no evidence of erosion or hiatus. The dwellings are mainly filled with the lapilli tuff and maintain their architectural structures such as roofs, walls, and floors that partly remain original wood without scorches. The lack of burned charcoal on the wood indicates that the lapilli tuff emplaced in low temperature. The general characteristics of the lapilli tuff indicate debris flow deposition. Poor sorting and massive facies are suggestive of rapid deposition of sediments. Lack of significant destruction in the ruins implies that the debris flow flowed in quite gentle manner. The Heian eruption of Towada volcano caused abundant ash falls (To-a and OYU pumice), pyroclastic flow (KPf), and lahar (Atsumiya flood deposits; Hayakawa 1985). The volcanic ash layer and the lapilli tuff layer at the Katagai-Ienoshita ruins can be correlated with To-a and Atsumiya flood deposits, respectively.

Keywords: Lahar, Towada volcano

## Applicability evaluation of the drone-mounted thermal infrared camera to geothermal monitoring at Sumikawa site, Akita Prefecture

\*Makoto Kobayashi<sup>1</sup>, Yoshinori MAEJIMA<sup>2</sup>, KEN-ICHI TOKITA<sup>3</sup>

1.Dia Consultant co., Ltd., 2.Maechan net. co., Ltd., 3.Iwate University

To understand the volcanic activity, it is important to monitor of earthquakes, crustal movement, geothermal activity throughout volcanic quiescence. Especially, the monitoring of geothermal activity is useful as a continuous observation, because the occurrence of high-temperature anomaly and change of heat discharge at the surface are closely related to the movement of magma and hydrothermal systems under the volcano, and also the monitoring of geothermal activity is simple, convenient and cost-effective compared with others.

This presentation would introduce a case study of thermal monitoring at the Sumikawa hot spring where a small phreatic explosion occurred in 1997. In particular, we observed the thermal distribution of the surface using a drone-mounted thermal infrared camera on the 18<sup>th</sup> October, 2015. And a temperature distribution map with high spatial resolution, roughly 5 cm, was generated from the data. This high resolution map would be made it possible for us to acquire the precise information of geothermal anomaly at the relatively small fumarolic area. Therefore, this method could complement the conventional observing approach of geothermal activity by performing repeatedly with proper timing.

Keywords: drone, geothermal monitoring, temperature distribution map, Sumikawa site



## Activization of Zao volcano within the past 100 years and the present activity

\*Akio Goto<sup>1</sup>, Noriyoshi Tsuchiya<sup>2</sup>, Nobuo Hirano<sup>2</sup>, Takahiro Watanabe<sup>2</sup>, Tetsuya Matsunaka<sup>3</sup>, Miwa Kuri<sup>4</sup>, Masaaki Uno<sup>2</sup>, Atsushi Okamoto<sup>2</sup>, Kengo Nakamura<sup>2</sup>, Sumiaki Machi<sup>1</sup>

1.Center for Northeast Asian Studies, Tohoku University, 2.Graduate School of Environmental Studies, Tohoku University, 3.Tandem Accelerator Complex, University of Tsukuba, 4.International Research Institute of Disaster Sciences, Tohoku University

In the recent 100 years major activities occurred on Zao volcano in 1918, 1939, 1966 and continued several years. After the 2011 Tohoku Earthquake increase in seismic activity was reported on 21 active volcanoes in Japan (JMA, 2014). While Zao volcano was out of them, volcanic tremor was observed for the first time in Jan. 2013, and a tremor and preceding tilting occurred in April (JMA, 2013). In addition, partial turbidity was found on Okama crater lake in Oct. 2014. We have started temperature monitoring of fumaroles and springs on Maruyama-sawa geothermal area (hereafter indicated as Maruyama-sawa), 1.5 km NE of Okama in 2012, temperature monitoring and chemical analysis of Okama and Maruyama-sawa water in 2013. We also have watched the confluence of Nigori-kawa and Firiko-zawa (Niizeki-onsen), 1.6 km east of Okama, where hot dense springs appeared in the past activity. Here we review the last three major activities focusing on Okama, Maruyama-sawa and Niizeki-onsen to compare with the present activity.

In 1918 Okama changed its color and then gas emitted from bottom (Omori, 1918), which lasted until 1928. The depth in 1928 was 61 m (Anzai, 1961). Some change accompanied an earthquake at Maruyama-sawa on 12 Aug. 1918 (Imada et al., 1985), although the detail is unclear. Tori-jigoku, killing animals by dense volcanic gas, had formed by 1935 (Anzai, 1961). Niizeki-onsen, developed by tunneling between 1907 and 1908 (sanitation department of Miyagi prefecture, 1969), lowered its temperature in 1917 winter and decreased the discharge by 1/3 in Jun. 1918. Although the temperature recovered temporarily, it was closed due to dry up in 1921.

In 1939 Okama changed its color on the end of July, followed by gas emission and temperature rise. Temperature in the bottom mud was >250 °C in Aug. 1940 (Anzai, 1941). The last turbidity was on Sep. 1942. Maruyama-sawa had weak fumarole activity in Jul. 1939 (Toraishi and Tominaga, 1940), but small explosion occurred on 10 Feb. (Toraishi and Tominaga, 1940) or 16 Apr. (Anzai, 1941), 1940. Niizeki-onsen recovered effusion 18 m away from the old vent in Jun. 1939, and new hot spring appeared 500 m upstream along Nigori-kawa (Ueno, 1940). Temperature was 88 °C on Feb. 1940 (Toraishi and Tominaga, 1940) and ph was 0.3 on May 1940 (Anzai, 1941). A 2 m wide and over 100 °C solfatar was found on the northern slope of the riverside.

No anomaly occurred on Okama in 1966 activity: no gas emission, unchanged depth (27 m line) between 1955 and 1968 (Shida et al., 1969) and monotonous decrease in  $\text{Ca}^{2+}$  and  $\text{SO}_4^{2-}$  concentrations between 1955 and 1983 (Shida et al., 1969; Sato and Kato, 1985). In contrast Maruyama-sawa activated its fumarole. At Niizeki-onsen steaming ground appeared on the slope and highly acidic hot spring effused along Nigori-kawa, whose temperature, ph, electrical conductivity (EC) were 77 °C, 0.3, >5 S/m on Oct. 1967 (Shida, 1968).

Based on our observation the present activity seems to be similar to that from 1966 so far. Except  $^{129}\text{I}/^{127}\text{I}$  ratio that may relate to seismic activity (Matsunaka et al., 2014), no obvious change has been observed on Okama; the depth is around 25 m, and  $\text{Ca}^{2+}$  is 60–70 mg/kg which is almost equal to or slightly lower than that in 1983. Temperature of Maruyama-sawa fumarole is almost constant, but the fumarolic steam has become prominent gradually, especially since autumn of 2014. In addition a trace of mud effusion was found in Oct. 2015. We confirmed in Sep. 2015 that Niizeki-onsen has reactivated upwelling. Temperature, ph and EC on 3 Sep. and 28 Oct. were 32.1 °C and 34.1 °C, 2.3

and 2.0, 0.126 S/m and 0.789 S/m.

Imada et al. (1985) pointed out the center of the activity had moved from Okama to Maruyama-sawa.

Except Okama the present activity also resembles that from 1939. We should continue the survey with having the 1940 Maruyama-sawa small explosion in mind.

Keywords: Zao volcano, 2011 Tohoku Earthquake, activization

## Temporal change of a hydrothermal system beneath Azuma volcano inferred from the Analysis of N-type events

\*Tatsuya Torimoto<sup>1</sup>, Mare Yamamoto<sup>1</sup>, Satoshi Miura<sup>1</sup>, Sadato Ueki<sup>1</sup>

1. Graduate School of Science, Tohoku University

### 1. Introduction

Understanding a hydrothermal system beneath volcano is a key to predict volcanic activities because surface volcanic phenomena are strongly controlled by the physical state of subsurface hydrothermal system. For that purpose, the analysis of N-type events, which are considered to be a resonance of underground fractures, may be a suitable way to estimate the physical properties of fluids inside the fractures (e.g., Kumagai and Chouet, 2000). At Mt. Azuma, N-type events are frequently observed around the time of appearance of a new fumarole on November 11, 2008, and these events have also been observed in recent years. In this study, we analyzed spectral characteristics of N-type events to infer the temporal evolution of hydrothermal system beneath Mt Azuma.

### 2. Data and Methods

We used vertical-component waveform data recorded at permanent stations TU.AZM (Tohoku Univ.) and V.AZJD (JMA), and apply the Sompì method (e.g., Kumazawa et al, 1990) to estimate four parameters (frequency, damping factor, initial amplitude, initial phase) characterizing each observed waveform. In this study, we mainly examine the time variation of frequencies, quality factors, and spectrum ratios of dominant namiso (wave elements) estimated by the Sompì method to interpret temporal variation of physical parameters of volcanic fluids.

### 3. Result and Discussions

The temporal variations of oscillatory characteristics of N-type events during two representative time periods from August, 2008 to November, 2008 (Period I) and from October, 2009 to December 2009 (Period II) are summarized as follows: During Period I, dominant frequency gradually shift from 4.0 Hz to 3.0 Hz, while the corresponding Q factors are almost constant. The spectrum ratios between lower mode and higher modes becomes larger as time passes. During Period II, dominant frequency becomes lower in the former part of the period, and settles down to 1.0 Hz. Quality factors and spectrum ratios during this period is almost constant.

These temporal variations of oscillatory characteristics of N-type events are interpreted in terms of temporal evolution of hydrothermal system as follows: During the Period I, the density ratio between fluid inside fractures and surrounding rock becomes larger while the velocity ratio is almost unchanged. This implies that the fluid inside fractures is a mixture of liquid and gas components, and the fraction of gas component becomes smaller during this period. During the Period II, the physical properties of fluid are at stable conditions and it implies steady supply of fluids into the crack.

The fact that the frequencies of most dominant mode in the period I is around 3 Hz while that of the period II is around 1 Hz also indicates that the gas fraction in the hydrothermal fluid during the Period I is larger than that of the Period II, and suggests a long-term variation of hydrothermal system.

Keywords: Azuma, fracture, hydrothermal system, N-type events

## Resistivity structure beneath the fumarolic area of Nasu-Chausu-dake inferred from the DC resistivity survey

\*Takahiro Kishita<sup>1</sup>, Wataru Kanda<sup>2</sup>, Shinichi Takakura<sup>3</sup>, Kaori Seki<sup>1</sup>, Yasuo Matsunaga<sup>1</sup>

1.EPS, Tokyo Tech., 2.VFRC, Tokyo Tech., 3.AIST

Chausu-dake is an active stratovolcano located in the mid-southern part of the Nasu volcanic group. Its volcanic activity started about 16000 years ago, and six large-scale eruptive activities including the magma ejection and many phreatic explosions were reported. The last one was activity during 1408-1410, and a lava dome was formed in the summit area. Phreatic explosions on July 1st, 1881 formed two craters on the northwestern side and western side of the lava dome. Recently, phreatic explosions occurred in these craters in 1953, 1960, and 1963, and fumarolic fields are formed today.

In this study, we carried out the DC resistivity survey in two fumarolic zones and revealed the detailed subsurface resistivity structure. Of the two resistivity survey lines, we referred to the line crossing the northwestern crater as "line A" (total length: 380m, electrode spacing: 10m) and the other line crossing the western crater as "line B" (total length: 300m, electrode spacing: 10m). Measurements were performed for each line by using the Wenner electrode array and Eltran electrode array which have different sensitivity to subsurface structure each other. The observed data were converted to the apparent resistivity distribution with different electrode spacing, and the 2D resistivity model was inferred using a 2D inversion program based on Sasaki (1981) which solves the non-linear least squares method using finite element meshes. The resistivity structure models obtained by this way were compared with the geological map of Nasu volcano presented by Yamamoto and Ban (1997), and with the resistivity model that was estimated from the AMT data of Aizawa et al.(2009).

As the result, we interpreted high resistivity zones near the surface as the andesitic lava and/or pyroclastic rocks which erupted about 100 thousand years ago, and low resistivity zones corresponded to a hydrothermal fluid and/or the hydrothermally altered zone because the fumarolic gases and the altered rocks were seen at the surface. The resistivity structure model of the line B showed that the low resistivity zone extends to the south of the crater, which is consistent with the 1D model of Aizawa et al.(2009).

In this study, we could interpret only the shallow resistivity structure because the obtained data was of low quality to infer a deep structure. To constrain a deeper and wider subsurface structure and to identify the presence of hydrothermal fluid, we are planning to carry out the AMT survey over the whole area of lava dome.

Keywords: Nasu volcano, fumarolic zone, DC resistivity survey, resistivity structure

## Resistivity structure of Kusatsu-Shirane volcano inferred from a magnetotelluric survey

\*Yasuo Matsunaga<sup>1</sup>, Wataru Kanda<sup>2</sup>, Shinichi Takakura<sup>3</sup>, Takao Koyama<sup>4</sup>, Yasuo Ogawa<sup>2</sup>, Kaori Seki<sup>1</sup>, Atsushi Suzuki<sup>1</sup>, Zenshiro Saito<sup>1</sup>

1.Department of Earth and Planetary Sciences, Graduate School of Science, Tokyo Institute of Technology, 2.Volcanic Fluid Research Center, Tokyo Institute of Technology, 3.National Institute of Advanced Industrial Science and Technology, 4.Earthquake Research Institute, University of Tokyo

Kusatsu-Shirane volcano is an active volcano located in the northeastern part of Gunma prefecture. There are some craters on the summit area, one of which is the Yugama crater where lake water shows strongly acidic nature. High seismicity is frequently observed beneath the crater. Several hot springs located in the foot of the volcano discharge abundant hot spring water. For these reasons, there seems to be a highly developed hydrothermal system beneath the volcano.

According to the geochemical studies, fumaroles in the summit area, lake water in the Yugama crater and hot springs in the flank are derived from a two-phase hydrothermal fluid reservoir located beneath the Yugama crater. In contrast, hot springs located in the foot of Mt. Moto-Shirane discharge more primary fluids which are mixtures of high temperature volcanic gases and meteoric water (Ohba et al., 2000). In addition, audio-frequency magnetotelluric (AMT) surveys conducted along an E-W profile of the volcano found a 300m-1000m thick conductive layer beneath the eastern slope. This conductor was interpreted as the smectite-rich layer of Pliocene volcanic rocks that plays a role of low-permeable cap separating the fluid path to the hot spring of the eastern slope and the path to the hot spring of the foot of the volcano (Nurhasan et al., 2006). Another AMT survey conducted around the Bandaiko hot spring revealed the existence of a conductor extending to a deeper part beneath the hot spring (Kanda et al., 2014).

These studies revealed the generating process of various kinds of hot spring water and the shallow structure in the area to some extent. However, a deep structure of the volcano has not been understood yet. We conducted a wideband magnetotelluric (MT) survey across Mt. Moto-Shirane to reveal the pathway of hydrothermal fluid from the deeper part, and the location of heat source, that is, the magma reservoir of the volcano.

The survey was carried out at 12 sites along a 10km long E-W profile from the Manza hot spring area via the summit area of Mt. Moto-Shirane to the Bandaiko hot spring. We inverted the observed data by using the code developed by Ogawa and Uchida (1996) to obtain a 2-D resistivity section. Impedance phase and apparent resistivity were used for the inversion, in which the data showing 3-D features were eliminated in advance.

Obtained resistivity structure was characterized by the following features.

- (1) Conductive body extending from the summit area to the deeper part of the western flank
- (2) Conductive layer at the shallow part of the eastern flank
- (3) Large resistive block at the deeper part of the eastern flank

The conductive layer (2) may correspond to the Pliocene volcanic rocks which were found by the previous AMT survey. Beneath this conductive layer, a resistive block (3) lies. Because the observed data was affected by the artificial electromagnetic signals, we need to examine the data carefully to confirm whether the model is true or not. We will give a presentation on the some results of analysis in a poster session.

Keywords: Resistivity structure, Magnetotellurics, Kusatsu-Shirane Volcano

## Precise hypocenters in active hydrothermal systems determined by the double-difference technique: Implications for fluid flows at during an inflation event at Kusatsu-Shirane Volcano in 2014

\*Tomoyoshi Kuwahara<sup>1</sup>, Akihiko Terada<sup>2</sup>, Yohei Yukutake<sup>3</sup>, Wataru Kanda<sup>2</sup>, Yasuo Ogawa<sup>2</sup>

1.Graduate School of Science and Engineering, Tokyo Insutitute of Technology, 2.Volcanic Fluid Research Center, Tokyo Insutitute of Technology, 3.Hot Springs Research Institute of Kanagawa Prefecture

Earthquake swarms occurred beneath the Shirane pyroclastic cone at Kusatsu-Shirane Volcano in 2014. The seismic activity was followed by an inflation at shallow depth beneath the cone and changes in geomagnetic field and chemical compositions of volcanic gas emitted around the cone. These unusual activities are likely caused by accumulation of hydrothermal fluid at shallow depth beneath the cone. MT surveys revealed that a low permeable layer probably composed of Smectite exist at shallow depth beneath the cone (Ogawa et al., personal communication). Such a subsurface structure may play an important roles in fluid storage and triggering of phereatic eruptions. To understand a relation between subsurface structure and fluid flow, precisely determined hypocenters give valuable clues (Yukutake et al., 2011). Applying the double-difference technique (Waldhauser and Ellsworth, 2000), we precisely relocated hypocenters which occurred in 2013-2014.

To obtain initial locations of hypocenters for applying the Double-Difference technique, reliable seismic velocity structure is necessary. However, it is not well known beneath the cone. Kuwahara et al. (2015) developed a simple 1-D model composed of two layer. Minimized average residuals of P-wave travel times suggest that optimal seismic velocities of upper and lower layer are 2.5 km/s and 4.8 km/s, respectively, which correspond to figures estimated by controlled source seismic experiments (Onizawa et al., 2005; Takeda et al., 2004). A height of bottom of upper layer is estimated to 1,500 m a.s.l. that corresponds to the height of the bottom of low permeable layer, suggesting the upper layer is mainly composed of volcanic rock altered by hydrothermal activities. On the basis of the velocity model mentioned above, we obtained the initial hypocenters of 251 events. For the analysis, we selected events which the P- and S-wave arrival times obtained at six and at least three stations respectively, including three bore-hole type. The cross-correlation measurement consisted of 86,089 P-wave and 37,413 S-wave.

Relocated hypocenters concentrate on the height of 950-1,000 m a.s.l. beneath the center of Yugama crater lake. In March 2014, at the beginning of earthquake swarms periods, relocated hypocenters are same as events in 2013. One of notable feature is that earthquakes began to occur at shallower depth of 1,100-1,300 m a.s.l. from the end of April 2014. In May 2014, an increase in water temperature of Yugama crater lake were observed. Subsurface inflation monitored by tilt meters suggests a fluid storage rate was highest in May 2014. We believe that hydrothermal fluid supplied from depth began to accumulate under the low permeable layer in March 2014. The fluid began to fracture the low permeable layer, and penetrate into shallower part at the end of April. Finally, the fluid began to eject mildly from the lake bottom from May 2014.

Acknowledgement: We are grateful to Dr. Shin'ya Onizawa, Dr. Tomoki Tsutsui and Mr. Rintaro Miyamachi for the field work.

Keywords: Kusatsu-Shirane Volcano, microearthquakes, double-difference method

## Volcanic activity of Asama volcano in 2015

\*Sayaka WADA<sup>1</sup>, MASAMICHI NAKAMURA<sup>1</sup>, Yoshihiro Otsuka<sup>1</sup>, Sei IIJIMA<sup>1</sup>

### 1. Japan Meteorological Agency

After the end of April, 2015, volcanic earthquakes occurred near Asama volcano have been increased and in June the emission of sulfur dioxide have been increased rapidly. In recognition of the increase in volcanic activity, JMA issued a Near-crater Warning on 11 June and raised the Volcanic Alert Level from 1 to 2. Thereafter, small eruption occurred on 16 and 19 June. In our poster, we report the activity of Asama volcano in 2015 including the activity before and after eruption. Volcanic seismicity became relatively high from the end of April 2015 at Asama volcano. It became the highest in June, and decreased gradually. Amounts of sulfur dioxide emission had increased in June and decreased gradually. Therefore, there would be some correlation between seismic activity and amounts of sulfur dioxide. The glow was observed after 16 June. The thermal activity has remained at high levels.

The volcanic deformation observed by tiltmeters and EDM (Electronic Distance Measurements) after June 2015, by GNSS observation after May 2015. The expansive deformation was confirmed from the data of tiltmeters. We used the model of a point pressure source and tried to estimate the pressure source of this deformation. For data analysis, we use a software package "MaGCAP-V" (MRI, 2008). The best fit model is a point pressure source located in the west of Asama volcano. The deformation detected by GNSS measurements suggests that there is the source which is deeper than the source inferred by the data of tiltmeters because the movement of GNSS has preceded the movement of tiltmeters.

In our poster, we discuss these results in detail and compare with the past activity.

Acknowledgements: We used the data observed by GSI and NIED. We also used a software package "MaGCAP-V" (MRI, 2008). We would like to express my gratitude to them.

Keywords: Asama volcano, eruption, volcanic deformation

## Temporal change of SO<sub>2</sub> discharge at Asama volcano

\*Yoshihiro Otsuka<sup>1</sup>, Minoru TAKEO<sup>2</sup>

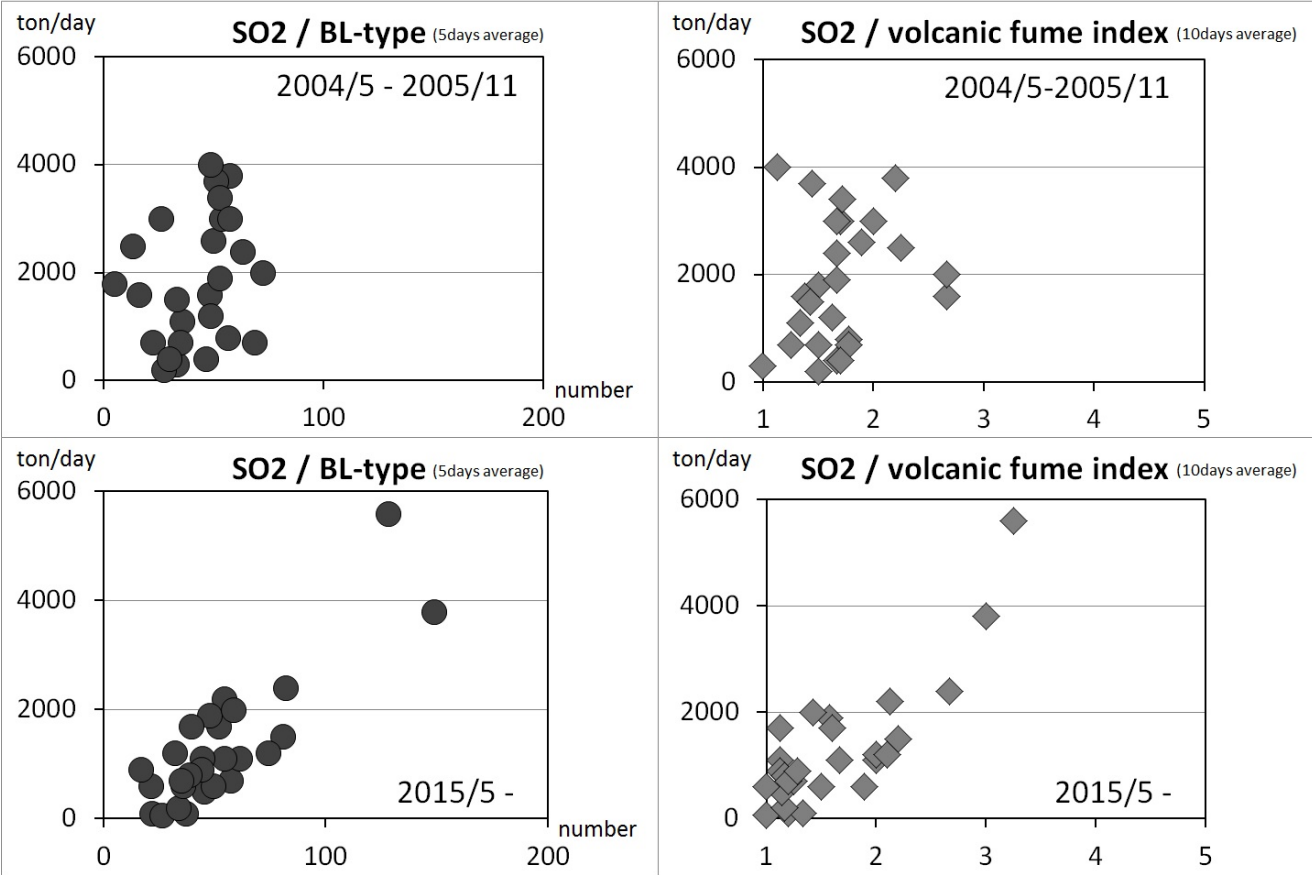
1.Seismology and Volcanology Department,JMA, 2.Earthquake Research Institute, University of Tokyo

Japan Meteorological Agency (JMA) has been observed amount of SO<sub>2</sub> emission at Asama volcano since July 2002, for the purpose of monitoring the volcanic activity. Based on the observed SO<sub>2</sub> discharge data, we investigate correlations among daily amount of SO<sub>2</sub> emission, volcanic fume index, and frequency of volcanic earthquakes dividing the term into eruption (June 2002 - April 2004, May 2004 - November 2005, August 2008 - July 2009, and May 2015 -) and non-eruption periods.

A positive correlation between frequency of BL-type volcanic earthquake and SO<sub>2</sub> discharge is confirmed during the 2015 eruption period; that between volcanic fume index and SO<sub>2</sub> discharge is in a similar way. The similar correlations are recognized during the eruption periods in 2008 and 2009. On the other hand, we can't make certain of correlations between frequencies of BL-type event and volcanic fume indexes during the eruption periods in 2003 and 2004; we frequently observed increments of SO<sub>2</sub> emission without increase of BL-type earthquakes and volcanic fumes. (fig.1) A very long-period pulse, hereafter we call it VLP, is an impulsive motion with a dominant period longer than 5 seconds accompanied by a tilt change, which is excited by a sudden gas emission (Maeda and Takeo, 2012). Weak correlations are confirmed between the frequencies of VLP and BL-type event, and between the frequency of VLP and SO<sub>2</sub> discharge. However, there are several examples of large amount of SO<sub>2</sub> emission with a few occurrence of VLP. During non-eruption periods, the daily SO<sub>2</sub> discharge rate could not exceed 2000 ton/day even though the increment of BL-type activity. The increment of SO<sub>2</sub> emission seems to be plausible data indicating a volcanic eruption potential, and the positive correlations among SO<sub>2</sub> emission, volcanic fume, and daily frequency of volcanic event are confirmed during the 2008, 2009, and 2015 eruption periods. However, there are some observations that SO<sub>2</sub> emission represented weak correlations with the frequencies of BL-type event and with the volcanic fume indexes even though the eruption periods (2003 and 2004). The gas emission system seems to fluctuate along the volcanic activity.

Keywords: Asama volcano, SO<sub>2</sub>, seismic waveform, volcanic fume





## Measurements of soil CO<sub>2</sub> flux at Asama volcano, Japan before and after minor eruptions in June 2015

\*Masaaki Morita<sup>1</sup>, Toshiya Mori<sup>1</sup>, Ryunosuke Kazahaya<sup>2</sup>, Hiroshi Tsuji<sup>3</sup>

1.Geochemical Research Center, Graduate School of Science, The University of Tokyo, 2.Research Institute of Earthquake and Volcano Geology, Geological Survey of Japan, AIST, 3.Earthquake Research Institute, The University of Tokyo

Volcanic degassing is not only from plumes or fumaroles in craters but also from soil emanations on volcano flanks. In this soil degassing, carbon dioxide (CO<sub>2</sub>) is an important species because of its high abundance in magmatic volatiles and its low solubility in magma. Many previous studies have reported on variations of soil CO<sub>2</sub> flux and its spatial distribution corresponding to changes of volcanic activity [e.g., Hernández *et al.*, 2001, *Science*; Carapezza *et al.*, 2004, *Geophys. Res. Lett.*; Pérez *et al.*, 2006, *Pure Appl. Geophys.*]. Therefore, it is important to monitoring soil CO<sub>2</sub> flux for understanding relations of volcanic degassing and volcanic activity changes.

At Asama volcano, Japan, minor eruptions occurred on 16th and 19th June 2015 that were the first eruptions since 2009. After these eruptions, a measurement of soil CO<sub>2</sub> flux was conducted on 29th October 2015. Here we compare the data of 2015 to those of inactive period in 2012–2014 [Morita *et al.*, *Bull. Volcanol.*, *accepted*] and discuss on fluid ascent before and after the 2015 eruptions. Soil CO<sub>2</sub> flux was measured using an accumulation chamber method [Parkinson, 1981, *J. Appl. Ecol.*; Baubron *et al.*, 1990, *Nature*; Chiodini *et al.*, 1998, *Appl. Geochem.*] at 54 sampling points in the eastern side of Kamayama flank and Maekake crater rim. A spatial distribution of measured flux was obtained from an average of 100 realizations by sequential Gaussian simulation [Deutsch and Journel, 1998; Cardellini *et al.*, 2003, *J. Geophys. Res.*].

As a result, a spatial distribution of high soil CO<sub>2</sub> flux anomalies in eastern Kamayama flank and eastern Maekake crater rim is similar to that for the 2012–2014 observations reported in Morita *et al.* [*Bull. Volcanol.*, *accepted*]. Comparing the flux values of the 2015 and the 2012–2014 measurements, an average flux of the 100 realizations was about 5–10 times higher in eastern Maekake crater rim and was not changed or a little lower around Kamayama crater rim. Morita *et al.* [*Bull. Volcanol.*, *accepted*] reported that soil CO<sub>2</sub> emitted from the eastern side of the summit probably ascend from a hydrothermal fluid layer corresponding to a low electrical resistive body that resides in the shallow part of the volcano flank [Aizawa *et al.*, 2008, *J. Volcanol. Geotherm. Res.*]. The increase of soil CO<sub>2</sub> flux in eastern Maekake crater rim likely reflect an increasing supply of magmatic volatiles to the hydrothermal fluid layer from the depth. Different responses of soil CO<sub>2</sub> flux between Kamayama and Maekake crater rims may correspond to differences of fluid pathway and ascent process. To ascertain relations between soil CO<sub>2</sub> flux variations and the fluid ascent process from the depth, further repeated observations of soil CO<sub>2</sub> flux and detailed comparisons to the volcanic activity are necessary.

Keywords: Asama volcano, Soil CO<sub>2</sub> flux, Fluid ascent

## A permeability evolution model for the 2014 eruption of Mt. Ontake inferred from tilt waveform analyses

\*Yuta Maeda<sup>1</sup>, Aitaro Kato<sup>1,2</sup>, Toshiko Terakawa<sup>1</sup>, Yoshiko Yamanaka<sup>1</sup>, Shinichiro Horikawa<sup>1</sup>, Kenjiro Matsuhira<sup>1</sup>, Takashi OKUDA<sup>1</sup>

1.Earthquake and Volcano Research Center, Graduate School of Environmental Studies, Nagoya University, 2.Earthquake Research Institute, The University of Tokyo

During 450 s before the onset of Mt. Ontake 2014 eruption, very long period (VLP) seismic events and a summit-uplift tilt change were observed. Our waveform inversion solution of the largest VLP event, that took place 25 s before the eruption onset, was an NNW-SSE striking tensile crack at a 600 m depth beneath the eruptive vent region; this result was interpreted as an opening and a closing of one of the preexisting seismic faults caused by ascent of water vapor (Maeda et al., 2015, EPS). Our waveform inversion of the tilt change pointed to a semi-vertical tensile crack at 1 km depth that inflated by  $10^6 \text{ m}^3$ . The tilt waveform is well explained by a linear function of time during the first 168 s, then switched to an exponential growth at a time constant of 84 s (Maeda et al., 2015 VSJ fall meeting). Interpretations of these results were kept unsolved at that time.

In this presentation, we show our latest model of the tilt change developed after the 2015 VSJ fall meeting. We assume that the inflation of the crack was caused by boiling of underground water at a constant depth (pressure: 20 MPa; depth: ~1 km).

The linear function of time is explained by boiling of underground water under a constant heat supply from depth. Using the volume change rate estimated from the waveform inversion, the heat supply rate is estimated to be  $10^{10} \text{ J/s}$ , consistent with the surface heat emission estimated after the 2014 eruption (Terada et al., 2014 VSJ fall meeting).

To realize the exponential function, a positive feedback process is needed such that a larger amount of water vapor in the crack leads to more rapid boiling of underground water. As long as a single large crack ( $10^6 \text{ m}^3$ ) filled with water vapor is considered, a slow growth lasting for up to 450 s is difficult to realize according to the force balance of Lister and Kerr (1991, JGR). We then regard the tilt source to be a region of many small subparallel cracks filled with water vapor, and model this system as a vertical permeable flow driven by the buoyancy of water vapor. The Darcy velocity equation suggests that the permeability is the only quantity that could significantly vary with time. We therefore consider the following positive feedback: the larger the water vapor in the source volume, the larger the porosity, permeability, and Darcy velocity, leading to faster water vapor migration upward from the boiling depth, which is compensated by increasingly rapid boiling of underground water. We quantified this idea and obtained an exponential growth of the water vapor volume under a proportional relation between the porosity and permeability. The observed time constant of 84 s is explained by a realistic permeability in this model.

In summary, the source process before the Mt. Ontake eruption is modeled by initial boiling of underground water under a constant heating, followed by exponential acceleration of the boiling rate caused by increased porosity and permeability, VLP events caused by ascent of the water vapor, and finally the eruption.

Keywords: Mt. Ontake, Phreatic eruption, Tilt

## The rainfall correction of E-W component of the tiltmeter at Mt. Ontake Tanohara (2)

\*Kazuhiro Kimura<sup>1</sup>, Katsuhisa Kawashima<sup>2</sup>, Matsumoto Takane<sup>2</sup>, Akihiko SASAKI<sup>3</sup>, Tsutomu Iyobe<sup>4</sup>, Masaki Nakahashi<sup>5</sup>, Akio Kobayashi<sup>1</sup>

1.Meteorological Research Institute, 2.Research Institute for Natural Hazards and Disaster Recovery, Niigata University, 3.Faculty of Science, Shinshu University, 4.Graduate School of Engineering, Kyoto University, 5.Japan Meteorological Agency

Most of active volcanoes of Japan are snowcapped during winter. And most of tiltmeters for volcano monitoring are influenced by meltwater.

Kimura and Nakahashi(2015) tried rainfall correction of E-W component of the tiltmeter at Mt. Ontake Tanohara by using the precipitation only, and were able to get the good result for the period when rainfall is liquid (from June to October). As a result, they were able to confirm a tilt change of the mountain rise from around September 10, 2014 in the same timing that earthquakes increased under the summit of Mt. Ontake. However, they cannot correct the influence of meltwater from March to May every year. The meltwater data are necessary to correct influence of meltwater. Kawashima et al.(2015) observed the snow and meteorological data at Mt. Ontake Tanohara, and calculated the amount of meltwater from November, 2014 through May, 2015. Kimura et al.(2015) tried the rainfall correction of E-W component of the tiltmeter at Mt. Ontake Tanohara by using the precipitation and the amount of meltwater, and were able to correct the influence of meltwater of 2015.

The snow and meteorological observation at Mt. Ontake Tanohara was started November, 2015 again. As of January, 2016, there is very less snow than last year, we show the result of the rainfall correction of the tiltmeter at Mt. Ontake Tanohara by using the precipitation and the amount of meltwater of 2016.

### References:

Kawashima K., T. Iyobe, T. Matsumoto, K. Kataoka, K. Izumi, A. Sasaki, K. Suzuki, T. Saito (2015): Research Activities Ontake Volcano from the Viewpoint of Snow-Volcano Interrelations, proceedings of JSSI & JSSE Joint Conference - 2015 in Matsumoto, C3-1.

Kimura K., K. Kawashima, T. Matsumoto, T. Iyobe, A. Sasaki, M. Nakahashi (2015): The influence of meltwater on the borehole tiltmeter for volcano monitoring - Trial of meltwater correction for tiltmeter data of EW component at Mt. Ontake Tanohara -, proceedings of JSSI & JSSE Joint Conference - 2015 in Matsumoto, C3-5.

Kimura K., M. Nakahashi (2015): The rainfall correction of E-W component of the tiltmeter at Mt. Ontake Tanohara (1), proceedings of the Japan Geoscience Union Meeting, SVC45-P24.

Keywords: tiltmeter, Mt. Ontake, rainfall correction, meltwater

## Identification and emplacement mechanisms of the September 2014 eruptive products from Ontake volcano, Japan, inferred from magnetic petrology

\*Takeshi Saito<sup>1</sup>, Kyoko S Kataoka<sup>2</sup>, Takane Matsumoto<sup>2</sup>, Katsuhisa Kawashima<sup>2</sup>, Tsutomu Iyobe<sup>3</sup>, Akihiko Sasaki<sup>1</sup>, Keisuke Suzuki<sup>1</sup>

1.Faculty of Science, Shinshu University, 2.Research Institute for Natural Hazards and Disaster Recovery, Niigata University, 3.Graduate School of Engineering, Kyoto University

Phreatic eruption occurred at Ontake volcano on the 27th Sept. 2014, have produced wide variety of deposits around the volcano. The eruption column reached to about ten thousand meters high and resulted in thin ash fall deposits extended 100km to the east. Small pyroclastic flow deposits were emplaced at southern slope of the volcano edifice. Though steam emission without additional volcanic products have been observed after the initial intensive activity, heavy rain falls triggered a lahar which transported volcanic materials deposited at around the craters to the foot of the volcano. This study focuses on eruption processes and transport and emplacement mechanisms of the eruptive products. Preliminary results were reported in 2015 JpGU meeting. This time, we will report magnetic petrological features of the eruptive products of Ontake 2014 and discuss emplacement mechanisms of the materials.

Magnetic minerals in the eruptive products are characterized by abundant pyrite and small amount of titanomagnetites. Thermomagnetic analysis indicated that pyrite is stable under 380°C and changes to magnetite above 380°C, suggesting the eruptive materials did not suffer high temperature of more than 380°C just before and during the eruption. Magnetic hysteresis parameters of the materials ejected at the initial stage of the eruption were relatively concentrated around the bottom right corner of the total distribution at Day plot, whereas the other materials were scattered at the upper left. It is suggested that the materials by the initial stage of the eruption contain larger magnetic minerals. On the other hand, field observation and granulometric analysis of the deposits including magnetic minerals indicated that the materials derived from the initial stage are composed of well-sorted fine ash, inconsistent with magnetic hysteresis results. There is a possibility that heavy magnetic minerals bearing iron tend to fall rapidly, resulted in higher concentration of larger magnetic minerals in the materials ejected at the initial stage.

These rock magnetic characters can be used as a marker of the eruptive products. Thin fine ash layer found at the upstream of the Nigori-kawa River, about 3 km south from the vent area, showed similar rock magnetic features with those of the materials caused by the initial stage, whereas such deposits cannot be traced further downstream from the point. The deposit could be derived from ash cloud of pyroclastic flow or from ash fall itself by the initial stage. Approximately 2m thick lahar deposits containing sediments derived from the 2014 eruptions were found along the river, suggesting emplacement of the pyroclastic flow impacted upstream areas of the catchment. Turbidity of the river decreased significantly after a year of the eruption, but a certain amount of the 2014 materials were contained in the river water. This is suggestive of perennial transportation of volcanic materials sourced from the vent area even in the present time.

Keywords: Ontake, phreatic eruption, magnetic mineral, pyrite

## Study on crack size in anisotropic media in Hakone volcano

\*Ryou Honda<sup>1</sup>, Yohei Yukutake<sup>1</sup>, Shin'ichi Sakai<sup>2</sup>, Yuichi Morita<sup>2</sup>

1.Hot Springs Research Institute of Kanagawa Prefecture, 2.Earthquake Research Institute, University of Tokyo

We have studied properties of anisotropic media in Hakone volcano, such as depth dependence of anisotropic intensity and/or its time variations. In this study, we consider the characteristic size of the crack system in the anisotropic media in Hakone volcano. To do so, we examined the confidence band in the frequency domain of the parameters obtained in the S-wave splitting analysis based on the method proposed by Mizuno et al (2001).

Mizuno et al (2001) proposed a quantitative manner to estimate errors in phase differences between two quasi-S waves obtained by a splitting analysis. The phase differences should be constant (confidence band) under the assumption that a considered wavelength is much longer than the size of the cracks. As a frequency becomes higher, the phase differences become frequency-dependent. Therefore, we can estimate the lower limit of the wavelength, that is, the upper limit of crack size from a confidence band of phase differences.

We estimated the upper limit of crack size as 200 ~ 300m in the assumed velocity structure. However, lower limits of wavelength obtained for some observation sites (e.g., KIN and OWD) are longer than those for the other sites. Yukutake et al (2013) reported that there is a low b-value zone beneath the fumarolic area (Owakudani). The low b-value zone is expected to include relatively large cracks. The spacial variations of estimated crack size may be caused by rays passing through the low b-value zone.

Keywords: anisotropy, S-wave splitting, Hakone volcano

## Magnetic variation of total intensity associated with volcanic activity observed around Owakudani, Hakone Volcano

\*Tetsuya Yamamoto<sup>1</sup>, Kazuki Miyaoka<sup>1</sup>, Masatake Harada<sup>2</sup>, Jun Takenaka<sup>2</sup>, Akimichi Takagi<sup>1</sup>

1.Meteorological Research Institute, Japan Meteorological Agency, 2.Hot Springs Research Institute of Kanagawa Prefecture

Volcanic event of Hakone in 2015 began in late March by slight extension of baseline length observed by GNSS network, and in late April the volcanic seismicity increased including many felt earthquakes as well as fumarole of Owakudani became more active. InSAR analysis revealed that a local uplift was take place in a part of Owakudani from May to June. After these, on June 30, eruption occurred at the nearest neighbor of the locally uplifted area in Owakudani. Though the eruption was tiny, a group of vents was created. Since July the activities were going down, the extension of the GNSS baseline was stopped and the seismicity decreased.

Associated with phreatic eruption, the type of eruption expected at Owakudani, hydrothermal activity often causes thermal demagnetization of underground rock in rather shallow place and results in magnetic change on the surface. For Kusatsu-Shiranesan and Meakandake where phreatic eruption occurred in recent years, observed magnetic variation of total intensity is one of indices used for assessment of the volcanic activity. For Owakudani, the magnetic intensity is also thought to be a hopeful data for the volcanic monitoring, we carried out repeat observation of magnetic intensity around Owakudani from May to November in 2015.

It was revealed from the observation that the magnetic intensity decreased by about 1nT from July to September, after the eruption, at the stations in the northern part of Owakudani. In the same period, a slight increase of the intensity was possibly occurred at a station in the southern part. These kind of magnetic variation is expected when underground rock get magnetized, and it will be possible by cooling of heated rock. Beneath Owakudani, the rock temperature seemed decreased from July to September. It might be happened by the creation of the vents in the eruption at the end of June and they made the cooling more effective. Assuming the temperature decrease was occurred beneath the locally uplifted area in Owakudani before the eruption, and the depth was 500m from the surface, the obtained magnetic moment was estimated as  $2-3 \times 10^6 \text{Am}^2$ .

Keywords: Hakone, magnetic variation, volcanic activity

Volcanic ash erupted from Owakudani fumarolic area of Hakone volcano on June 30, 2015, and its soluble components

\*Muga Yaguchi<sup>1</sup>, Takeshi Ohba<sup>1</sup>, Masakazu Sago<sup>1</sup>, Asako Sekimoto<sup>1</sup>

1.Department of Chemistry, School of Science, Tokai University

Volcanic ash erupted from Owakudani fumarolic area of Hakone volcano on June 30, 2015, was collected, and their constituent minerals, chemical compositions, and water soluble components were analyzed.

Smectite, pyrite, tridymite, cristobalite, gypsum, anhydrite, plagioclase and quartz were detected in the volcanic ash by XRD and microscopic observation. This mineral assemblage indicates that the volcanic ash was derived from relatively low-temperature alteration zone of the hydrothermal system beneath the Owakudani fumarolic area. The volcanic ash contains relatively lower concentrations of some elements such as Na, K, Ca and Mg than andesitic lava in the Owakudani area (Takahashi et al. 2006), supporting that the volcanic ash was derived from hydrothermal alteration zone. Water soluble components seemed to be derived from thermal water because high amount of  $\text{Cl}^-$  and  $\text{SO}_4^{2-}$  (12.2 and 6.6g/kg, respectively) and Cl/S ratio of 5 were detected. Considering that there are thermal waters which have Cl/S ratio of about 2 at depth around 29-36m (Watanuki, 1966) and that of 7-18 at depths around 500m (Oki and Hirano, 1974), volcanic ash seems to be erupted from depths of around 500m below the surface, or more shallow depth.

Keywords: Hakone volcano, phreatic explosion, volcanic ash, hydrothermal mineral, water soluble component



## Water quality characteristics of Lake Nyos, Cameroon

\*Muga Yaguchi<sup>1</sup>, Mumbfu E Mimba<sup>1</sup>, Ajiro Takuya<sup>1</sup>, Takeshi Ohba<sup>1</sup>, Gregory Tanyileke<sup>2</sup>, Joseph V Hell<sup>2</sup>

1.Department of Chemistry, School of Science, Tokai University, 2.IRGM, Cameroon

In 1986, Lake Nyos in Cameroon released a large amount of CO<sub>2</sub> and killed more than 1700 residents. Subsequent investigation revealed that the CO<sub>2</sub> is originated in degassing magma and is ascending from the bottom of the lake with thermal water (e.g., Kusakabe et al., 1989; Ohba et al. 2012). Although controlled degassing started at Lake Nyos in 2001 and have resulted in reducing CO<sub>2</sub> content of the lake (e.g., Kusakabe et al. 2008), investigations regarding chemical components except CO<sub>2</sub> content is also important to ensure gas disaster prevention.

In this study, chemical compositions of the water samples collected from various depths in the lake Nyos and volcanic rocks collected from lake rim were analyzed. TDS of the lake increases with depth. The ionic dominance pattern for cations is Fe<sup>2+</sup> > Mg<sup>2+</sup> > Ca<sup>2+</sup> > Na<sup>+</sup> > K<sup>+</sup> at the bottom of the lake, whereas the anion is dominated mainly by HCO<sub>3</sub><sup>-</sup> with only a very small amount of Cl<sup>-</sup> and SO<sub>4</sub><sup>2-</sup>. Except for HCO<sub>3</sub><sup>-</sup> derived from CO<sub>2</sub>, whose origin has already been described, the concentration of dissolved components are 40 ~ 380 mg/L and Na/(Na+Ca) weight ratios are about 0.3 ~ 0.4, indicating that the water quality of the lake is affected by water-rock interaction. Good correlation was observed between chemical compositions of lake water and whole-rock compositions of the rock samples, supporting this inference. Assuming that the chemical components of the lake water are derived from rock dissolution, the solubility of the elements seem to be basically controlled by the ionic potential (Z/r), elution rate of elements of large Z/r (e.g., Al, Ti and Cr) were small compared to elements of small Z/r (e.g., Na, K, Ca, Mg, and Mn). Additional study in consideration of pH condition and equilibrium state of minerals is important to determine the water-rock interaction processes that affect the water quality.

Keywords: Cameroon, Nyos, Crater lake, Limnic eruption, Water quality

## Change of Izu Ohshima GNSS height at 2012

\*Hiroyuki Takayama<sup>1</sup>, Tetsuya Yamamoto<sup>1</sup>, Shin'ya Onizawa<sup>2</sup>

1.Volcanological Division 1st laboratory, Meteorological Research Institute, 2.Japan Meteorological Agency

Takayama et. al.(2015) showed the change of GNSS height around Mt. Mihara. After that, all stations in Izu Ohshima is change in GNSS height at 2012.

On all stations in Izu Ohshima, we approximate GNSS height by line from 2009 to 2011 and after 2013. Rate after 2013 minus rate from 2009 to 2011 are the changes at 2012. These changes are large near north of caldera. They are small at north and south island.

We plot the changes against distance from north of caldera. We plot a rate of rise by Yamakawa-Mogi model of depth 5km on this graph. If we set  $2.1 \times 10^6$  square meter per year, the changes coincide with the rate of rise by Yamakawa-Mogi model. This means that the rate of rise increases  $2.1 \times 10^6$  square per meter at 2012.

Keywords: GNSS, Height, Izu Ohshima Island

## Volcanic activity in Nishinoshima volcano 2013-2016

\*tomozo Ono<sup>1</sup>, Taisei Morishita<sup>1</sup>, Shogo Hamasaki<sup>1</sup>, Kenji Nogami<sup>2</sup>

1. Japan coast Guard, 2. Tokyo Institute of Technology

Since activity starting on November 20, 2013, a volcanic activity at Ogasawara Islands (Bonin Islands) Nishinoshima volcano has continued an active volcanic activity for about 2 years. But the volcanic activity was declining finally, and the eruptive activity wasn't confirmed any more by an investigation after 22 December 2015.

The Japan Coast Guard has been carrying out observation of Nishinoshima volcano in cooperation with the Tokyo Institute of Technology since the volcanic activity's restart was confirmed.

A detailed report is done about a change in the activity style of the eruptive after the flank eruption of volcanic cone on 7 July, 2015.

There was a lava flow which reaches an east-south side coastline from the northeast side of the formed volcanic cone on the south side of Nishinoshima from after May, 2015 to around July.

The volcanic activity of this period has been eruption successively.

And, the summit eruption became dormant at early morning on 6 July, 2015, Japan coast Guard survey vessel was investigating.

And flank eruption has begun from the volcanic cone's north side around 10:50 about 4 hours later. Next day, The eruption resumed from the summit crater of volcanic cone at early morning on 7 July, 2015.

The two big craters were formed to the top of the volcanic cone as a result of flank eruption on July 6-7.

It's the activity style in intermittent eruption of the strombolian type from the activity that strombolian eruption is continued more continuously, it changed.

There were no expansion of land area for lava flow like before on July 2015, because the volume of lava decreased.

The vulcanian eruption was a sound with eruption and infrasonic wave in airplane on 17 November, 2015.

Eruptive activity wasn't admitted in December, 2015, and the temperature in the crater also fell to the surrounding temperature level.

There are no reports of the eruptive activity current as of January, 2016.

Keywords: volcano, Nishinoshima

Precision surveying of the lava flow in Nishinoshima volcano -What has been found from the ultra- low-altitude imaging by the UAV? -

\*Tatsuro Chiba<sup>1</sup>, Hisashi Sasaki<sup>1</sup>, sonoka tsukuda<sup>1</sup>, Kenji Nogami<sup>2</sup>

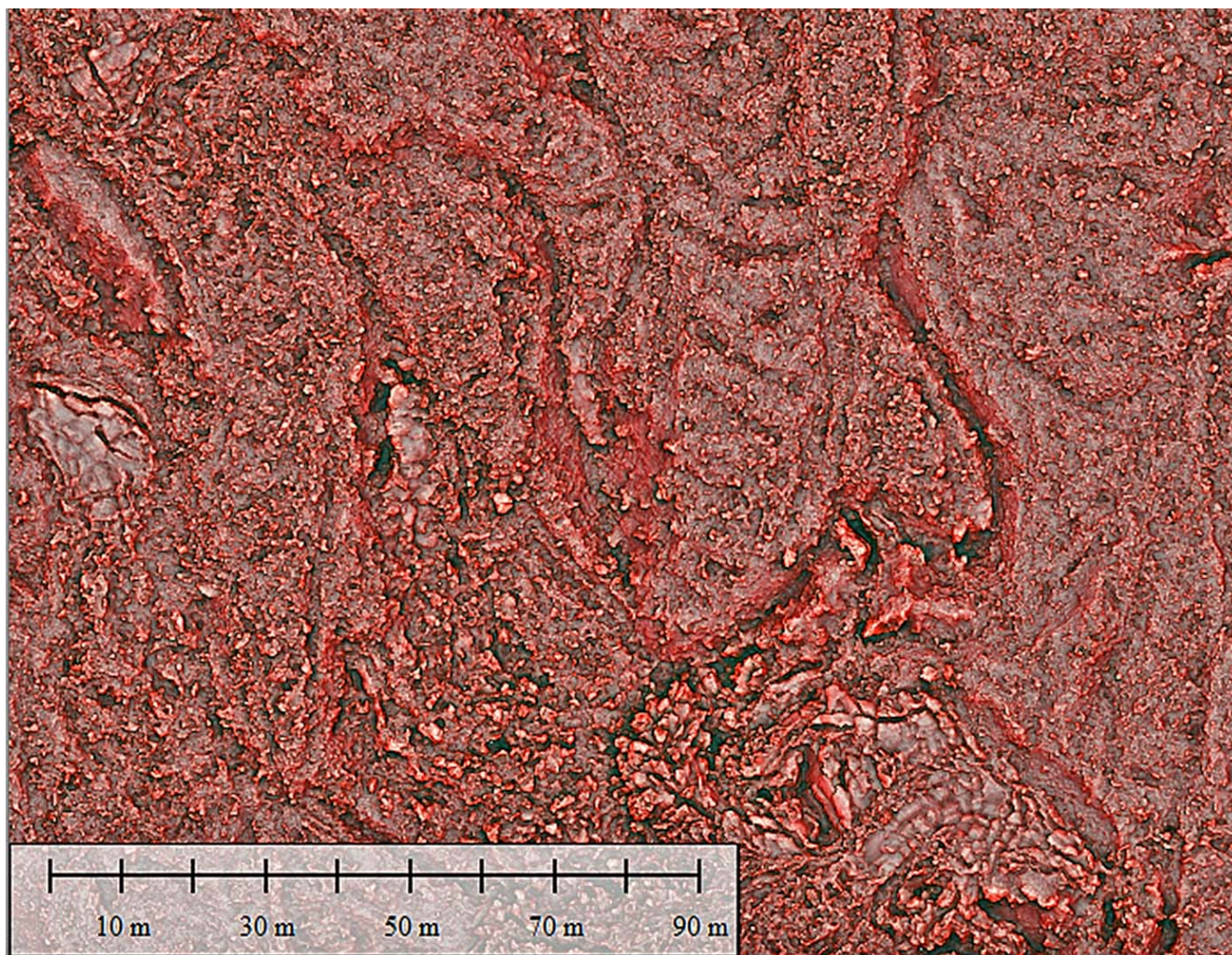
1.Asia Air Survey Co., Ltd., 2.Tokyo Tech University

The Nishinoshima volcano started eruption in November, 2013. Because Nishinoshima was a remote island, the surveying interval was long with several months from several weeks, and the detailed observation of the lava flow situation was difficult. Japan Broadcasting Corporation (NHK) had photographed Nishinoshima island in its active volcanic activity, in a period from May to July, 2015 (Table 1). On May 9th and 12th, NHK launched unmanned aircraft from Chichi-jima island of Ogasawara Islands, and captured images of the island with a single-lens reflex camera for pre-test of a research project. From June 28 to July 3, NHK launched an unmanned helicopter (UAV) from a ship anchored at the point of 4 km from the crater and captured movies and images of the lava flow and the crater in the eruption. The unmanned helicopter had recorded imagery of high resolution and high quality, including 4k video, at 120m flight height above the ground. This project had been collected massive data of Nishinoshima island in its active volcanic activity. From the world-wide point of view, it can be said that this is the first time of collecting repeatedly imagery of volcanic activity from very close position, including lava flow and erupting crater, in a short period of time. In this study, we made 5cm and 25cm DEM based on these images using the SfM (Structure from Motion) software and generated a red relief image map. This resolution has enough precision in order to grasp the width of the crack that occurred on the lava flow surface and the change. We distinguished small impact crater, volcanic bombs, depression fake crater and hornito around the scoria cone. And we distinguished two types of lava flow, one is a'a lava flow and another one is branched tube type lava flow. The a'a lava flows have compressed ridge and levee in surface. The tension cracks are developed on surface of branch tube type lava. The width of cracks become to wide in 4days. And the front of this lava flow was proceeded to a sea shore at the same time. These evidences suggest to inflation of lava flow triggered by molten lava saturation in a tube. This type structure of the branched inflated lava tubes were founded any fields, (1) Jyo-ga-saki shore of Izu Peninsula, (2) 2nd lava flow of Taisho lava in Sakura-jima volcano, (3) Aokigahara lava field of Fuji volcano. The flow speed of a'a lava are faster than branch type lava.

#### Acknowledgment

This result of paper is a part of collaborative research with Japan Broadcasting Corporation (NHK). We are deeply grateful to NHK collected and provided valuable data from the aspects of enhancing volcanic research and spatial technology.

Keywords: photogrametry, UAV, lava inflation



## Shallow Seismic Structure at Nishinoshima Volcano

\*Chiaki Okada<sup>1</sup>, Azusa Nishizawa<sup>1</sup>, Mitsuhiro Oikawa<sup>1</sup>

1. Hydrographic and Oceanographic Department, Japan Coast Guard

Nishinoshima island is located at about 1000 km southward from Tokyo, belonging in the volcanic front of the Izu-Ogasawara (Bonin) arc-trench system. Since an eruption resumed at southeast side of the Nishinoshima mainland in November 2013, for the first time in the almost 40 years, the area of Nishinoshima expands taking in Nishinoshima mainland with a large amount of volcanic lava. Although volcanic activity calms down gradually as of January 2016, it still continues.

Investigating underground structure around Nishinoshima becomes important to understand the volcanic activity of Nishinoshima. The information of underground structure of volcanoes can be expected to elucidate the transfer systems of magma and volcanic fluids accompanied by volcanic activity. Also, we can determine the location of volcanic earthquake more precisely using estimated seismic velocity structure.

Seismic explorations have been done such as Fuji volcano, Aso volcano and Kuchinoerabujima volcano. The seismic exploration results, for example at Aso volcano, revealed the existence of high seismic velocity body centered on the volcanic crater. Additionally Japan Coast Guard (JCG) carried out several ocean bottom seismographic observation at submarine volcanoes such as Myojin-sho and Fukutoku-oka-noba. The results of survey at Fukutoku-oka-noba showed there is the material which attenuates seismic waves under the volcanic body. However there is not so much detailed information about seismic velocity structure of Nishinoshima volcano.

JCG carried out overall geological and geophysical surveys to elucidate the present volcanic activity in detail using S/V *Shoyo* during June to July 2015. The survey includes seismic refraction measurements, using Ocean Bottom Seismograph (OBS) and airgun system, and the seismic reflection measurements using a single channel seismic streamer. The purpose of this measurement is to estimate preliminary shallow crustal seismic velocity structure around Nishinoshima. In this report, we show the results of fan shooting and seismic refraction measurement around Nishinoshima volcano.

In this survey, we shot totally 11 survey lines which went along right over OBSs deployed by JCG, Earthquake Research Institute (ERI) and Meteorological Research Institute (MRI). There are 2 or 3 OBSs in every survey line and the survey line lengths are almost 20 km. Total airgun volume is 3000 (1500x2) inch<sup>3</sup> (about 49 L) and shot interval is 40 seconds.

Based on the results of fan shooting used each OBS's record section, we found the area where the amplitude of seismic waves attenuate depending on the direction of traveling waves. This area might exist just under the volcanic body of Nishinoshima volcano.

In the seismic refraction measurements, the first arrivals of refracted seismic wave of about 4 km/s were observed in each record section at epicentral distances between 3 to 8 km. Many seismograms recorded the first refracted arrivals at the epicentral distances over 10 km. In some record sections, we also found the later phases of around 2 km/s which can be interpreted as reflected seismic signals. According to the preliminary P-wave velocity model obtained by the 2-D ray tracing method, a layer of 2 km/s as the topmost layer has a thickness of around 1.5 km. We could explain observed travel times if the P-wave velocity of the underlying layer will be around 4.5 km/s.

Keywords: Nishinoshima, Shallow crustal structure, Seismic refraction measurement





## Estimation of source location of volcanic earthquakes beneath Nishinoshima volcano applying the envelope correlation method to ocean bottom seismometer data

\*Yutaka Nagaoka<sup>1</sup>, Akimichi Takagi<sup>1</sup>, Kenji Nakata<sup>2</sup>, Kazuhiro Kimura<sup>2</sup>

1.Volcanology Research Department, Meteorological Research Institute, 2.Seismology and Tsunami Research Department, Meteorological Research Institute

Meteorological Research Institute deployed five ocean bottom seismometers (OBS) around Nishinoshima volcano to investigate the source location of volcanic earthquakes. The observation period is from June 21 to October 2, 2015.

As a preliminary analysis, we picked up 45 earthquakes from 30-minute-long OBS data (2015/6/21 07:00:00-07:30:00), converted them into RMS envelope in 4-8 Hz, and estimated source locations applying the envelope correlation method (Obara, 2002). Most earthquake sources located almost right beneath the volcano with a wide distribution in a vertical section. A further analysis is expected to figure out more precise source locations of volcanic earthquakes and to reveal the eruption processes.

Keywords: Nishinoshima volcano, source location, envelope correlation



The re-analysis of the EM data associated with the 2014 eruption, Aso volcano.

\*Mitsuru Utsugi<sup>1</sup>

1.Aso Volcanological Laboratory, Institute for Geothermal Sciences, Graduate School of Science, Kyoto University

On Aso volcano, magmatic eruption was occurred at Nov. 2014, first time in 21 years. Around the Nakadake 1st crater, which is the most active crater of Aso volcano, we conducted continuous geomagnetic field observation (since 1991). From these observations, we obtained the data which suggest the subsurface thermal state had drastically changed before the beginning of the eruption. From the continuous geomagnetic field (total field) observation, significant temporal change was observed. This temporal change began from Oct. 2014, one month before the eruption. The sense of this change is demagnetization and it suggests subsurface temperature was increased. This change was continuing to the end of Apr. 2015. In our study, we re-analysed the data of the temporal change of total field on the period of Oct. 2014 to Apr. 2015. In this study, we tried to decompose the observed change into regional geomagnetic change, periodic change and smoother trend with removing the noise influence based on the method proposed by Hujii and Kanda (2008). As the result, we obtained a clear trend which means the total field change related to the volcanic activity in very high resolution. From this result, it is possible to obtain important information about the magma movement related to the eruption of 2014. In our presentation, we will show the detail about our observation data and results of the data decomposition as well as the model for the movement of subsurface heat sources which is derived by the equivalent source analysis.

Keywords: geomagnetic total field, volcano-magnetic change, thermal demagnetization

Compositional variation of Holocene volcanic products  
from the northwestern part of Aso central cones

\*Masataka Kawaguchi<sup>1</sup>, Toshiaki Hasenaka<sup>1</sup>, Nobutatsu Mochizuki<sup>1</sup>, Hidetoshi Shibuya<sup>1</sup>, Yasushi Mori<sup>2</sup>

1.Graduate School of Science and Technology, Kumamoto University, 2.Kitakyushu Museum of Natural History and Human History

We described the petrography of Holocene volcanic products from the northwestern part of Aso central cones and compared their bulk rock compositions with the result of paleomagnetic study. We examined their genetic relationship by fractional crystallization model.

Holocene volcanic products of this area gradually changes to more unfractionated magma type, from Kishimadake to Ojodake, Komezuka, with time. Paleomagnetic directions determined by Yato et al. (2013) showed that the simultaneous eruptions occurred at different volcanoes. They also showed that the three volcanoes repeatedly erupted after intervals of quiescence. Tamai (2015MS) divided lavas of Kishimadake, Ojodake and Komezuka into 5 stages using magneto-stratigraphy. Kishimadake lava of stage 3 is different from that of stage 1. One is similar to Komezuka lava and has an intergranular texture. The other has an intersertal texture. Mineral assemblage is the same. Ojodake and Komezuka lava show little change in composition, mineral assemblage and texture throughout all stages.

All of the three range from 1.7 to 2.3 in  $\text{FeO}^*/\text{MgO}$  ratio with 51.0-53.5 wt.%  $\text{SiO}_2$ . Ojodake and Komezuka lavas differ in  $\text{FeO}^*/\text{MgO}$  ratio even though they have the same  $\text{SiO}_2$  content. It suggests that steady-state recharge and eruption occurred in the magma supply system for several hundred years. In addition, coeval lavas from different volcanoes, of different chemical compositions, indicate multiple magma chambers were present. Because the Rayleigh fractional crystallization model did not reveal parent-daughter pairs, simple fractional crystallization of the observed phenocryst assemblage do not account for compositional variation of Holocene volcanic products.

Keywords: Aso, central cones, post-caldera volcanism, Holocene, paleomagnetic directions, chemical compositions

## Continuous soil diffuse CO<sub>2</sub> flux measurement at Aso volcano, Japan

\*Toshiya Mori<sup>1</sup>, Masaaki Morita<sup>1</sup>, Akihiko Yokoo<sup>2</sup>, Takahiro Ohkura<sup>2</sup>, Yuichi Morita<sup>3</sup>

1.Geochemical Research Center, Graduate School of Science, the University of Tokyo, 2.Aso Volcanological Laboratory, Institute for Geothermal Sciences, Graduate School of Science, Kyoto University, 3.Earthquake Research Institute, The University of Tokyo

Carbon dioxide is a major volcanic gas component which gives important information for monitoring volcanic activities. This gas is not only emitted as volcanic plumes from craters and fumarolic areas but also widely emitted through soil surface of volcanoes as invisible emission called "diffuse degassing". There are several advantages for monitoring the soil diffuse degassing, because the soil gas usually do not have corrosive acidic gases and its temperature are generally low. Thus, it is much easier to carry out continuous monitoring compared to that for high temperature fumarolic gases. Many precursory changes have been reported related to soil diffuse flux of CO<sub>2</sub> prior to the volcanic eruptions or to significant changes of volcanic activities. We set up a CO<sub>2</sub> flux station (West systems, Italy) for continuous monitoring of soil CO<sub>2</sub> diffuse degassing at Aso volcano, Japan, in early Jan. 2016. The station was set about 1 km south-west from the rim of a currently active crater of Mt. Nakadake near Hondo observatory of Kyoto University. The station is powered by solar panel system and measures the soil CO<sub>2</sub> flux every hour by the accumulation chamber method together with various meteorological parameters such as air temperature, air pressure, humidity, precipitation, wind speed and etc. At least until mid Feb. 2016, the CO<sub>2</sub> flux has been low ranging below 0.28 moles/m<sup>2</sup>/day. In the presentation we will introduce our measurement at Aso volcano, discuss influence of various meteorological elements to the diffuse CO<sub>2</sub> flux, and compare the flux with the volcanic activities of Aso volcano.

Keywords: Aso volcano, volcanic gas, CO<sub>2</sub> diffuse degassing

## Temporal variation of source locations and occurring conditions of continuous tremors at Aso volcano

\*Misa Ichimura<sup>1</sup>, Akihiko Yokoo<sup>1</sup>, Tsuneomi Kagiya<sup>1</sup>, Shin Yoshikawa<sup>1</sup>, Hiroyuki Inoue<sup>1</sup>

1. Graduate School of Science, Kyoto University

In November 2014, magmatic eruptions started at Aso volcano after 20 years dormancy. About one year before this eruption activity, a new eruptive vent was opened and several ash emissions occurred in January 2014. At this period, significant changes in both amplitude and peak frequency of continuous tremors had been recognized. The amplitude of 5-10 Hz band-filtered seismograms recorded at station SUN increased gently until December 22, 2013 (Stage I). The peak frequency increased from 2 to 3 Hz. Until December 30 (Stage II) the amplitude increased rapidly (3 Hz). After a sharp amplitude decrease on December 30, the amplitude took high value until January 2, 2014 (2 Hz, Stage III). From 2 to 3 January it reduced sharply. The amplitude increase similar to Stage I was observed for 10 days (3 Hz, Stage IV). From 13 to 20 January, it took very low value with 1.8 Hz peak (Stage V).

In this study, we focus this two-months stage of volcanic activities to understand source process of the continuous tremors.

For locating tremor sources, we perform a grid searching using a spatial distribution of amplitude ratios of the tremors recorded at five seismic stations around the crater. Estimated source locations distribute from the ground surface to a depth of 700 m beneath the crater and migrate through the analyzed period. The source depths in Stage I to IV are 260, 180, 190, 350 m, respectively. Distribution of these source locations connects the ground surface and the upper end of the crack-like conduit (Yamamoto et al., 1999). It also passes through a low resistivity area (Kanda et al., 2008). This may indicate the shallowest pathway of volcanic fluids, which has never been revealed.

Julian (1994) suggested that continuous tremors caused by oscillation of channel walls through which fluids pass. Using this model, we find that both amplitude and peak frequency of the oscillation depend on conditions of both channel thickness and output fluid pressures. For instance, increase of channel thickness makes amplitude to increase. The increase in the thickness can be regarded as expansion of a fluid pathway according to increase of fluid supply (Aki et al., 1977). Additionally, as an output pressure increases, both amplitude and frequency increase as well. Increase and decrease of the output pressure can relate to choke and widening of the pathway, respectively.

Based on all information aforementioned we suppose qualitatively temporal variation of source locations and occurring conditions of the continuous tremors at Aso volcano as follows. In Stage I, we observed the increase of both tremor amplitude and peak frequency. This was caused by increase of fluid pressure in the pathway to reflect supplying of larger amount of volcanic fluids. In order to satisfy this pressure increasing, a conjunctive portion at the upper edge of the crack-like conduit that connects to a narrow pathway into the crater was widened. In Stage II, observed increasing of amplitude was owing to an expansion process of the whole part of this narrow pathway. At the end of this stage when we observed both amplitude and frequency dropped, pressure in the upper part of the pathway decreased due to an opening of the vent. In Stage III, the pathway was still enlarging to transport the fluids, which caused large tremor amplitude. The fluid supply then decreased. We detected it as a sharp decrease of tremor amplitude and increase of the peak frequency. In Stage IV, fluid supply increased again. To satisfy the increase of the fluid pressure, the upper part of the crack-like conduit was expanded again. However, observed amplitude

was not so large rather than the Stages II and III because establishment of the pathway had been already completed in those stages. At the end of this stage, occurrence of ash eruptions led to pressure drop in the shallower portion of the pathway so that we could detect both the amplitude and frequency decreased.

Keywords: volcanic tremor, Aso volcano

## Monitoring volcanic long period tremors from Aso volcano in 2014-2015

\*Yurie Mukai<sup>1</sup>, Kazuya Yamakawa<sup>1</sup>, Akiko Takeo<sup>2</sup>, Takuto Maeda<sup>2</sup>, Kazushige Obara<sup>2</sup>

1.Department of Earth and Planetary Science, the University of Tokyo, 2.Earthquake Research Institute, the University of Tokyo

### Introduction

Aso volcano is one of the most active volcanoes in Japan and has erupted repeatedly more than a thousand years since the dawn of history. It has been proposed that long period tremors (LPTs) are caused beneath Aso volcano by the elastic interaction between the volcanic gasses or ash passing the crack-like vent, and the wall of the vent. This LPTs have a dominant period of about 15 s. By monitoring the LPTs from Aso volcano for two years from 2014 to 2015, we revealed the relationship between LPTs and eruptive activities.

### The monitoring of LPTs

We used three-component broadband seismograms from seven F-net broadband seismograph network stations operated by National Research Institute for Earth Science and Disaster Prevention around Aso volcano. First, we investigated the changes in daily power spectrum for each component and each station. The continuous signal with a dominant period of 8-12 s was observed at time periods from October 2014 to April 2015, and from September to October 2015. These periods well agree with Strombolian eruptions and occurrence of volcanic tremors reported by Japan Meteorological Agency. Furthermore, this signal was not observed in the same season in the previous year. Therefore, it is interpreted as LPT signal rather than seasonal changes of microseisms. The signal amplitude was dominated in the radial and vertical component measured from Aso volcano, and this suggests that it was Rayleigh waves of the LPT.

Then, we detected LPTs by applying the matched filter technique. We first selected a LPT event with high signal-to-noise ratio as a template event, and prepared three-component waveforms at the seven stations. We then calculated the cross-correlation coefficient between the template and continuous waveforms, with sliding the time window through the continuous waveforms for two years, to compute the sum of 21 cross-correlation coefficients as a function of time. When the sum of the coefficients exceeded a threshold set based on the median absolute deviation, we detected an event as a LPT. The amplitude ratio between the template and detected events were also estimated by a waveform fitting method. We also applied the same analysis to records from six stations because a record of one station was unavailable for a period in 2015.

As a result, we detected LPTs with wider dynamic range in amplitudes, including amplitudes smaller than 100 nm/s, which previous study (Sandambata et al., 2015) excluded from their analysis. In addition, we observed that the amplitude of LPTs dropped sharply only from the end of December 2014 to January 2015 during the continuous eruption from November 25th, 2014 to May 21st, 2015.

### Changes in frequency-amplitude distribution

We divided the analysis period into 21 stages based on the trend of the time-series of LPT amplitude and calculated frequency-amplitude distribution for each stage. Previous study (Sandambata et al., 2015) showed that the distribution follows the power-law distribution rather than the exponential distribution just after the Strombolian eruption in November 2014 and interpreted that the characteristic amplitude scale was lost by the Strombolian eruption. We obtained the similar result during this period. We note that the all stages in 2015 activities show that they follow exponential distribution, and this suggests the peculiarity of the Strombolian eruption in November 2014. On the other hand, smaller LPTs dominated from the end of December 2014 to January 2015 compared to other stages. Japan Meteorological Agency reported that grayish white

fumes were observed from November to December 2014 and from March to May 2015, whereas white fumes were observed from January to February 2015. Our result and the reported phenomena indicate that the change in the main component of the fumes from water vapor to volcanic ash had some effect on the amplitude of LPTs.

Keywords: Mount Aso, Volcanic tremor, Long period tremor, Frequency-amplitude distribution, Rayleigh wave

Tilt changes associated with eruptions by the tiltmeter array at Aso volcano.

\*Rintaro Miyamachi<sup>1</sup>, Takahiro Ohkura<sup>2</sup>, Hiroyuki Inoue<sup>2</sup>, Takeshi Matsushima<sup>1</sup>, Shiori Fujita<sup>1</sup>, Hiroshi Shimizu<sup>1</sup>

1.Institute of Seismology and Volcanology, Faculty of Sciences, Kyushu University, 2.Aso Volcanological Laboratory, Faculty of Science, Kyoto University

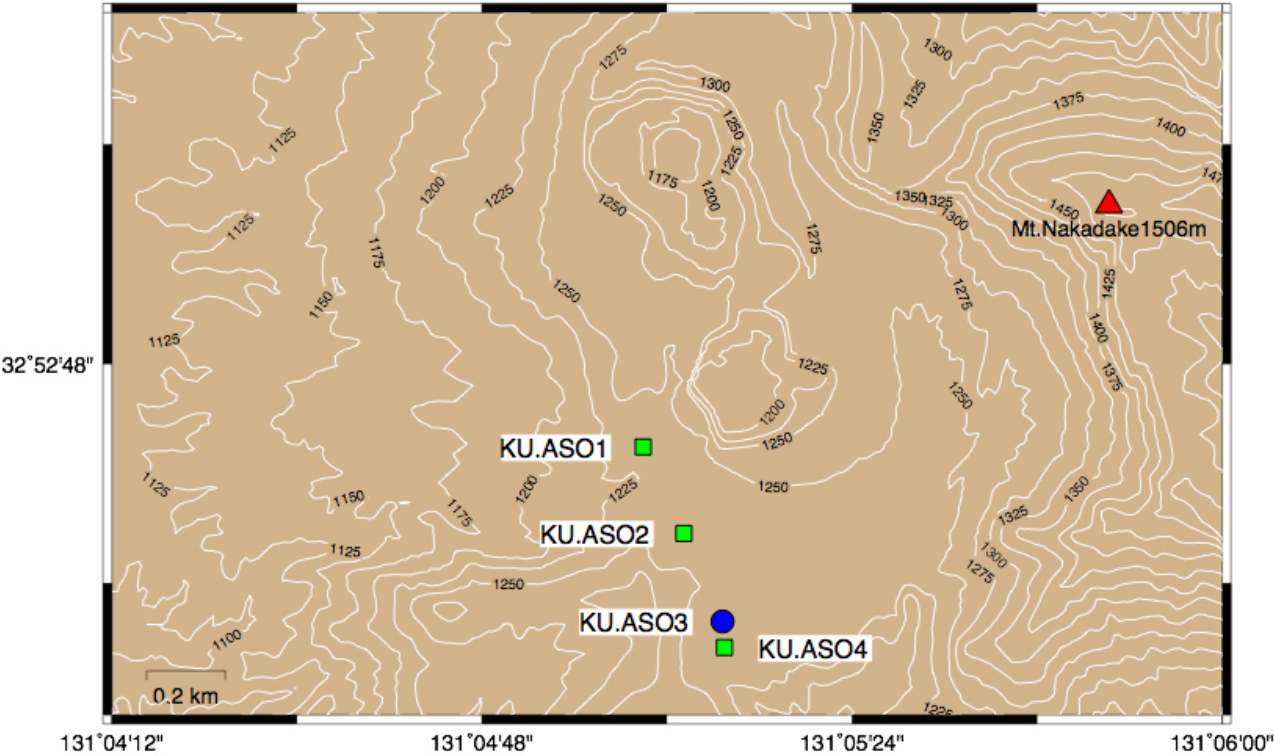
Aso volcano started magmatic eruptions from November 25, 2014. Eruptive activity once became quiet in mid 2015. However, a phreatomagmatic eruption occurred on 14 September 2015, and phreatic eruptions have sporadically occurred until February 2016. We investigate the space-time variation of pressure sources associated with volcanic eruptions in order to understand the eruption process in the shallow volcanic conduit of Aso volcano.

In general, an observation using tiltmeter is arranged so as to surround the volcano, for the estimation of location of pressure sources. In this study, however, a tiltmeter array deployed in a straight line to the first crater of Nakadake, assuming the pressure sources locate beneath the crater. By calculating the cross-correlation of tilt variations recorded at each station, we can estimate the depth change of pressure source with time associated with eruption at the first crater of Nakadake of Aso volcano.

The tiltmeter has been installed three points (KU.AS01, KU.AS02, KU.AS04) to the south of the first crater of Nakadake (Fig.1). At KU.AS01 and KU.AS02, the tiltmeters were set in the ground. In addition, we have installed a microphone and a broadband seismometer at KU.AS01 and KU.AS03, respectively. The observation started from July 14, 2015, and we successfully observed the tilt changes associated with eruptions of 14 September, 23 October and 7 December 2015.

Keywords: Aso volcano, Tilt array





## Source depth of Strombolian eruptions at Aso volcano in April 2015

\*Kyoka Ishii<sup>1</sup>, Akihiko Yokoo<sup>1</sup>, Tsuneomi Kagiya<sup>1</sup>, Takahiro Ohkura<sup>1</sup>, Shin Yoshikawa<sup>1</sup>, Hiroyuki Inoue<sup>1</sup>

1. Graduate School of Science, Kyoto University

At the Nakadake 1st crater of Aso volcano, magmatic eruptions had started in November 2014 after 22 years dormancy. This eruption activity lasted until May 2015. It was a first time for us to observe the eruptions using a network of seismo-acoustic sensors deployed around the crater. We have stations equipped with a low-frequency microphone (ACM) and a short-period seismometer (KAF) on the crater rim. They are situated at 260 m SW and 230 m SWW from the active vent, respectively. On the NNW flank of the volcano (830 m distance), a broadband seismometer (UMAB) is installed. In this study, we analyze seismo-acoustic data acquired at these three stations in the 19:00-20:00 JST (GMT+9:00) on 24 April 2015 to estimate source depths of Strombolian eruptions.

At each Strombolian eruption, characteristic seismo-acoustic signals were observed. They were typically started by a downward phase of low-frequency ( $<0.1$  Hz) seismic velocity to the UMAB station. This wave corresponded to a long period tremor (LPT; Yamamoto et al., 1999, GRL). A couple of seconds later (1.7-5.4 s), higher frequency (5-10 Hz) seismic velocity arrived to the KAF station. Infrasound wave was detected at ACM about 1 s after the seismic arrival to KAF. The infrasound wave (peak frequency is  $\sim 0.5$  Hz) was started by a compression phase, however in 0.1 s later a high-frequency content ( $>10$  Hz) was added on it. We can recognize a strong positive correlation ( $R=0.92$ ) between Root-Mean-Squared (RMS) amplitude of the seismic velocity at KAF and that of 10 Hz high-passed infrasound wave at ACM. The time delay between the arrivals of these two signals was 0.93-1.56 s (mean 1.2 s).

To estimate source depth of each Strombolian eruption, we assumed that a space in the conduit through which infrasound wave propagates was occupied with hot volcanic gases. On the basis of a composition ( $\text{H}_2\text{O}:\text{SO}_2:\text{CO}_2=90:4:4$ ; Shinohara, Pers. Comm., 2016) and a temperature data (330-360 K at the vent), the sound velocity inside the conduit was estimated to be 410-430 m/s. We also considered that seismic signals observed at KAF are composed of the P wave ( $V_p=3.3$  km/s; Tsutsui et al., 2003, BVSJ). It resulted in the source depth of each Strombolian eruption to be 70-380 m. This depth is consisted with a shallow region above an upper edge of the crack-like conduit (300 m; Yamamoto et al., 1999, GRL).

We intended that signals of LPT arrived to UMAB was 1.7-5.4 s earlier from the arrival time of high-frequency seismic wave to KAF. Because LPT is resulted from a resonant oscillation of the fluid-filled crack-like conduit beneath the active crater (Yamamoto et al., 1999, GRL), Strombolian seems to relate the source of LPT as well. According to a near-field effect, the phase velocity of the LPT has a value between those of the P and S waves (3.3 and 1.9 km/s; Sudo and Kong, 2001, BV). It indicates that ascending speed from the source location of the LPT, at the center of the crack-like conduit (1.6-1.8 km; Yamamoto et al., 1999, GRL), to the depth of Strombolian eruption we could estimate (70-380 m) is 300-700 m/s. It is too fast to consider that the volcanic fluids (magma and gases) migrate upward with this velocity. At the present, we interpret it as a pressure wave; it is radiated from the LPT source at the same time of the LPT occurrence and propagates inside the crack-like conduit to the depth of Strombolian eruption. Estimated speed of the pressure wave (300-700 m/s) is accountable either when andesite molten magma (sound velocity is 2.3-2.5 km/s; Murase and McBirny, 1973, BGSA) includes bubbles at a few vol.% (Morrissey and Chouet, 2001, JVGR), or when  $\text{H}_2\text{O}$  vapor steam contains small amount of ash particles ( $<10$  vol.%). The time delay of 0.1 s between arrival times of the 0.5 Hz and  $>10$  Hz infrasound waves at ACM may become a clue to understand detailed process of Strombolian eruption at the depth.

Keywords: Aso Volcano, Strombolian eruptions, Aso 2015 Eruption

## New fumarole activity at the southwest rim of Ioyama in Kirisima volcanoes, Southern Kyushu

\*Yasuhisa Tajima<sup>1</sup>, Toshio Furuzono<sup>2</sup>, Setsuya Nakada<sup>3</sup>, Jun Funasaki<sup>4</sup>, Observation members Kirisima nature guide club<sup>2</sup>

1.Nippon Koei Co.,LTD., 2.Kirishima nature guide club, 3.Earthquake Research Institute, The University of Tokyo, 4.Miyazaki Local Meteorological Office

A new fumarole appeared on the southwest rim of the Ioyama old crater in the Kirisima volcanoes on December 14<sup>th</sup>, 2015. Previously, two main fumarole zones were active in Ebinokogen site: the Ebino fumarole zone in the west and the Ioyama fumarole zone in the east (Geothermal Research Department, the Geological Survey of Japan (GSJ), 1955). The Ebino fumarole zone was very active from the 1940s to 1960s (Council for conservation of nature of Ebinokogen, 1987). Temperatures were measured by GSJ at depths of 1 m in the Ebino fumarole zone and observed 96°C in 1954. In the 1940s to 1960s, this zone moved to the west, and the activity decreased until 1970s.

The center of the Ioyama fumarole zone is about 0.8 to 1 km to the east of the center of the Ebino fumarole zone (Geothermal Research Department, GSJ, 1955). Records from sulfur mining indicate that the Ioyama fumarole zone has been active before AD 1900. The oldest fumarole temperature was recorded over 80°C in Ioyama measured by Oda Ryohei on August 12<sup>th</sup>, 1916 (Oda, 1922). Akiko Yoshano described the fumarole in a short Japanese poem in 1929. The temperature of the fumarole in the Ioyama fumarole zone reached between 96 and 120°C in 1954 (Geothermal Research Department, GSJ, 1955). The highest temperature in the Ioyama fumarole zone was recorded as 247°C in March 1975 (Kagiyama, 1979) and five measurements over 150°C in August 1987 (Kagiyama, 1987). However, the activity of this zone declined in 1990s, and we could not find the fumarole in 2008.

The first volcanic tremor was observed on August 14<sup>th</sup>, 2014 under the periphery area of Karakunidake. And volcanic earthquakes and tremors were observed occasionally from July 2015 (JMA Homepage). A member of the Kirisima nature guide club found a very small fumarole on the afternoon of December 14, 2015 on the southwest rim of Ioyama old crater. A fumarole had previously been identified at this location in the Ioyama fumarole zone. The fumarole temperature was 80°C on this day. We observed temperatures between 93 and 96°C in the fumarole on December 25<sup>th</sup> and 27<sup>th</sup>. This new fumarole and high temperature area has continued to expand to the north and south of the original location as of February 2016. We are monitoring changes in the temperature, direction of movement, and location of the fumaroles.

Observation members of Kirisima nature guide club: Kentaro Haraguchi, Takeji, Nagatomo, Takamichi Higashi, Midori Baba, Hideaki Yoshinaga.

Keywords: Kirisima volcanoes, Ioyama, fumarole

## Chemical and isotopic composition of the fumarolic gas sampled at Mt Iwoyama, Kirishima volcanic area, Japan

\*Takeshi Ohba<sup>1</sup>, Muga Yaguchi<sup>1</sup>

1.Department of chemistry, School of Science, Tokia University

### Introduction

Mt Iwoyama is one of the active volcanoes in Kirishima volcanic area, located on the northern flank of Mt Karakuni. Mt Iwoyama was formed at the eruption in 1768 (Imura and Kobayashi, 2001). According to the observation by Japan Meteorological Agency (JMA), in the early of April 2014, the number of volcanic earthquakes increased. In July 2015, volcanic tremors occurred several times. On 15<sup>th</sup> Dec 2015, a new discharge of fumarolic gas was noticed on the top of Mt Iwoyama. Those observations indicate the increase of volcanic activity of Mt Iwoyama. In general, the composition of fumarolic gas changes along the progress of volcanic activity. We sampled the newly discharged fumarolic gas on 22<sup>th</sup> Dec 2015 and report the analytical result with interpretations.

### Sampling of fumarolic gas

The position of fumarolic gas was N31deg56min48.3sec, E130deg51min10.5sec. The surrounding area of fumaric gas was covered with whitish altered rock. The temperature of gas was 97.2C. No fumarolic gas other than the observed one was noticed.

### Results and discussions

The concentration of HCl was lower than the analytical detection limit. The SO<sub>2</sub>/H<sub>2</sub>S ratio was 0.027, similar to the value in 1994 (Ohba et al., 1997). The H<sub>2</sub>O-CO<sub>2</sub>-S ternary composition indicates the CO<sub>2</sub> enrichment compared to the gas in 1994. The isotope ratio of H<sub>2</sub>O (dD) was -91 per mill, lower than -55 and -80 per mill, the values of two fumarolic gases in 1994. A part of water vapor in the observed fumarolic gas seems to be removed by the condensation before the discharge at fumarole, because the isotope ratio was low and the fumarolic gas has appeared at the place with no discharge of fumarolic gas, which means the channel of volcanic gas in crust was cool and it removes the enthalpy of water vapor. The H<sub>2</sub>O-CO<sub>2</sub>-S ternary composition and isotopic ratio of H<sub>2</sub>O can be estimated with the calculated addition of H<sub>2</sub>O removed by condensation. The estimated composition and ratio were similar to the fumarolic gases in 1994 and 1991 at Mt Iwoyama. The N<sub>2</sub>-Ar-He ternary composition indicated He enrichment relative to the gases sampled in 1991 and 1994. Kita et al (1993) reported the He enriched endmember in fumarolic gases at some volcanoes in south-east part of Japan such as Mt Unzen-Fugendake. If the He enriched endmember is contained in the sampled fumarolic gas, a magma should be involved with nature different from the degassing magma in 1994. Because the number of sampled fumarolic gas is only one, we need to continue the sampling and analysis to confirm the N<sub>2</sub>-Ar-He ternary composition.

### Acknowledgements

This study was supported by JSPS KAKENHI (15K12485). We sincerely thank Dr K Kokubo of JMA and Fukuoka Regional Headquarters JMA, for the assistance of fumarolic gas sampling.

Keywords: Active volcano, Volcanic gas, Geochemistry

## Volcanic tremor recorded on two seismic arrays at Kirishima volcano, Japan

\*Manami Nakamoto<sup>1</sup>, Satoshi Matsumoto<sup>1</sup>, Hiroshi Shimizu<sup>1</sup>

1. Institute of Seismology and Volcanology, Faculty of Science, Kyushu University

The Kirishima volcano complex is a group of more than 20 volcanoes in southern Kyushu Island, Japan. The 2011 eruption of Shinmoedake, one of them, was preceded by phreatic events on August 22, 2008 and continued until September 7, 2011. After that we found no remarkable volcanic activity at the volcano. Recently, however, it is observed that fumarolic gas is rising at Ioyama and crustal deformation studies point out ground uplift around the area. Because volcanic earthquakes and tremors also occurred, it is necessary to pay attention to change on the activity. Volcanic tremors are considered to be oscillations that occur in the magma supply system. Therefore, it is important to investigate location of their source and characteristics for understanding the conditions and processes of volcanic activity. We carried out two seismic array observations at Kirishima volcano to reveal source location of volcanic tremor.

It is difficult to locate tremor sources by conventional methods using travel times because we cannot pick the arrival time correctly. One useful method of estimating the source locations is array analysis, which uses data from a dense seismic network in small area. Generally, a seismic array can decompose waves approaching from many directions and determine the slowness of each wave. Although location of the source cannot be uniquely determined by only one seismic array, multiple array enable us to estimate the source location. We deployed two seismic array on August 30, 2014. One consisted of 7 seismometers located near Ohata pond 5 km away from Shinmoedake crater, and the other consisted 7 seismometers located at Shinyu hot springs 3km away from the crater. They were installed with a sensor interval of 200-350 m, and signals from the seismometers were recorded by a data logger with 250 Hz sampling frequency. We use the combination of two array to determine the tremor sources. Moreover, we can also detect temporal change by array analysis.

From August 30, 2014 to October 5, 2015, two volcanic tremor were recorded at our site. We analyzed the tremor which occurred on July 26 at 9:23, 2015 and its duration was about 150 seconds. Peak frequency of the tremor was about 2-3 Hz. As the result of semblance analysis with 2-4 Hz band-pass filter, we found that the tremor was radiated from WSW direction to Ohata array and from north direction to Shinyu array, corresponding to Ioyama area.

Keywords: Kirishima volcano, volcanic tremor, seismic array

## Continuous relative gravity observation at Sakurajima Volcano: Short-period gravity changes before and after eruptions

\*Tsuyoshi Kurihara<sup>1</sup>, Takahito Kazama<sup>1</sup>, Keigo Yamamoto<sup>2</sup>, Masato Iguchi<sup>2</sup>

1.Kyoto University, 2.DPRI, Kyoto University

Mass movement in a volcano leads to minute gravity changes on the ground, along with crustal deformations. Since the amplitude of the gravity changes depends on the density of the mass moving in the volcano, gravity observation is useful to directly understand the mechanism of the crustal deformations, such as melt supply from the deep underground and magma degassing in a magma chamber. In Sakurajima Volcano (Kagoshima Prefecture, Japan), crustal deformations have been observed to discuss preparation processes for eruptions with broadband time periods from seconds to years (e.g., Iguchi et al., 2008; Hotta et al., 2016). Okubo et al. (2013) also collected absolute gravity values at Arimura (2.1 km south-southeast from the Showa crater of Sakurajima Volcano) continuously, and observed the 10-micro-Gal gravity decrease associated with the magma ascent in a volcanic conduit. However, they only focused on the absolute gravity changes with the period of more than a few days, because the short-period absolute gravity values they collected were noisier than the long-period ones. Precise continuous gravity changes should be collected with the high sampling rate, in order to understand broadband activities of Sakurajima Volcano in terms of mass movement.

We were thus motivated to discuss the short-period processes of mass movements in Sakurajima Volcano, using the continuous relative gravity data sampled every one minute. The gravity data were collected by a Scintrex CG-3M relative gravimeter at Arimura Observatory from September 2010 to December 2015. The gravity data was dominated by several disturbances such as the instrumental drift, the long-period tidal effect with periods of more than a day, and the short-period tidal effect with periods of less than a day, which should be corrected from the original gravity data to retrieve gravity signals associated with volcanism. We first corrected the gravity changes due to the instrumental drift and long-period tides, by subtracting synthetic gravity changes expected by a spline function, which was calculated from the two-day average values of the original gravity data. We also corrected the short-period tidal effect by a tidal analysis software, BAYTAP-G (Tamura et al., 1991). Moreover, we reduced the effect of ground vibrations by stacking the two-day-long gravity data, which was cut off from the corrected gravity time series in 2013 and 2014 on the condition that the median time of the two-day window corresponds to the time of an eruption with a volcanic plume of >3000 m altitude. Note that we individually analyze the gravity data during the non-explosive eruption at 10:18 JST, 26 September 2013, because the small ground vibration enabled us to recognize volcanic gravity signals directly.

The stacked gravity data for the 2013 eruptions showed a slow decrease of about -20 micro-Gal since 12 hours ahead of the eruptions. The stacked gravity data for the 2014 eruptions also showed a rapid increase of about +30 micro-Gal in 30 minutes just after the eruptions. In addition, whereas no significant tilt variations were observed during the eruption on 26 September 2013, the simultaneously obtained gravity data showed a slow decrease since about 5 hours before the eruption, and the gravity value returned to the original level just after the eruption. These gravity changes can be explained by the inflation/deflation of a magma chamber below Sakurajima Volcano or the ascent/descent of magma mass in a volcanic conduit. In this presentation, these possibilities will be discussed quantitatively to understand the short-period process of mass movement in Sakurajima Volcano.

Keywords: relative gravity, gravity change, Sakurajima Volcano, magma, short period, density



## Spectral Ratio Analysis of Explosion Earthquakes at Sakurajima Volcano

\*Mohammad Hasib<sup>1</sup>, Takeshi Nishimura<sup>1</sup>

1. Department of Geophysics, Graduate School of Science, Tohoku University

Sakurajima volcano has been quite active, and hundreds of small explosions of vulcanian type occur every year, throwing ash to heights of up to a few kilometers above the mountain. Sakurajima volcano generates many explosions with various sizes, but we still have not well understood what physical parameters control the magnitude of explosion. In the present study, therefore, we investigate the source characteristic of explosion earthquakes that are associated with vulcanian explosions at Sakurajima volcano.

We analyze explosion earthquake waveform that are recorded by JMA for the two years from 2012 to 2013. The seismogram are recorded by short period seismometers with a natural frequency of 1 Hz and a sampling frequency of 100 Hz. We analyze Up-Down (U) component at SRB station which is located at a distance about 2 km from the active crater (Showa crater).

We reduce the site effect and propagation effect in the observed seismogram by using spectral ratio method to retrieve the source characteristic of explosion earthquake. We classify the explosion earthquake waveform by using RMS amplitude into 4 classes. The RMS amplitude is calculated for about 400 s from the onset of the earthquake. The RMS amplitude ranges up to  $470 \times 10^{-3}$  nm, and we divide the explosion earthquakes into class I ( $0$  nm -  $30 \times 10^{-3}$  nm), class II ( $30 \times 10^{-3}$  nm -  $60 \times 10^{-3}$  nm), class III ( $60 \times 10^{-3}$  nm -  $90 \times 10^{-3}$  nm) and class IV ( $90 \times 10^{-3}$  nm -  $150 \times 10^{-3}$  nm). We calculate the spectral ratios of class II, III and IV to the smallest class (I). We calculate the spectral ratios by setting a time window every 10 sec from the onset to coda wave.

The obtained spectrum amplitude ratio can be described by a flat level at low frequency range ( $0$  Hz -  $1$  Hz) and that at high frequency range ( $4.5$  Hz -  $10$  Hz). The spectrum amplitude ratio gradually decreases in the intermediate frequency range ( $1$  Hz -  $4.5$  Hz). The corner frequencies at  $1$  Hz -  $4.5$  Hz does not change significant (change slightly) for the ratio of classes II, III and IV. Analysis of direct waves that begins from the onset for 10 sec show the following characteristics: Ratios at low frequency range for classes III and IV are about 1.6 and 3 times larger than that for class II, while ratios at high frequency range for class III and IV are about 1.3 and 2 times larger than that for class II. Analysis of coda waves that begins 50 sec from the onset show the following characteristics: Ratios at low frequency range for classes III and IV are about 1.4 and 1.9 times larger than for class II. On the other hand, ratios at high frequency range for class III and IV are about 1.06 and 1.1 times larger than that for class II. The ratios for coda waves are slightly smaller than those for direct waves, which implies differences in the source processes between the initial explosion and following continuous ash emissions.

Keywords: Spectral Ratio Analysis, Sakurajima Volcano, Explosion Earthquake

Temporal variation of the ACROSS signals during a period from January to August, 2015 in Sakurajima volcano, Japan.

\*Koshun Yamaoka<sup>1</sup>, Hiroki Miyamachi<sup>2</sup>, Hiroshi Yakiwara<sup>2</sup>, Yuta Maeda<sup>1</sup>, Toshiki Watanabe<sup>1</sup>, Takahiro Kunitomo<sup>1</sup>, Ryoya Ikuta<sup>3</sup>, Takeshi Tameguri<sup>4</sup>, Hiroshi Shimizu<sup>5</sup>, masashi watanabe<sup>1</sup>, Masato Iguchi<sup>4</sup>

1.Earthquake and Volcano Research Center, Graduate School of Environmental Studies, Nagoya University, 2.Graduate school of Science and Engineering, Kagoshima University, 3.Faculty of Science, Shizuoka University, 4.Disaster Prevention Research Institute, Kyoto University, 5.Graduate school of Science, Kyushu University

Quantitative monitoring of magma transport process is essentially important for understanding the volcanic process and prediction of volcanic eruptions. To realize this monitoring, an active monitoring system using a vibration source called ACROSS has been operated in Sakurajima Volcano since September 2012 (Yamaoka et al., 2014; Miyamachi et al., 2013; 2014).

From our previous observational studies, we obviously found that the amplitude and travel times of the daily transfer functions (the ACROSS signal) vary temporally. In particular Maeda et al. (2015) revealed that the amplitude of the ACROSS signals in the later phases became small in several hours before and after explosive eruptions. In this report, we show a long-term temporal change for the ACROSS signals observed with the remarkable volcanic activity that occurred in Sakurajima volcano on August 15, 2015.

#### DATA

Our ACROSS system is composed of two vibrators: one vibrator (SKR1) with a signal frequency range of 7.510Hz +/- 2.50Hz and the other (SKR2) with the range of 12.505Hz +/- 2.50Hz. The seismic signals from the ACROSS sources are routinely monitored with more than 20 permanent and 5 temporal seismic stations in and around Sakurajima volcano. The signals recorded at the seismic stations are deconvoluted with the ACROSS source function to obtain the transfer function between the source and the receivers.

The ACROSS system was continuously operated until 18 August, 2015 after five month failure of inverter system. We successfully replace the broken inverter with a normal one by managing transferring inverters from one source to another. The fixed ACROSS system started operation at the beginning of January 2015, but the operation was suspended on 18 August, 2015 because of the signal contamination to a monitoring seismic station for the volcano. We use the data in 2015 to check the temporal change of transfer functions between the ACROSS source and the seismic stations in Sakurajima island.

#### RESULTS

We calculated the daily transfer functions for each station by every 1 day stacked data during a period of January to August 2015. Transfer functions in Sakurajima volcano indicate large temporal variation especially in later phase part comparing to the other site such as Awaji or Tokai area where ACROSS system is being operated. In many of the transfer function connecting between the ACROSS source and the stations remarkable change can be seen at the end of July, 2015, though causal relationship to the volcanic event on 15 August is not clear. We also need to make a quantitative investigation on the meteorological effect to the transfer functions.

#### Reference

Yamaoka et al. (2014) Earth Planets, Space, Doi:10.1186/1880-5981-66-32  
Maeda et al. (2015) Geophys. Res. Lett., Doi: 10.1002/2015GL064351

Keywords: structure, temporal variation, magma

Unknown later arrivals in controlled source seismograms in northern Kagoshima Bay region.

\*Tomoki Tsutsui<sup>1</sup>, Takeshi Tameguri<sup>2</sup>, Masato Iguchi<sup>2</sup>, Haruhisa Nakamichi<sup>2</sup>

1.Akita University, 2.Kyoto University

We will present unknown later arrivals in the controlled source seismograms which detected in northern Kagoshima Bay area, and will discuss their origin and structure in the area.

Project Sakurajima 2008 had been conducted with chemical explosion for the sake of exploring magma system and its background structure on November 2008 (Iguchi et al., 2009). A dataset of first arrival time has been analyzed down to 4km below sea level by Miyamachi et al. (2013) and Tameguri et al. (2012). They presented that velocity is lower inside of Aira Caldera than that of outside.

On the other hand, the seismograms also include following two prominent later arrivals which have never been discussed;

1. The phase arrives on 7 to 8 seconds over the stations in south Sakurajima through Osumi Peninsula,
2. The phase arrives on 8 seconds over the stations in Shirahama through Uranomae in north eastern Sakurajima.

The arrival 1 appears definitely clear in southeast shore of Sakurajima. Its apparent velocity is just above 7 km/s and then is asymptotically closing that of the first arrival. The similar later arrival appears in other seismograms across the same region of the midpoints. The arrival 2 appears definitely clear at Wariishizaki point, north shore of Sakurajima. Its apparent velocity is over 8 km/s. No similar arrival appears in any seismograms across the same region of the midpoints.

Considering those characteristics of each arrival, the arrival 1 is interpreted as PP reflection and the arrival 2 as PS conversion. Then, assuming wave types, interface model for the reflection and the conversion have been considered, which can explain their travel time better. An interface at 11 km below sea level appears better fit with both of their travel times. Moreover, the mid points and the estimated converted points coincide with each other at the central area of northern Kagoshima Bay. The reflection and the conversion occur at the same interface because of the model and their identical apparent velocity.

The central area of northern Kagoshima Bay involves inflation sources beneath, which have been presented by Mogi (1958); Yokoyama (1971); Eto et al. (1997); Yamamoto et al. (2013); and Iguchi et al. (2013). The interface coincides with those inflation sources. It is of interest that the interface at the center of northern Kagoshima Bay can associate with possible deep magma reservoir which feeds magma to Sakurajima Volcano.

Keywords: Volcano, Sakurajima Volcano, Crustal structure, Seismology

## Seismic activities with regards to the eruptions of Kuchinoerabujima in 2014 and 2015 observed by V-net network

\*Keita Chiba<sup>1</sup>, Toshikazu Tanada<sup>1</sup>

1.National research institute for earth science and disaster prevention

Kuchinoerabujima, which is located about 12km west of Yakushima, is a volcanic island. Explosive eruptions occurred at Shindake in Kuchinoerabujima in 2014 and 2015. It was reported that a new fissure was generated in the western part of the crater of Shindake in the eruption in 2014, according to Coordinating Committee for Prediction of Volcanic eruption in Japan. In addition to this phenomenon, it is also reported that seismic source time functions with regards to these eruptions are different between the eruptions in 2014 and 2015. The north-south component of the source time function was dominant in the eruption in 2015 although only the vertical component of source time function is dominant compared to other components (Matsuzawa: personal communication). To reveal the relationships between these phenomena and seismic activities, we determined the hypocenters and performed waveform analyses using the data-set by Japan Meteorological Agency (JMA) and National Research Institute for Earth Science and Disaster Prevention (NIED) in this study. We assumed half-space with  $V_p=2.5\text{km/s}$  as a velocity structure. The datasets are composed of 165 events from July 27, 2014 to August 3, 2014 (before the eruption in 2014) and 958 events from April 15, 2015 to June 4 in the eruption in 2015 (507 events before the eruption and 451 events after the eruption). It was found that the hypocenter distribution before the eruption in 2014 concentrated in the western part of Shindake and the hypocenter distribution before the eruption in 2015 tends to be distributed over north and south direction in the vicinity of Shindake. The locations of these hypocenters are thus consistent with the location of the fissure generated by the eruption in 2014 and the source time function with the dominant component of north and south direction estimated in the eruption in 2015. On the other hand, it was found that the direction of particle motion of events after the both eruptions tends to be consistent with that by both eruptions. Changes of the corner frequency of the events were not observed before and after the eruption, in both eruptions. From the hypocenter distribution before the eruption in 2015, it is thus implied that eruption products moved to the north and south direction, using an existing weak line generated by the events with the distribution of the north and south direction in the vicinity of the Shindake before the eruption in 2015.

Keywords: Kuchinoerabujima, hypocenter distribution, seismic source time function

## Quantitative understanding of volcanic activities by a combinational use of geophysical and geochemical data - a case study of magmatophreatic eruptions at Kuchierabu volcano, SW Japan

\*Shogo Komori<sup>1</sup>, Tadafumi Ochi<sup>1</sup>, Ryunosuke KAZAHAYA<sup>1</sup>, Takahiko Uchide<sup>1</sup>, Akiko Tanaka<sup>1</sup>

1.National Institute of Advanced Industrial Science and Technology

Generally, magma ascent to a shallow part of a volcanic edifice induces swarms and crustal deformations. Newly-developed cracks and fractures would promote the magma ascent and release of volcanic gases from the magma. The released gases develop a hydrothermal system beneath the edifice, by mixing with the shallow groundwater. When the gas and heat fluxes increase and/or the ascending magma body encounters the groundwater system, phreatic / magmatophreatic eruptions would be induced because of unstable pressure-temperature conditions of the system.

Geophysical and geochemical data (i.e., seismicity, total magnetic intensity, resistivity, InSAR, GPS, and volcanic gas composition) are powerful tools to understand such the various volcanic activities. Also, numerical simulation programs such as HYDROTHERM and STAR can quantitatively evaluate the pressure-temperature conditions beneath the volcano associated with the hydrothermal activity. Therefore, it is expected that the combinational use of the above data and simulations could quantitatively and precisely evaluate the volcanic activity, which might also improve the prediction of the volcanic activity.

Based on the above concept, a working group was established by the authors, to enable the combinational use of the data for the quantitative evaluation of the volcanic activity. In this study, our group will introduce a case study of the magmatophreatic eruption at Kuchierabu volcano, SW Japan, occurred in August 2014 and May 2015. Numerical simulation of the hydrothermal system using the HYDROTHERM software (Hayba and Ingebritsen, 1994) estimates the temporal evolution of the pressure-temperature conditions after the increased flux of volcanic gas and heat and/or the encounter of the magma body. By combining with the previous studies and observed data [i.e., resistivity structure and demagnetized sources (Kanda et al., 2010), volcanic gas data, GPS, and InSAR], our group will try to quantitatively understand the mechanism of the magmatophreatic eruption

Keywords: Kuchierabu volcano, phreatic eruption, hydrothermal system

## A 3-D resistivity model of Kuchi-erabu-jima volcano

\*Wataru Kanda<sup>1</sup>, Mitsuru Utsugi<sup>2</sup>, Yasuo Ogawa<sup>1</sup>

1.Volcanic Fluid Research Center, Tokyo Institute of Technology, 2.Institute for Geothermal Sciences, Graduate School of Science, Kyoto University

### 1. Introduction

In Kuchi-erabu-jima volcano, a phreatic eruption occurred on Aug.3, 2014 after the preparation period of about 20 years. The existence of magma was presumed in the shallow edifice by several observational evidences such as a large amount of SO<sub>2</sub> degassing and volcanic glows, which resulted in a phreatomagmatic eruption accompanied by the pyroclastic flow on May 29, 2015. In this presentation, we report on the three dimensional (3-D) resistivity model of Kuchi-erabu-jima volcano inferred from reanalysis of the AMT (audio-frequency magnetotellurics) data obtained in 2004, in order to reexamine the preparation zone of phreatomagmatic eruption.

### 2. AMT data

The AMT data were acquired at a total of 27 sites around the Shin-dake crater during September to November of 2004. A part of the data has already published as the two dimensional (2-D) model along the WNW-ESE measurement line (Kanda et al., 2010). As a result, we found a low resistive zone thinly spreading near the surface of craters, and another conductive zone over the whole edifice at depths of 200-800m. These conductive zones were interpreted as layers containing low-permeable clays which were formed by the hydrothermal alteration. A groundwater layer was located between these low-permeable layers, which was considered to constrain the behavior of variation sources of the geomagnetic field and the deformation. However, we performed a 3-D modeling by using all the data obtained at 27 sites because these results were obtained by two-dimensional assumption, and because the data more than a half was not used.

### 3. 3-D modeling

The 3-D inversion code developed by Siripunvaraporn and Egbert (2009) was used. Full components of impedance tensor of 15 frequencies between 2 and 3000 Hz (error floor: 5%) were used for calculation. Horizontal mesh size around the Shin-dake crater was set to 40 m and the vertical size was 10-15m, a total of 64x64x66 meshes was discretized. Topographic and bathymetric features were accounted for in the model and resistivity blocks corresponding to seawater were fixed at 0.33  $\Omega$ m during the inversion process. Although a detailed resistivity distribution around the craters was obtained at present, it is necessary to examine its sensitivity because the site is unevenly distributed along the several trails. We will report the outline of these results.

This work was supported by JSPS KAKENHI Grant Number 15H05794.

Keywords: Kuchi-erabu-jima, resistivity structure, preparation zone of volcanic eruption

## Formation mechanism of the sulfur chimney at Mt. Iwo-dake, Satsuma-Iwojima Is., Japan

\*Ryoko Furukawa<sup>1</sup>, Toshiro Yamanaka<sup>1</sup>, hisashi Oiwane<sup>2</sup>, Masafumi MURAYAMA<sup>3</sup>, Hitoshi CHIBA<sup>4</sup>

1. Graduate School of Natural Science and Technology, Okayama University, 2. Mishimamura Village, Kagoshima Prefecture, 3. Center for Advanced Marine Core Research, Kochi University, 4. Department of Earth Sciences, Okayama University

Mt. Iwo-dake stood on Satsuma-Iwojima Is. is one of the most active volcanos in Japan. Many fumaroles have been active everywhere, and the fumaroles involved significant native sulfur deposits around them. Therefore, many parts of the mountain slopes have been decorated in yellow. In addition, quite high temperature fumaroles up to 900 °C have been observed in the summit crater, so there is a quite rare site where we can access such high temperature fumaroles. Another characteristic of the volcano is occurrence of chimney made up only of native sulfur on the fumaroles. Some of them are growing over 1 m high. Such sulfur chimney has been rarely reported all over the world. In this study we propose how to form such sulfur chimney made on the fumarole. Moreover, we will discuss about physicochemical condition in the volcano based on sulfur isotopic compositions of fumarolic gas and sulfur deposit.



## Ground Deformation around the Domestic Active Volcanoes detected by D-InSAR of ALOS-2/PALSAR-2

\*Shinobu Ando<sup>1</sup>, Takuro Kodama<sup>2</sup>, Shin'ya Onizawa<sup>2</sup>, Satoshi Okuyama<sup>3</sup>

1.Seismology and Tsunami Research Department, Meteorological Research Institute, 2.Japan Meteorological Agency, 3.Volcanology Research Department, Meteorological Research Institute

ALOS-2, was launched on May 24, 2014, has an L-band SAR (PALSAR-2) in the same way as ALOS/PALSAR. PALSAR-2 is of help to understand of a ground surface state, and its interferometric coherence is highly effective for the crustal deformation observation. Furthermore, PALSAR-2, is also very short repeat observation cycle (14days), has a higher resolution sensor than PALSAR. Therefore, higher resolution data can be acquired and we analyzed more frequently and are expected to be useful for disaster prevention and mitigation. After the calibration period of about half a year after the launch, ALOS-2 / PALSAR-2 data has been published on November 25, 2014. Current operational plan of ALOS-2 / PALSAR-2 is continue to be focused on the accumulation of the base map, but a lot of archive data have accumulated in the around active volcano because of early two years have passed from the start of observation.

We have analyzed the ground deformation caused by the earthquake and volcanic activity at domestic and overseas using ALOS-2 / PALSAR-2 data. And then, our analysis results are provided to each department of the JMA, and are used to the study of volcanic activity evaluation and seismic analysis results. In this presentation, we mainly report on the analysis results of around the domestic active volcano.

Some of PALSAR-2 data were prepared by the Japan Aerospace Exploration Agency (JAXA) via Coordinating Committee for the Prediction of Volcanic Eruption (CCPVE) as part of the project 'ALOS-2 Domestic Demonstration on Disaster Management Application' of the Volcano Working Group. Also, we used some of PALSAR-2 data that are shared within PALSAR Interferometry Consortium to Study our Evolving Land surface (PIXEL). PALSAR-2 data belongs to JAXA. We would like to thank Dr. Ozawa (NIED) for the use of his *RINC* software (Ver 0.36). In the process of the InSAR, we used Digital Ellipsoidal Height Model (DEHM) based on 'the digital elevation map 10m-mesh' provided by GSI, and Generic Mapping Tools (P.Wessel and W.H.F.Smith, 1999) to prepare illustrations.

Keywords: ALOS-2/PALSAR-2, InSAR, Domestic Active Volcano

## Volcanic tremor accompanied with crustal deformation

\*Koji Kato<sup>1</sup>, Akimichi Takagi<sup>5</sup>, Fujimatsu Jun<sup>2</sup>, Kobayashi Tsukasa<sup>3</sup>, Hiramatsu Hideyuki<sup>4</sup>

1.Japan Meteorological Agency, 2.Sapporo Regional Headquarters.JMA, 3.Sendai Regional Headquarters.JMA, 4.Fukuoka Regional Headquarters.JMA, 5.Meteorological Research Institute

Recently, Volcanic tremor accompanied with crustal deformation are observed many volcanoes. We will introduce their data.

## Deployment of the automatic Multi-gas stations for volcano monitoring by JMA

\*Akimichi Takagi<sup>1</sup>, Keita Torisu<sup>2</sup>, Hiroshi Shinohara<sup>3</sup>

1.Volcanology Research Department, Meteorological Research Institute, 2.Seismology and Volcanology Department, Japan Meteorological Agency, 3.National Institute of Advanced Industrial Science and Technology

In order to help to monitor volcanic activities, the automatic Multi-gas station systems are going to be deployed at four active volcanoes in Japan by JMA. This station has already been installed at Kusatsushirane and Azuma volcanos. Later this year, more two stations will be installed at two volcanoes, Kuju and Ontake.

This telemetric monitoring system was improved from the prototypal Multi-gas system which had been developed by the Advanced Industrial Science and Technology (Shinohara, 2005). This system can detect five gas components, SO<sub>2</sub>, H<sub>2</sub>O, CO<sub>2</sub>, H<sub>2</sub> and H<sub>2</sub>O. This station captures drifted atmosphere involving diffused volcanic gases released from fumarole by pump absorption, not by insertion of pipe to fumarole directly. Though this system cannot measure absolute value of gas concentration, this can get composition ratio based on multiple gas components. There are several studies that change of the composition ratio accompanied by volcanic activity by repeated survey (Ossaka et al., 1980). In the past, gas concentrations have not been monitored continuously by stable-maintained systems in active volcanoes in Japan, so this system is expected to accumulate effective data which contributes to evaluate volcanic activity and to detect premonitory phenomenon for phreatic eruption.

This system is needed to be installed near volcanic crater where gas is generated. At such area, power source and communication line are not prepared. So this has independent power system used solar panels and telemetry system used satellite communications. Observation is once per day and measurement time is 40 minutes at 13:00 every day for electric power saving. However, in the case of gas concentration exceeds the threshold value. Extra-measurement is done up to three times a day. Data is transmitted to headquarters of JMA immediately after measurement then it is supposed to be transferred to the MRI and AIST.

Keywords: Multi-gas system, volcanic gas, phreatic eruption

## Installation of geomagnetic total field observation stations to active volcanoes by Japan Meteorological Agency

\*Akira Yamazaki<sup>1</sup>, Makoto Nishida<sup>1</sup>, Tomofumi I<sup>1</sup>, Hideyuki Hirahara<sup>1</sup>, Masaki Nakahashi<sup>2</sup>

1.Kakioka Magnetic Observatory, 2.Volcanology Division, Japan Meteorological Agency

Due to the eruption of Ontake volcano on September 27, 2014 which became worst volcanic disaster after the Second World War, Japan Meteorological Agency (JMA) decided to strengthen volcanic observation system for prediction of phreatic eruption. Geomagnetic total field observation was adopted one of the strengthened observation system, because it has an advantage to monitoring of hydrothermal circulation under a volcano. From such process, we decided installation of geomagnetic total field observation stations in 2015 fiscal year at four active volcanoes (Tarumae, Azuma, Ontake, Kirishima) in Japan.

We planned that six Overhauser magnetometers are installed approximately within one km from a target crater at each volcano for monitoring the thermal activity beneath the crater, and one Overhauser magnetometer at the foot of each volcano as reference station. Also, one flux-gate magnetometer to measure three components geomagnetic field is installed at the reference station to correct external magnetic field disturbance such as a magnetic storm. The resolution of the Overhauser magnetometer is 0.01nT, and that of the flux-gate magnetometer is 0.001nT. We adopted solar-battery method as supply system, and it works over one hundred days without solar supply due to snow in winter season. The measurement data is transmitted to JMA using satellite or FOMA communication lines.

We selected the observation sites, where the topography is relatively flat and available sunshine for solar supply, approximately within one km from a crater. To avoid the vehicle noise, the observation sites were separated more than 200 m from a roadway. It is known that the annual variations caused by the temperature dependency of magnetization of rocks or soil around the observation site become big at high magnetic gradient observation site. To do the annual variations as small as possible, we selected less than 20 nT/m of magnetic gradient site by conducting magnetic survey around the observation site.

On the Tarumae volcano, there is a fumarolic activity at the summit lava dome. According to the repeat magnetic survey since 1998 by Sapporo Volcanological Center, JMA, magnetization has been progressing after 2010 beneath the lava dome. We selected the observation stations around the lava dome with reference to the result of the repeat magnetic survey. On the Azuma volcano, there is a fumarolic activity at the Oana crater located the south-east slope of Mt. Issaikyo. According to the repeat magnetic survey since 2003 by Sendai Volcanological Center, JMA, demagnetization has been progressing beneath the Oana crater. We selected the observation stations around the Oana crater with reference to the result of the repeat magnetic survey. On the Ontake volcano, we selected the observation stations around the Jigokudani crater which erupted on September 27, 2014. On the Kirishima volcano, the thermal activity is high accompanying with sometime occurrence of volcanic tremor around the Ioyama crater at Ebino plateau. We selected the observation stations around the Ioyama crater for the purpose of the monitoring of the underground thermal activity around the Ioyama crater.

Keywords: Japan Meteorological Agency, geomagnetic total field, active volcano, hydrothermal system, phreatic eruption, Overhauser magnetometer

## Effective utilization of geospatial information for intensified volcano activities

\*Yuki Kurisu<sup>1</sup>

### 1.GSI of Japan

Japan is one of the volcano-abundant countries in the world. Japan saw volcanic activities frequently occurred in Kuchino-erabujima volcano, Sakurajima volcano, Mt. Aso and Mt. Hakone, gave social influences such as evacuation in 2015. Disaster Mitigation measures such as quick and accurate evacuation, are important in order to protect people's lives and property from a volcanic disaster. Geospatial Information Authority of Japan (GSI) has contributed to mitigate volcanic disaster damages in recent years, by providing related organs and general public with necessary geospatial information. The author will highlight the effective use of three kinds of geospatial information among which GSI has provided for volcanic disaster mitigation.

The first is geospatial information about crustal deformation. Volcanic crustal deformation caused by movement of magma and vapour is so important information that it infers volcanic activity status under ground. In the case of Kuchino-erabujima and Mt. Hakone, the GSI deployed mobile GNSS observation equipment (REGMOS : Remote GNSS Monitoring System) in order to monitor crustal deformation more accurately. In addition, the result of SAR Interferometry complementarily detected ground surface deformation in an area-wide manner. Local crustal deformation detected at Owakudani, Mt. Hakone by SAR interferometry was considered to speedy volcanic alert level operated by Japan Meteorological Agency. Further crustal deformation enabled volcanic estimation source model to compare current situation with the past eruptions in the case of Sakurajima. The provision of such geospatial information through the Coordinating Committee for Prediction of Volcanic Eruption supported experts' decision making.

The second is aerial / satellite image. Aerial photo is very important because we can visually understand the damage of disaster. While manned flight just above a volcano is difficult during eruption, effort in taking oblique photo enabled to grasp the situation around crater in the case of Mt. Aso. Aerial photo taken by UAV made it possible to understand the disaster situation in detail. The GSI interpreted denuded land, pyroclastic flow and lahar using UAV images. The GSI also extracted surface change by a volcanic disaster using a pair of Landsat 8 images. Thanks to these geospatial information, we could understand the entire damage.

The third is hazard map and elevation map. They are very important to conduct volcanic disaster response operation. The GSI provided volcanic disaster response maps on which disaster prevention facility is described, relief map and 3D map on which detailed topography is draw. Land Condition Map of Volcano enabled to compare past damage of eruptions. These information is effective for efficiency disaster response.

Geospatial information is essential for effective and efficient volcanic disaster response. In tandem with disaster management organizations, GSI will continuously provide useful geospatial information in support of disaster response, rescue work and restoration activities.

Keywords: geospatial information, crustal deformation, SAR(synthetic aperture radar), grasping the damage of disaster, UAV(Unmanned Aerial Vehicle)

## A trial for evaluation of explosivity in monogenetic volcanism using grain size characteristics of pyroclasts

\*Rina Noguchi<sup>1</sup>, Nobuo Geshi<sup>1</sup>

1.National Institute of Advanced Industrial Science and Technology

Monogenetic volcanoes are formed in relatively small and short-duration eruptions, but some of them with explosive phenomena due to magma-water interactions (e.g., Wohletz and Sheridan, 1983). In 1983, Nippana tuff ring in Miyakejima Island was formed by small but explosive magma-water interaction in half a day (Aramaki and Hayakawa, 1984). That was a violence event with base surges (Sumita, 1985). As noted below, this kind of eruption style (i.e., phreatomagmatic) is not included in Volcanic Explosivity Index (VEI) originally. Also, VEI has no resolution in small-scale eruptions. Therefore, we should focus on magnitude-free parameters to assess dangerousness of monogenetic volcanism.

Explosivity in monogenetic volcanism is not well evaluated in the previous work. In the first place, what is "explosivity"? Volcanic eruption can be divided in two types: explosive and effusive. According to Wohletz and Heiken, 2002, the explosive eruption is "in which the expansion of gases determines mass transfer processes" in the point of mass transfer system. The mainstream of classification for the explosive eruption is "Walker diagram" which typed by fall-out tephra thinning rate and grain size (Walker, 1973). Walker, 1980 showed five parameters for explain "bigness" of explosive volcanic eruptions: magnitude, intensity, dispersive power, violence, and destructive potential. Taking into account these parameters, Newell and Self, 1982 proposed VEI to explain explosive character of an eruption in historical times. The specific criteria of VEI are volume of ejecta, column height, and descriptive terms. In this index, phreatomagmatic eruptions including Surtseyan have never been considered originally. Hickson *et al.*, 2013 added Surtseyan at VEI 4--5, but it lacks in detail. Furthermore, VEI does not include characteristics of ejecta, such as grain size and shape which represents features of explosions.

This study focus on grain size characteristics of pyroclasts to evaluate the explosivity of monogenetic volcanism regardless of the magnitude of eruptions. I compare the characteristics among three type: magmatic, phreatomagmatic, and rootless. To characterize the grain size, I use fractal fragmentation theory which was applied to a scoria cone by Perugini *et al.*, 2011, and median grain size which relates with energy conversion efficiency in the magma-water interaction (Wohletz and McQueen, 1984). In this presentation, I will show a result of trial evaluation of explosivity in monogenetic volcanism especially focusing on a role of external water in eruptions.

Keywords: monogenetic volcano, explosivity, magma-water interaction